INFORMATION TO USERS

This material was produced from a microfilm copy of the original document. While the most advanced technological means to photograph and reproduce this document have been used, the quality is heavily dependent upon the quality of the original submitted.

The following explanation of techniques is provided to help you understand markings or patterns which may appear on this reproduction.

1. The sign or "target" for pages apparently lacking from the document photographed is "Missing Page(s)". If it was possible to obtain the missing page(s) or section, they are spliced into the film along with adjacent pages. This may have necessitated cutting thru an image and duplicating adjacent pages to insure you complete continuity.

2. When an image on the film is obliterated with a large round black mark, it is an indication that the photographer suspected that the copy may have moved during exposure and thus cause a blurred image. You will find a good image of the page in the adjacent frame.

3. When a map, drawing or chart, etc., was part of the material being photographed the photographer followed a definite method in "sectioning" the material. It is customary to begin photoing at the upper left hand corner of a large sheet and to continue photoing from left to right in equal sections with a small overlap. If necessary, sectioning is continued again – beginning below the first row and continuing on until complete.

4. The majority of users indicate that the textual content is of greatest value, however, a somewhat higher quality reproduction could be made from "photographs" if essential to the understanding of the dissertation. Silver prints of "photographs" may be ordered at additional charge by writing the Order Department, giving the catalog number, title, author and specific pages you wish reproduced.

5. PLEASE NOTE: Some pages may have indistinct print. Filmed as received.

Xerox University Microfilms

300 North Zeeb Road
Ann Arbor, Michigan 48106

76-19,211

ONYEGEGBU, Samuel Onuorah, 1945-
THE EFFECT OF SECONDARY INJECTION ON THE PERFORMANCE AND EXHAUST EMISSIONS OF AN OPEN-CHAMBER DIESEL ENGINE.

The University of Michigan, Ph.D., 1976
Engineering, mechanical

Xerox University Microfilms, Ann Arbor, Michigan 48106

THE EFFECT OF SECONDARY INJECTION ON THE PERFORMANCE AND EXHAUST EMISSIONS OF AN OPEN-CHAMBER DIESEL ENGINE

by

Samuel Onuorah Onyegegbu

A dissertation submitted in partial fulfillment
of the requirements for the degree of
Doctor of Philosophy
(Mechanical Engineering)
in The University of Michigan
1976

Doctoral Committee:

Professor Jay A. Bolt, Chairman
Associate Professor Francis E. Fisher
Professor William Mirsky
Professor J. Arthur Nicholls

DEDICATION

To the memory of my mother,

Christy Chukwuewezia Ajufoh Onyegegbu

ACKNOWLEDGMENTS

I would like to express my sincere gratitude and appreciation to Professor Jay A. Bolt for his inspiration, guidance, support, and encouragement throughout my years as a graduate student at the University of Michigan. I am indebted to him for developing my interest in this area of research and for suggesting this research topic. In addition, my thanks are extended to Professor Francis E. Fisher, Professor J. Arthur Nicholls, and Professor William Mirsky for their interest and cooperation throughout the course of this study. Particular gratitude is also due to Dr. Mohamed F. El-Erian, and Dr. Stephen P. Bergin for their valuable suggestions and help provided in numerous discussions before and during this research effort.

The financial support of the U.S. Public Health Service and later the Environmental Protection Agency, is gratefully acknowledged. I would like to express my gratitude to the Mechanical Engineering Department and the office of Financial Aids through Dr. Klinger for their support in the form of fellowships during my graduate studies.

I would like to thank Mr. Clement Ma and Mr. Ohannes Z. Karaoghlanian for their able assistance with experimental measurements. The help of the technicians and machinists of the Automotive Laboratory is greatly appreciated. Thanks are also due to Ms. Ruth Howard for her typing of the draft and final manuscript.

I would like to express special thanks to my wife, Nkadi, for her patience and understanding, and for making it very pleasant and comfortable for me to do all the writing of this thesis at home.

Finally, I would like to express my sincere thanks to my parents for all the love and opportunities they have shown me which enabled me to get to this stage of life. I wish my mother, who gave so much of herself for me, were alive to witness one of her dreams come true. She passed away in the middle of this work on March 7, 1975. May her soul rest in peace.

TABLE OF CONTENTS

	Page
DEDICATION	ii
ACKNOWLEDGMENTS	iii
LIST OF FIGURES	vii
LIST OF TABLES	xii
NOMENCLATURE	xiii
CHAPTER	
I. INTRODUCTION	1
1.1 Purpose and Background	1
1.2 Literature Review	4
1.3 Objectives and Scope of Investigation	10
II. TEST PROCEDURE, EQUIPMENT AND INSTRUMENTATION	12
2.1 Approach	12
2.2 General Description of Test Engine and Fuel System	20
2.3 Pressure and Needle Lift Measurements	30
2.4 Exhaust Gas Samping and Analysis	37
2.4.1 Sampling and Measurement of Unburned Hydrocarbons	41
2.4.2 Sampling and Measurement of Oxides of Nitrogen	45
2.4.3 Sampling and Measurement of Carbon Monoxide	53
2.4.4 Samping and Measurement of Smoke	53
III. EXPERIMENTAL RESULTS - FUEL INJECTION	58
3.1 Computation of Rate of Injection	58
3.2 The Secondary Injection Survey	61
3.2.1 Region of Operation in Which Secondary Injection Occurs	61
3.2.2 Magnitude of Secondary Injection and its Variation with Speed and Load	67
IV. DIESEL ENGINE COMBUSTION PROCESS	74
V. EXPERIMENTAL RESULTS - ENGINE PERFORMANCE AND EMISSIONS	76
5.1 Brake Mean Effective Pressure (B.M.E.P.)	76
5.2 Brake Specific Fuel Consumption (B.S.F.C.)	76
5.3 Smoke	80

TABLE OF CONTENTS (Continued)

		Page
5.4	Unburned Hydrocarbons	88
5.5	Oxides of Nitrogen	95
5.6	Exhaust Temperature	99
VI.	CORRELATION BETWEEN SECONDARY INJECTION AND ENGINE PERFORMANCE AND EMISSIONS	103
6.1	Correlation Based on Total Fuel-Air Ratio	109
6.2	Correlation Based on Main Fuel-Air Ratio	113
VII.	GENERAL DISCUSSION	122
VIII.	CONCLUSIONS	126
APPENDICES		
A.	EXPERIMENTAL DATA - FUEL INJECTION	128
B.	EXPERIMENTAL DATA - ENGINE PERFORMANCE AND EMISSIONS	137
REFERENCES		146

LIST OF FIGURES

Figure		Page
1.1	Secondary Injection Zone in a Speed, Fuel Delivery Plane	5
2.1	Comparison Between Conventional and Modified Pump Spill Port Areas	16
2.2	Comparison Between Original and Modified Spill Ports	17
2.3	Comparison Between Original and Modified Pump Delivery Valves	18
2.4	Fuel Flow Area of the Delivery Valve	19
2.5	Details of ATAC Engine Open Combustion Chamber	21
2.6	Details of Recesses in ATAC Engine Piston	22
2.7	Schematic of Engine Air System	25
2.8	Details of Exhaust Surge Tank	27
2.9	Closed Cooling System for Use of Ethylene-Glycol	28
2.10	Lubricating Oil Cooling System	29
2.11	Details of Crank Angle Degrees Marking Unit	31
2.12	Schematic Representation of the Diesel Fuel Injection System	32
2.13	Open-Chamber Combustion System Showing Details of Pressure Pick-up and Injector Location	36
2.14	Fuel Injector Fitted with a Needle Lift Detector and a Pressure Transducer	38
2.15	Circuitry for the Bently Distance Detector	39
2.16	Exhaust Gas Sampling System	40
2.17	Schematic Representation of the FID Instrument	42
2.18	Effect of Sample Probe Location on Unburned Hydrocarbon Measurement	44
2.19	Schematic Representation of the NOOD Instrument	47
2.20	Schematic Representation of the NDIR Instrument	48

LIST OF FIGURES (Continued)

Figure		Page
2.21	Effect of Sample Flow Rate on NO Measurement	50
2.22	Effect of Temperature and Material on Percent Conversion of NO_2 to NO, and NH_3 to NO	52
2.23	Details of the NO Converter	54
2.24	Schematic Representation of Smoke Sampling System	56
2.25	Schematic Representation of the Smoke Sample Probe	57
3.1	Needle Seat and Injector Holes Orifices	59
3.2	Equivalent Area for Fuel Flow Through Nozzle Orifices	62
3.3	Oscilloscope Records of Transient Fuel Line Pressure, Needle Lift, and Cylinder Pressure at Engine Speed of 1800 rpm and Total Fuel-Air Ratio of .0506	63
3.4	Oscilloscope Records of Transient Fuel Line Pressure, Needle Lift, and Cylinder Pressure at Engine Speed of 2400 rpm and Total Fuel-Air Ratio of .040	64
3.5	Fuel Injection Schedule for Conventional Injection System, at Engine Speed of 1200 rpm and Total Fuel-Air Ratio of .0294	65
3.6	Fuel Injection Schedule for Conventional Injection System, at Engine Speed of 1800 rpm and Total Fuel-Air Ratio of .0407	66
3.7	Zone of Secondary Injection in a Load, Speed Plane	68
3.8	Relationship Between Total Fuel-Air Ratio and Total Fuel Injected per Cycle for Various Engine Speeds	69
3.9	Relationship Between Total Fuel-Air Ratio and Main Injected Fuel per Cycle for Various Engine Speeds	70
3.10	Relationship Between Total Fuel-Air Ratio and Secondary Injected Fuel per Cycle for Various Engine Speeds	72
3.11	Relationship Between Total Fuel-Air Ratio and Percent Secondary Injection for Various Engine Speeds	73
5.1	Effect of Total Fuel-Air Ratio and Injection System Characteristics on BMEP for Engine Speed of 1200 rpm	77

LIST OF FIGURES (Continued)

Figure		Page
5.2	Effect of Total Fuel-Air Ratio and Injection System Characteristics on BMEP for Engin- Speed of 1800 rpm	78
5.3	Effect of Total Fuel-Air Ratio and Injection System Characteristics of BMEP for Engine Speed of 2400 rpm	79
5.4	Effect of Total Fuel-Air Ratio and Injection System Characteristics on BSFC for Engine Speed of 1200 rpm	81
5.5	Effect of Total Fuel-Air Ratio and Injection System Characteristics on BSFC for Engine Speed of 1800 rpm	82
5.6	Effect of Total Fuel-Air Ratio and Injection System Characteristics on BSFC for Engine Speed of 2400 rpm	83
5.7	Effect of Total Fuel-Air Ratio and Injection System Characteristics on Smoke for Engine Speed of 1200 rpm	85
5.8	Effect of Total Fuel-Air Ratio and Injection System Characteristics on Smoke for Engine Speed of 1800 rpm	86
5.9	Effect of Total Fuel-Air Ratio and Injection System Characteristics on Smoke for Engine Speed of 2400 rpm	87
5.10	Effect of Total Fuel-Air Ratio and Injection System Characteristics on Unburned Hydrocarbons for Engine Speed of 1200 rpm	89
5.11	Effect of Total Fuel-Air Ratio and Injection System Characteristics on Unburned Hydrocarbons for Engine Speed of 1800 rpm	90
5.12	Effect of Total Fuel-Air Ratio and Injection System Characteristics on Unburned Hydrocarbons for Engine Speed of 2400 rpm	91
5.13	Effect of Total Fuel-Air Ratio and Injection System Characteristics on Specific Hydrocarbon Emission for Engine Speed of 1200 rpm	92
5.14	Effect of Total Fuel-Air Ratio and Injection System Characteristics on Specific Hydrocarbon Emission for Engine Speed of 1800 rpm	93
5.15	Effect of Total Fuel-Air Ratio and Injection System Characteristics on Specific Hydrocarbon Emission for Engine Speed of 2400 rpm	94

LIST OF FIGURES (Continued)

Figure		Page
5.16	Effect of Total Fuel-Air Ratio and Injection System Characteristics on Oxides of Nitrogen for Engine Speed of 1200 rpm	96
5.17	Effect of Total Fuel-Air Ratio and Injection System Characteristics on Oxides of Nitrogen for Engine Speed of 1800 rpm	97
5.18	Effect of Total Fuel-Air Ratio and Injection System Characteristics on Oxides of Nitrogen for Engine Speed of 2400 rpm	98
5.19	Effect of Total Fuel-Air Ratio and Injection System Characteristics on Exhaust Temperature for Engine Speed of 1200 rpm	100
5.20	Effect of Total Fuel-Air Ratio and Injection System Characteristics on Exhaust Temperature for Engine Speed of 1800 rpm	101
5.21	Effect of Total Fuel-Air Ratio and Injection System Characteristics on Exhaust Temperature for Engine Speed of 2400 rpm	102
6.1	Comparison of the Rate of Injection Diagrams Used at an Engine Speed of 1200 rpm	105
6.2	Comparison of the Rate of Injection Diagrams Used at an Engine Speed of 1200 rpm	106
6.3	Comparison of the Rate of Injection Diagrams Used at an Engine Speed of 1800 rpm	107
6.4	Comparison of the Rate of Injection Diagrams Used at an Engine Speed of 1800 rpm	108
6.5	Effect of Secondary Injection on Percent Reduction of BMEP for Various Engine Speeds (Case I)	110
6.6	Effect of Secondary Injection on Percent Increase of BSFC for Various Engine Speeds (Case I)	111
6.7	Effect of Secondary Injection on Percent Increase of Smoke for Various Engine Speeds (Case I)	112
6.8	Effect of Secondary Injection on Percent Increase of Unburned Hydrocarbons for Various Engine Speeds (Case I)	114

LIST OF FIGURES (Continued)

Figure		Page
6.9	Effect of Secondary Injection on Percent Increase of Specific Hydrocarbon Emissions (Case I)	115
6.10	Effect of Secondary Injection on Percent Increase of BMEP (Case II)	116
6.11	Effect of Secondary Injection on Percent Reduction of BSFC (Case II)	117
6.12	Effect of Secondary Injection on Percent Increase of Smoke (Case II)	119
6.13	Effect of Secondary Injection on Percent Increase of Unburned Hydrocarbons (Case II)	120
6.14	Effect of Secondary Injection on Percent Increase of Specific Hydrocarbons (Case II)	121

LIST OF TABLES

Table		Page
I	Factors Affecting Duration of Injection	9
II	Engine Design Specifications	23
III	Fuel Injection System Specifications	33
IV	Fuel Specifications	34
V	Fuel Injection Experimental Data (Runs No. 1-5)	129
VI	Fuel Injection Data (Runs No. 6-10)	130
VII	Fuel Injection Data (Runs No. 11-15)	131
VIII	Fuel Injection Data (Runs No. 16-20)	132
IX	Fuel Injection Data (Runs No. 21-25)	133
X	Fuel Injection Data (Runs No. 26-30)	134
XI	Fuel Injection Data (Runs No. 31-35)	135
XII	Fuel Injection Data (Runs No. 36-40)	136
XIII	Performance and Emissions (Runs No. 1-5)	138
XIV	Performance and Emissions (Runs No. 6-10)	139
XV	Performance and Emissions (Runs No. 11-15)	140
XVI	Performance and Emissions (Runs No. 16-20)	141
XVII	Performance and Emissions (Runs No. 21-25)	142
XVIII	Performance and Emissions (Runs No. 26-30)	143
XIX	Performance and Emissions (Runs No. 31-35)	144
XX	Performance and Emissions (Runs No. 36-40)	145

NOMENCLATURE

Symbol	Definition
A	Area
a	Wave propagation velocity
API	American Petroleum Institute
ABDC	After bottom dead center
ATAC	Army Tank Automotive Command
ATDC	After top dead center
Ave.	Average
BBDC	Before bottom dead center
BHP	Brake horsepower
BMEP	Brake mean effective pressure
BSFC	Brake specific fuel consumption
BTDC	Before top dead center
C	Temperature, celsius
C.A.	Cam angle
C_c	Coefficient of contraction
C_d	Coefficient of discharge
d	Diameter
E	Bulk modulus of elasticity
EVC	Exhaust valve closing
EVO	Exhaust valve opening
Exh.	Exhaust
F	Temperature, Fahrenheit
FID	Flame Ionization Detector
gm.	Grams
hr.	Hour

NOMENCLATURE (Continued)

Symbol	Definition
I.D.	Inside diameter
Inj.	Injection
IVC	Inlet valve closing
IVO	Inlet valve opening
L	Length
	Needle lift
Max.	Maximum
Min.	Minimum
mm	Milimeter
NDIR	Non-Dispersive Infrared
NOOD	Nitric Oxide Optical Detector
O.D.	Outside diameter
OHV	Overhead valve
P	Pressure
$\frac{dp}{dt}$	Rate of change of pressure
ΔP	Pressure drop across nozzle orifices
ppm	Parts per million
psi	Pounds per square inch
Q	Fuel flow rate
rpm	Revolutions per minute
Sec.	Secondary
SMD	Sauter mean diameter
t	Time
TACOM	Tank Automotive Command

NOMENCLATURE (Continued)

Symbol	Definition
TDC	Top dead center
V	Velocity
$\frac{dv}{dt}$	Rate of change of velocity
ν	Kinematic viscosity
ρ	Mass Density
μ	Micron
Subscript	
b	Negative or backward wave
eff.	Effective
Equiv.	Equivalent
f	Fuel line
g	Cylinder gas
h	Nozzle holes orifice
i	Positive or forward wave
n	Needle seat orifice
orf.	Nozzle holes orifice
s	Nozzle sac

CHAPTER I

INTRODUCTION

1.1 Purpose and Background

Over the past ten years there has been an ever increasing awareness of the need to improve the quality of the air that we breathe. One of the major contributors to this air pollution problem has been the internal combustion engines of which the diesels now form only a small part. However, as the need for diesel-powered vehicles such as heavy-duty trucks increases, due largely to their simplicity and relatively low fuel consumption, so will the overall pollution from diesel engines increase.

It is also becoming increasingly imperative that engines be designed for better fuel economy and efficiency than is presently being realized. This is perhaps the only way to combat the energy shortage that is being forecast for the future, or else we must seek a cheaper and more abundant source of energy which is yet unknown to man.

The engineering approach to the solution of diesel emissions, fuel economy, power and efficiency lies in a better understanding of the functions of the various parts that constitute the diesel engine and their interactions with each other. These parts include the diesel fuel injection system and the combustion chamber.

It has been known for quite a while that the fuel injection process can have a profound influence on the combustion and resulting exhaust emissions and power of a diesel engine. It is also now known that given a combustion chamber design, the performance and emissions of a diesel engine are uniquely determined by the manner in which fuel

is injected into the combustion chamber. This fuel injection process or characteristic is in turn mainly determinated by the design of the fuel injection system.

Injection characteristics can be conveniently defined by the following:

a. timing

b. duration of injection

c. distribution and size of spray

d. rate or shape of the injection process

e. secondary injection

The effects of the first four defined injection characteristics on diesel engine power and emissions are very well documented in the literature on diesel engine combustion. The last injection characteristic is still a little understood phenomenon which, like the first four, is inherent in the jerk pump type fuel injection system. This is a second fuel injection into the combustion chamber which usually occurs after the main fuel injection has terminated. It is caused by high pressure waves remaining in the line after the initial closing of the needle and the delivery valve.

Experimental and analytical studies of diesel fuel injection systems, diesel engine combustion and emissions have been going on for many years at the University of Michigan. During most of this time the U.S. Army-Tank Automotive Command has sponsored research relating to combustion problems of highly supercharged diesel engines. During more recent years, TACOM and the Environmental Protection Agency have jointly sponsored research in the Automotive Engineering Laboratory of the University of Michigan concerning exhaust emissions of diesel

engines.

The Army sponsored research was initially concerned with the ignition delay and other combustion phenomena, with emphasis on high output conditions and coolant temperatures of up to 300°F. The variables studied included cylinder gas temperature, maximum cylinder pressure, charge density, engine speed, fuel-air ratio, and coolant temperature. Three types of fuel were used in these tests: Diesel No. 2, CITE, and Military gasoline. The tests were carried out on two engines: the Lister-Blackstone and the TACOM-1 engine.

More recent emission studies were carried out on the TACOM-1 engine using Diesel No. 2 fuel at higher cylinder pressures. Emission data including unburned hydrocarbons (H-C), oxides of Nitrogen (NO_x) and aldehydes were measured. This data was collected for both the open and the pre-type combustion chambers.

During these tests, it was observed that at high fuel deliveries, secondary injection occurred while using the open-chamber type combustion chamber. The secondary injection is easily noticed on the needle lift trace. It was also observed that the secondary injections once initiated grew with time before reaching a steady value. This generally resulted in a corresponding variation of emissions and performance data collected. Most noticeably, the smoke and unburned hydrocarbons readings increased with the incidence of secondary injection, prompting the need for a careful evaluation of the effects of secondary injection on diesel emissions and performance.

Meanwhile, the Environmental Protection Agency has for four years sponsored research on the diesel fuel injection system. This work resulted in an analytical simulation of the diesel fuel injection

system as well as design modifications to eliminate secondary injections from the fuel injection system while leaving the main injection unchanged. This study is documented in detail in the Ph.D. dissertation entitled, "Simulation and Control of Transient Flow in the Diesel Injection System," by M. F. El-Erian, (15) 1972.

Very few people have given attention to the effects secondary injections might have on the performance, exhaust emissions and smoke of diesel engines. Up to the present, there is no data published which give any quantitative or qualitative evaluation of the harmful or useful effects of this common characteristic of the jerk-pump type fuel-injection system. It will be the purpose of this thesis to obtain such useful information and publish the results which I believe will be very interesting and timely. It will contribute to the overall picture of the search for fuel injection characteristics which result in optimum combustion characteristics and minimum exhaust emissions.

1.2 Literature Review

A study by Bradbury, (8) 1950, showed that secondary injection generally occurred at conditions of simultaneously high load and high speed. Figure 1.1 shows the incidence of secondary injection as obtained by Bradbury in a typical jerk-pump injection system. It shows that a certain limited area of engine operation is free of secondary injection. Bradbury also studied the effect of pipe length and found a gradual retarding of secondary opening with increasing pipe length.

Mansfield, (32) 1965, in his studies stated that the level of pressure in the discharge system at the commencement of pump spilling

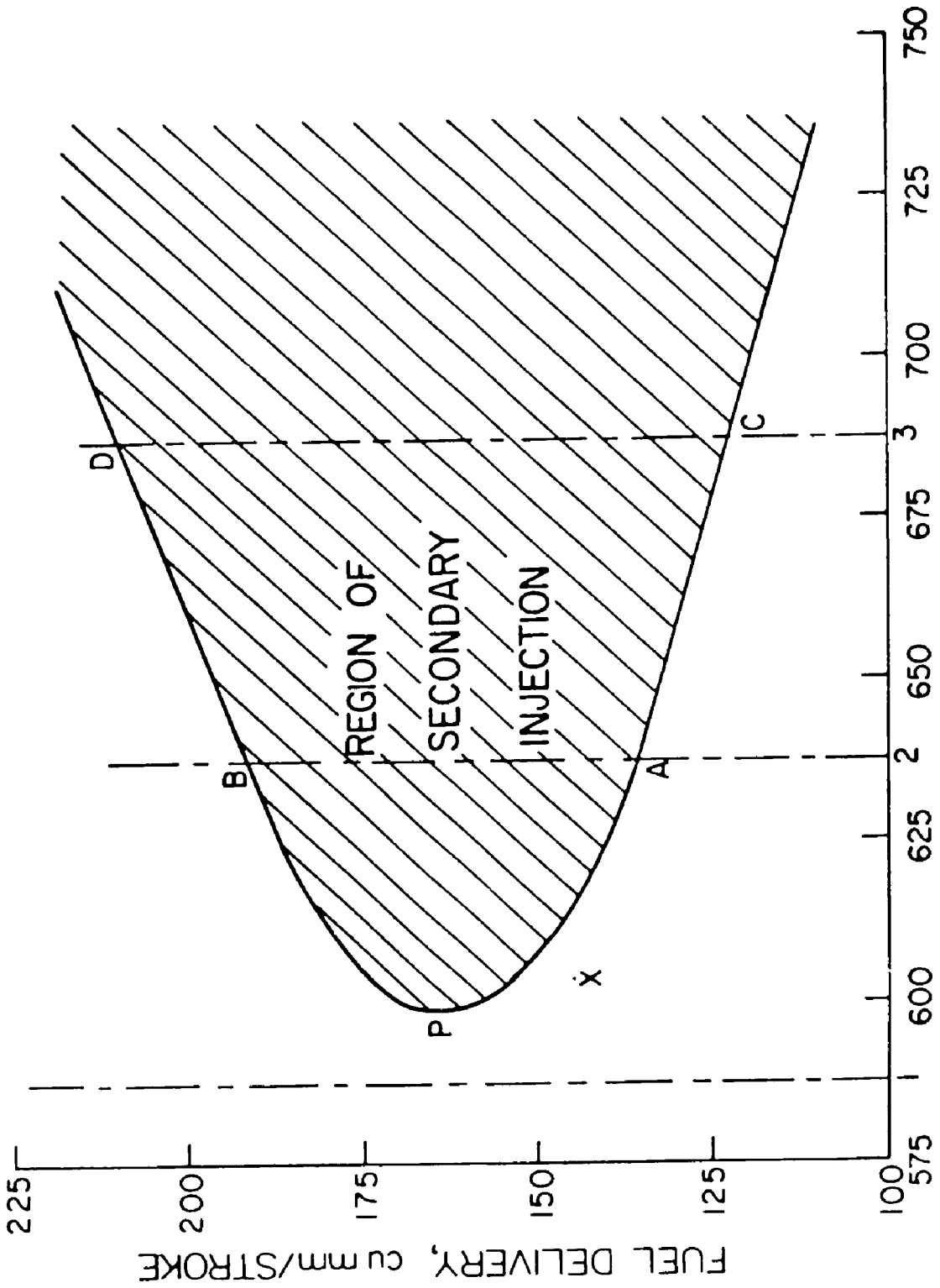


Figure 1.1 Secondary Injection Zone in a Speed, Fuel Delivery Plane

action determines whether or not secondary injection occurs. While studying the relationship between specific fuel consumption and mean effective pressure , Mansfield observed that the fuel consumption started increasing at about the point when secondary injection started occurring. He experimented with larger nozzle holes and found that they gave a lower fuel consumption at this high load condition, because the larger holes eliminated secondary injections at this condition. His overall conclusion was that small nozzle holes were preferred at part loads, but at high load when secondary injections occurred, larger nozzle holes were better.

Because of the lack of a thorough knowledge of the hydraulics of the diesel fuel injection system, and because the modern computer was not available to handle the complex equations, early attempts at eliminating secondary injection centered around experimental trial and error technique. Design changes were attempted mostly at the injector and high-pressure line. These changes include varying the injector pipe length and diameter, varying the needle opening pressure, and varying the number and size of the nozzle holes. Later on, changes have also been attempted at the pump. Judge, (25) 1967, showed that increasing the pipe length has the effect of damping out pressure waves and hence reducing secondary injection. This also results in altering the timing duration, shape and magnitude of the main injection. So while secondary injection is eliminated, the reduced main injection pressure produces poor fuel penetration and atomization and hence results in poor combustion. In short one defect is basically replaced by another defect. The other changes result in the same comparable weakness. Table I summarizes the effects of changing certain system components

on both the main and secondary injections as given by Burman and Deluca, (10) 1962.

Recent investigators now recognize that to satisfactorily eliminate secondary injection while minimizing changes in the main injection, main modifications have to be made in the injection pump. Dolenc and Lees (14), 1968, and Lustgarten and Dolenc (28), 1969, carried out tests using a pump plunger with a double stepped helix. Their results showed that less secondary injection was obtained and the engine performance was better than the origiral system.

Anders (1), 1971, in his investigations of the adaptation of injection pumps to meet the requirements of high-duty engines, cited secondary injection as one of the consequences of using small and light pumps to inject large quantities of fuel at high speeds. This, he observed, is due to excessive throttling effects occurring during the back flow after the end of delivery. He recommended the decrease of the dynamic flow delivery during spill by calculating geometrical control areas coupled with an aerodynamic design of the pump plunger helix.

In more recent times with the wide use of computers and a better understanding of the hydraulics of the injection system, accurate simulation of the injection system is now possible and has been done. Using these models, systematic and scientific analytical studies of ways to eliminate secondary injections have been investigated. Tateishi, Kushiyama, and Nagae (43), 1973, have studied the phenomenon during the end of fuel injection by graphical analyses and have proposed the following as a method for eliminating secondary injection and cavitation.

TABLE I

FACTORS AFFECTING DURATION OF INJECTION

Item	Direction of Change	Effect on Injection Duration: Main Injection	Effect on Injection Duration: Secondary Injection
Plunger Diameter	Increase	Decrease	Increase
Cam Velocity	Increase	Decrease	Increase
Nozzle Orifice Area	Increase	Decrease	Decrease
Tubing Bore	Decrease	Decrease	Decrease
Tubing Length	Increase	Decrease	Decrease
Trapped Fuel Volume	Decrease	Decrease	Decrease
Nozzle Opening Pressure	Increase	Decrease	Decrease
Nozzle Reciprocating Mass	Decrease	Decrease	Decrease
Nozzle Valve Lift	Decrease	Decrease	Decrease
Delivery Valve Retraction	Increase	Indefinite	Decrease

1. It is necessary to give a suitable velocity and duration of retraction of delivery valve.
2. Pressure drop during ending period of injection is controlled by opening area of spill port but not directly by revolutions per minute of engine.
3. Retraction of delivery valve has two different functions; to terminate injection rapidly, and to eliminate secondary injection.
4. In the conventional delivery valve, secondary injections may be avoided by adopting a large retraction volume but cavitation is also apt to be generated.

The major problem with this method is that the main injection is considerably altered.

In a more advanced work, El-Erian (15), 1972, developed an analytical technique to eliminate secondary injection through a redesign of the conventional pump spill port and pump delivery valve. These modifications did not alter the flow characteristics of the system significantly during the main injection and successfully dampened out the high-pressure transients that ultimately lead to secondary injection. To achieve this, the concept of average elastic energy as a control parameter was introduced. This is defined as the energy stored in the pipe line and volumes of the system due to elastic deformation of the fuel. He visualized that the pump adds energy in the form of flow work at the delivery valve end and this energy is stored in the pipe line and system volumes as elastic energy. Part of this energy is released at the injection nozzle during the injection period. If excessive uncontrolled elastic energy remains in

the system following the closure of the pump delivery valve, it will be released at the nozzle in the secondary injection period. A program was designed to release this high elastic energy in the system by controlling the fuel spilling at the port. The delivery valve must therefore be kept open during this control period. The rate of spilling at the port is controlled by the spill port design while keeping the delivery valve open longer is controlled by the size (diameter) of the delivery valve.

1.3 Objectives and Scope of Investigation

The major purpose of this research is to correlate diesel engine exhaust emissions and performance with secondary injections for the cases when secondary injections occur. To accomplish this, the following will have to be done.

1. Definition and identification of secondary injection characteristics, and a survey of the zone of secondary injection for a conventional American Bosch fuel injection system on a bench test rig.
2. Observation of the extent of influence of secondary injection on combustion characteristics in an engine as follows:
   - A. Power
     - a. Brake mean effective pressure
     - b. Brake specific fuel consumption
   - B. Emissions, or Completeness of Combustion
     - a. Black smoke
     - b. Unburnt hydrocarbons
     - c. Oxides of nitrogen
   - C. Noise and Engine Stresses
     - a. Shape and magnitude of cylinder pressure -

time trace.

3. Consideration of the engineering implications of the experimental results.

CHAPTER II

TEST PROCEDURE, EQUIPMENT AND INSTRUMENTATION

2.1 Approach

The approach to this problem is essentially experimental. Two fuel injection pumps were fitted to an engine, one at a time, and performance and emission data were taken with the engine run at various high load (fuel-air ratio) conditions and at three speeds. These speeds have been selected as 1200 rpm, 1800 rpm, and 2400 rpm.

One of the pumps is a conventional American Bosch fuel pump and the other is a modified American Bosch fuel pump. The conventional pump gives secondary injections at the running conditions while the modified pump gives the same main injection but no secondary injection at the running conditions.

To be able to understand the modifications made in the modified pump, it is convenient to explain the mechanics and sequence of fuel injection in a normal jerk type fuel injection system. The fuel injection system characteristics are better understood by a cause and effect study of events at the pump, the high pressure line, and the injector during the pump plunger stroke.

As the plunger begins its upward movement, the pressure in the pumping chamber increases only slightly. This rise is very small because the supply and spill ports are open. Midway in this movement the plunger covers both ports and the pumping chamber pressure begins to rise rapidly. The delivery valve opens when this pumping chamber pressure reaches a certain value. This is the beginning of the effective stroke.

Pressure waves P_i initiated by the plunger movement in compressing the fuel at the pumping chamber, propagate with the velocity of sound a_i through the fuel in the pressure line to the nozzle. If the pressure waves reaching the nozzle are less than the nozzle opening pressure, as the first waves obviously will be, the fuel velocity at the nozzle will fall to zero and a reverse pressure wave would be created (in other words the pressure wave will be completely reflected back). This reverse wave will reinforce the pressures in the pipe line by P_i while retarding velocities by a_i. At some point the reinforced waves reaching the nozzle equal and exceed the nozzle opening pressure. At this condition, the needle will open thus permitting fuel injection through the nozzle to the combustion chamber with combustion subsequently resulting. This is the beginning of the main injection. At the open needle, only part of the wave is reflected back and the resultant pressure wave determines the flow past the needle.

During the next important phase of the plunger stroke, the plunger helix begins to uncover the spill port. This reduces the pumping chamber pressure because of flow through the spill port. This lowering of the pumping chamber pressure causes the delivery valve to start closing. The valve closing causes negative pressure waves P_b and velocity waves a_b to travel down from the pump to the injector. The pressures in the line are reduced by P_b while the velocities are reinforced by a_b. When the pressure at the needle falls below the needle closing pressure, the needle begins to close. This is the end of the main injection. This needle closure in turn sends pressure and velocity waves down to the valve which at this time is closed.

We now have a system consisting of the fuel line with both ends

closed and pressure transients reflecting back and forth between the needle and the valve. If these pressure waves exceed the nozzle opening pressure on reaching the nozzle, the nozzle will open again, resulting in a second fuel injection within the cycle, after the end of the main injection. This is the cause of the phenomenon known as secondary injection.

Secondary injection is therefore very identifiable by the beginning of the second needle lift and the end of this needle lift within a cycle after the first needle lift.

As mentioned earlier in this chapter, two pumps were used in this research, a conventional pump and a modified pump. The difference between the two pumps are in the delivery valve sizes and the sizes and design of the spill ports.

The conventional spill port is replaced by three sets of ports so that the uncovering of the spill port is as shown in Figure 2.1. This is designed to control the rate of spill through the spill ports and hence the rate of closure of the delivery valve. The general idea is to close the delivery valve slow enough so that it is still open when the needle is closed. By staying open in this region, any high pressures in the line are relieved by flow out through the delivery valve. The flow areas through the modified delivery valve is kept the same as the original. However, a larger diameter valve is needed for it to stay open longer. Figure 2.2 shows a comparison between the original and modified spill ports while Figures 2.3 and 2.4 show a comparison between the original and modified delivery valves and their respective flow areas.

Now that secondary injection has been defined, it is convenient

to at this time specify parameters by which it could be measured for this study or any other studies. The important parameters are:

a. The timing or beginning of secondary injection

b. The duration or period of secondary injection

c. The distribution and size of spray during secondary injection

d. The rate or shape of the secondary injection process

The next step was the selection of points upon which attention will be focused for investigation. To represent the whole operating range of the engine for which secondary injection occurs in the conventional pump, it was decided to experimentally survey the range of fuel-air ratios and speed for which this phenomenon occurred. This helped to select points at which the secondary injection could relatively be classified as small, medium, or large. This classification is done according to the ratio of quantity of fuel injected during secondary injection in a cycle to the total quantity of fuel injected in a cycle. Each point is determined by a combination of speed and fuel-air ratio. For example, a combination of high speed and high fuel-air ratio will produce large secondary injection while a combination of the same high speed, and much smaller fuel-air ratio will produce small secondary injection. Also a combination of low speed and high fuel-air ratio will produce a medium secondary injection while a combination of the same low speed and a slightly smaller fuel-air ratio will produce small secondary injection.

Engine speeds of 1200 rpm, 1800 rpm, and 2400 rpm were chosen for testing. For each of these speeds, the fuel-air ratio is varied from about .03 to .055. This corresponds to a relative fuel-air ratio

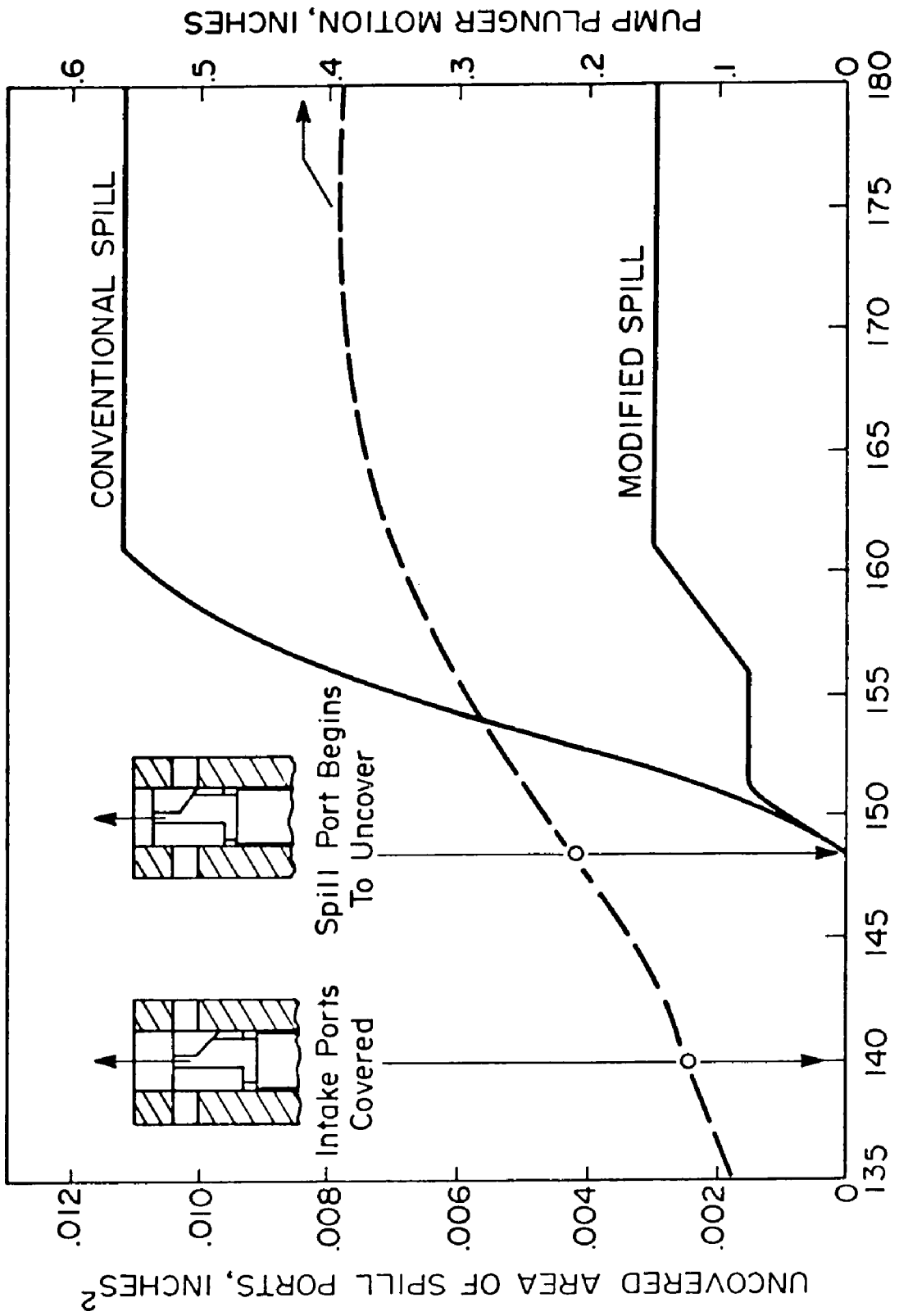


Figure 2.1 Comparison Between Conventional and Modified Pump Spill Port Areas

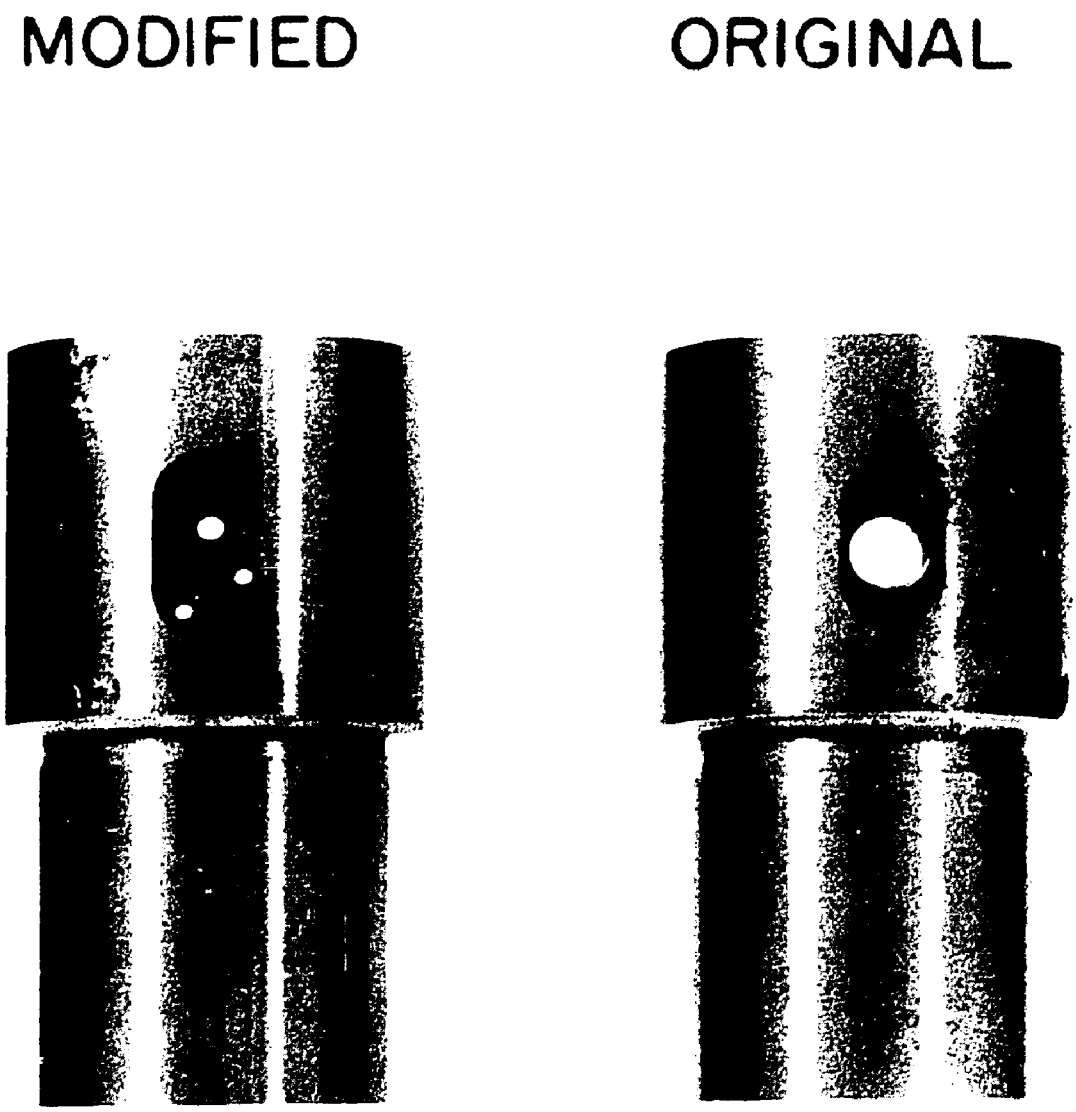


Figure 2.2 Comparison between Original and Modified Spill Ports

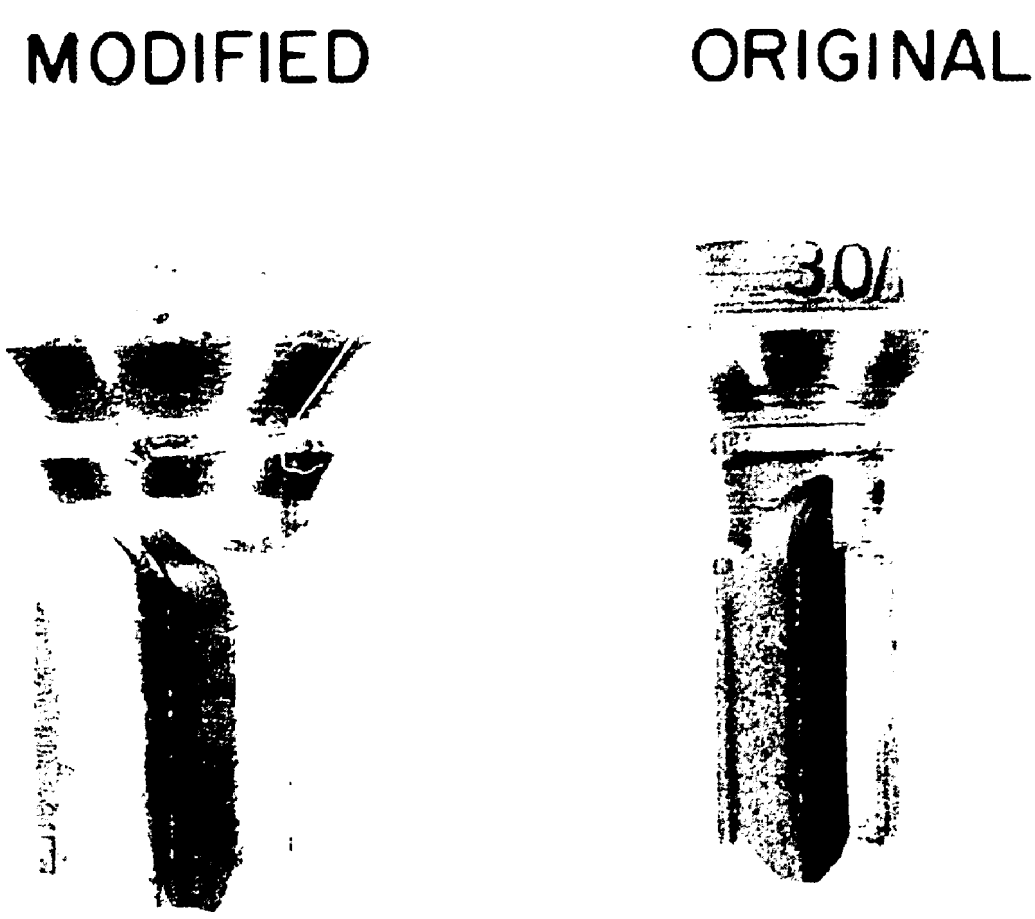


Figure 2.3 Comparison between Original and Modified Pump Delivery Valves

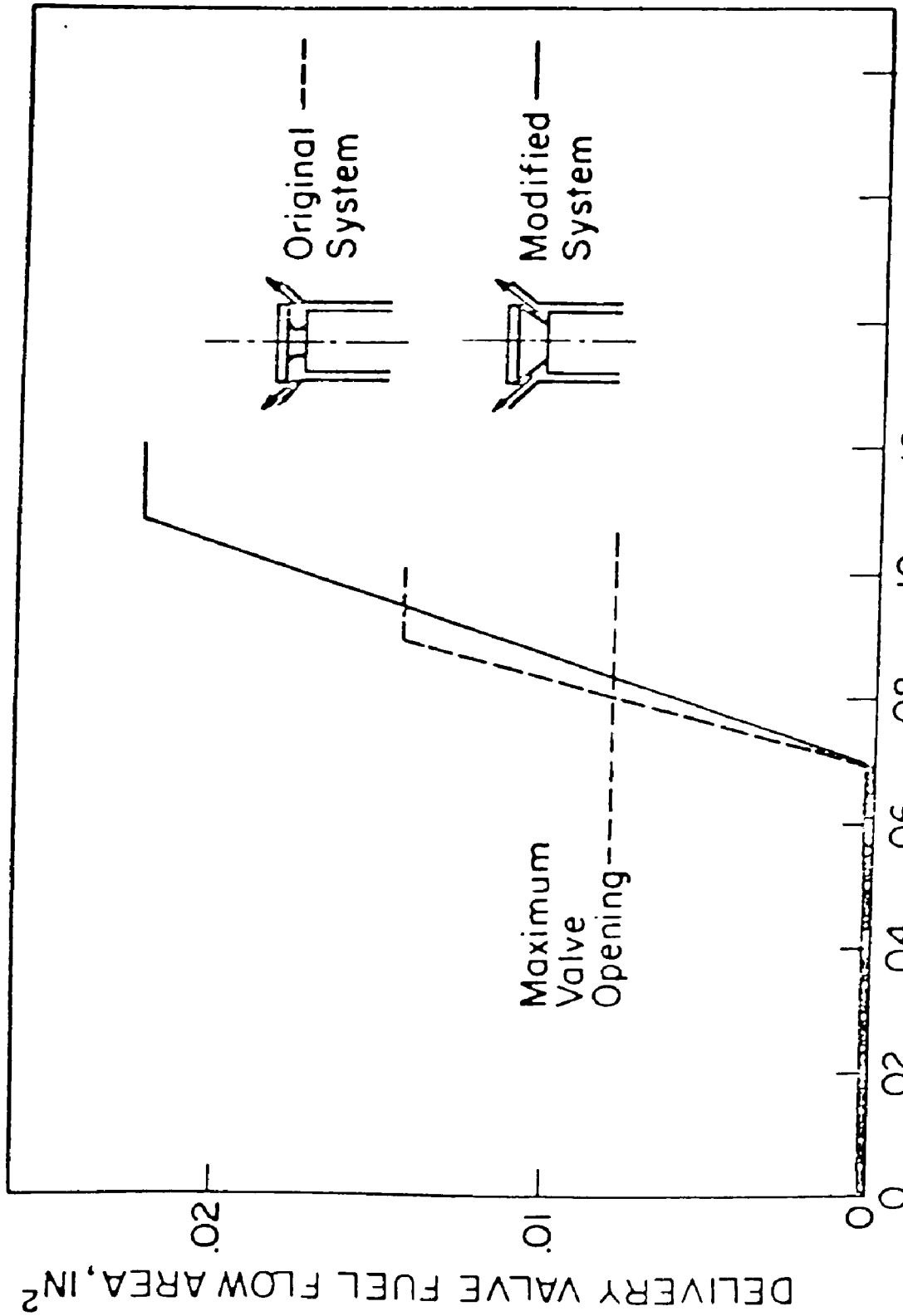


Figure 2.4 Fuel Flow Area Past the Delivery Valve. Comparison Between Conventional and Modified Designs

(fraction of stoichiometric) of approximately from .45 to .82. From the needle lift traces and calculations of mass of fuel injected per cycle for both total and secondary injections, the points to be investigated are selected.

2.2 General Description of Test Engine and Fuel System

The engine used for this experimental investigation is a high output single-cylinder, four-stroke cycle, open-chamber diesel engine, (the TACOM-1 engine). The engine is designed to operate at speeds of up to 3000 rpm and at outputs of up to 350 psi indicated mean effective pressure. The engine friction is high which results in low mechanical efficiency particularly at low loads. The cylinder has a bore of 4.5 inches, a stroke of 4.5 inches, and a compression ratio of 16.7:1. The cylinder head is flat with a 2.475 inch diameter and .8342 inch deep recess in the piston to generate high swirl in the combustion chamber. A schematic representation of the open chamber is given in Figures 2.5 and 2.6, while Table II lists the engine design specifications. Further details of the engine are given by Flynn and Johnson (18), 1957. Provision is made to supply the engine with air at any pressure from 0 to 3 atmospheres and at any temperature from room temperature to 450°F, with a mass flow rate of from 0 to 485 lbm/hr. The engine inlet air is supplied from the laboratory compressed air supply through a critical flow air meter. The critical flow design is chosen as it permits accurate air flow measurements regardless of the downstream pressure fluctuations caused by single cylinder engines. It also provides an easy means of supplying and controlling the air supercharge pressure. The air meter consists of four critical flow

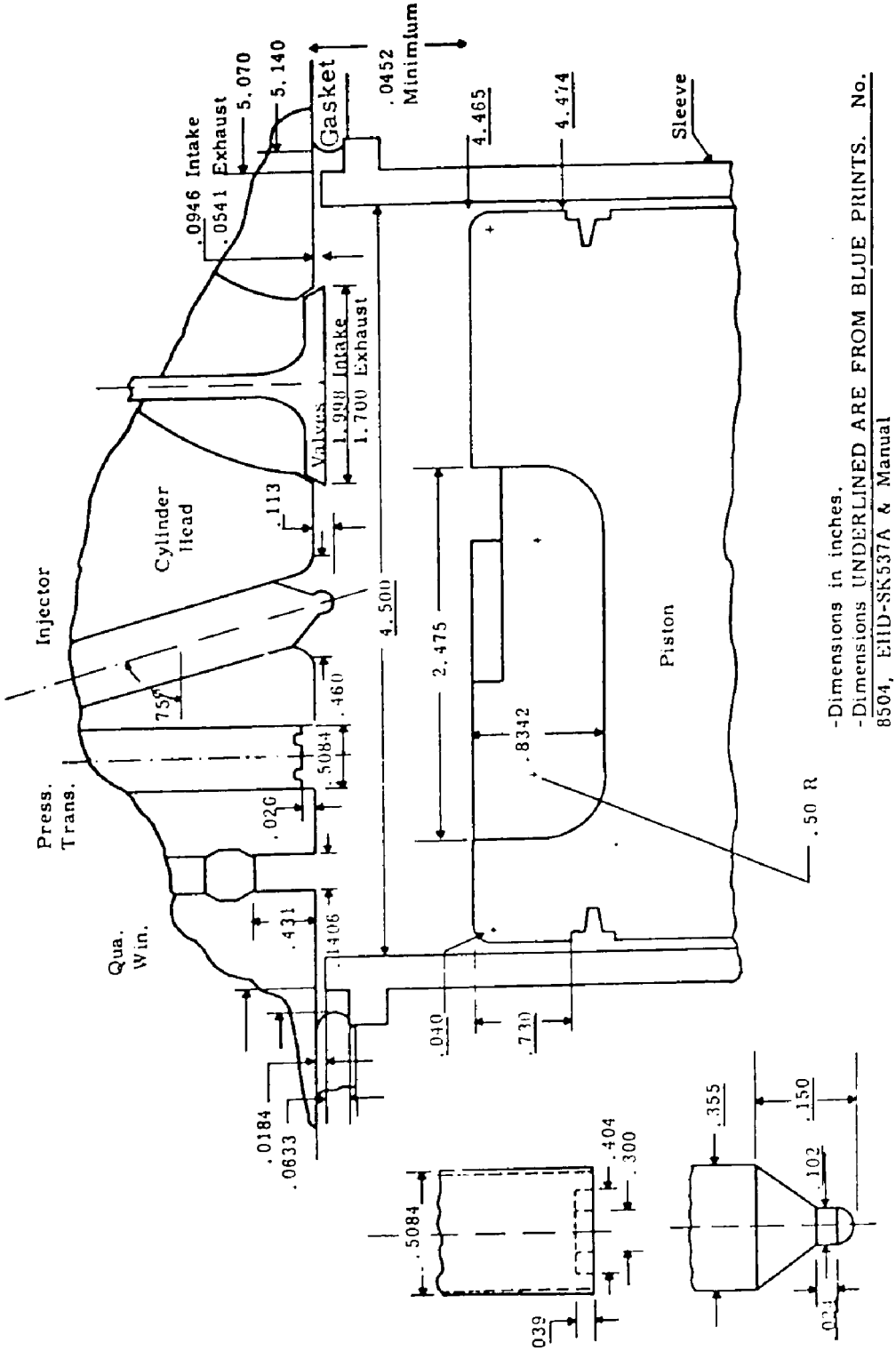


Figure 2.5 Details of ATAC Engine Open Combustion Chamber

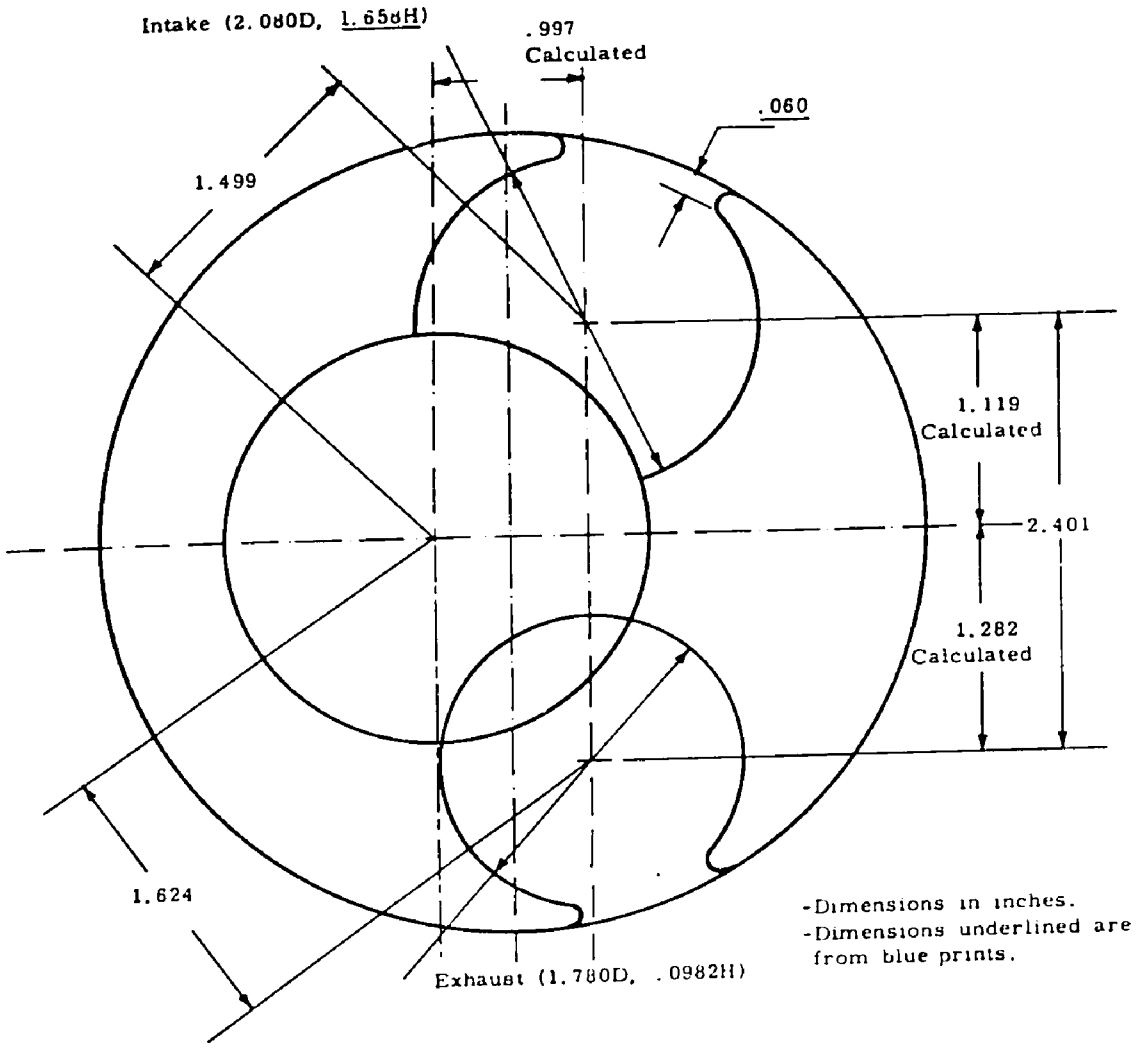


Figure 2.6 Details of Recesses in ATAC Engine Piston

TABLE II

ENGINE DESIGN SPECIFICATIONS

Displacement	71.5 $in.^3$
No. of Cylinders	1
Cycle	4
Bore	4.5 in.
Stroke	4.5 in.
Compression Ratio	16.1 (nominal)
Clearance Volume	4.76 $in.^3$ (nominal)
Connecting Rod Length	9.0 in.
Combustion Chamber	Open - bowl in piston
Maximum Engine Speed	3000 rpm
Flywheel Inertia	275 lb. $ft.^2$
Rotating Weight	4.7 lb.
Reciprocating Weight	7.8 lb.
Valve Actuation	Pushrod O.H.V.
Nominal Valve Timing	
-IVO° BTDC	20
-IVC° ABDC	40
-EVO° BBDC	50
-EVC° ATDC	10

orifices piped and valved together in parallel in such a manner that any single orifice or any combination of the orifices can be used to supply air to the engine. The upstream air pressure can be regulated to give any desired inlet air pressure and/or air flow. The air meter is calibrated to $\pm$ 1.0% accuracy. Figure 2.7 shows a schematic of the engine air system.

After the air leaves the air meter, it is passed through a chromalox electric air heater of 20 kilowatt capacity. The heater is thermostatically controlled and has the capacity to heat the maximum air flow from room temperature to 450°F. Smaller air flow rates can be heated to temperatures up to a maximum of approximately 800°F.

From the air heater, the air is directed to an inlet air surge tank of 5.6 ft.^{3} capacity. The purpose of the surge tank is to stabilize the pressure at the engine inlet. The tank is connected to the engine by a 10-inch section of flexible metal tubing and is insulated to minimize heat losses from the air.

A surge tank of 2.4 ft.^{3} capacity is also provided to stabilize the pressure at the exhaust. The exhaust back pressure is regulated by a gate valve located immediately after the exhaust surge tank. Because of the high temperature of the exhaust gases, it is necessary to cool the exhaust surge tank. This is accomplished by spraying water into the tank. The direction of the spray is such as not to interfere with the flow of gases from the engine to the tank or with the smoke meter probe.

This engine set up makes it possible to vary inlet air pressure and temperature as well as exhaust pressure independently of load and speed. Hence supercharged conditions can be readily simulated for

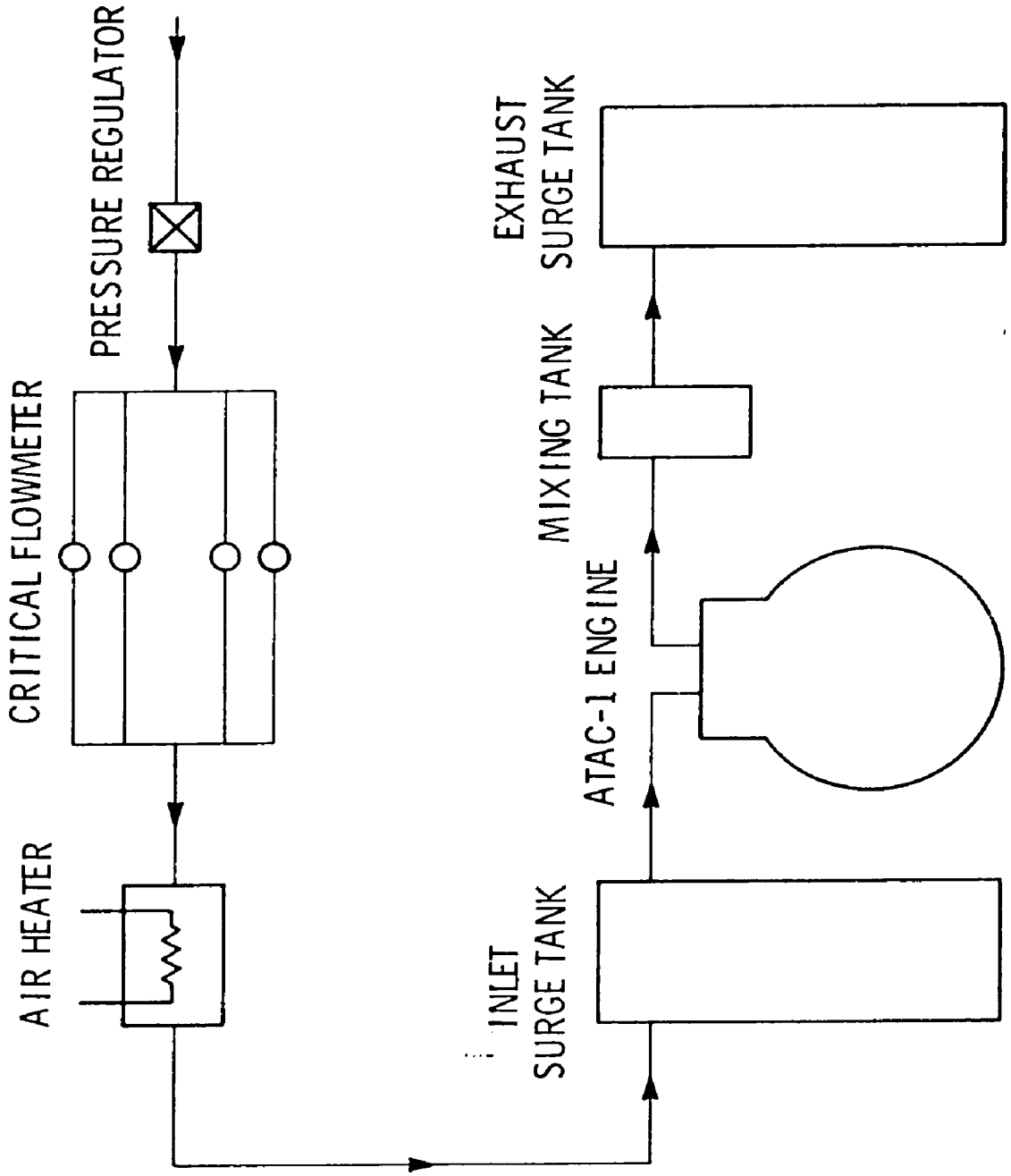


Figure 2.7 Schematic of Engine Air System

study. Figure 2.8 shows details of the exhaust surge tank.

The engine cooling system is shown schematically in Figure 2.9. The engine coolant is in a closed loop with a heat exchanger and so makes it easy for other coolants other than water to be used. A mixture of ethylene-glycol and water, which has a boiling point much above that of pure water has been used for this study. The coolant flow rate is measured by a standard ASME sharp-edge orifice and the coolant temperatures at the entrance to and the exit from the engine are measured by two iron-constantan thermocouples.

The flow rate of the lubricating oil is measured by a turbine type meter. The oil is cooled in a heat exchanger to a constant temperature of 200°F. The oil temperatures at the entrance to and the exit from the engine are measured by two iron-constantan thermocouples. Figure 2.10 shows a schematic of the oil cooling system.

The increase in oil and coolant temperatures as well as their respective flow rates can then be used to calculate the thermal load, which is the heat transfer from the gases to the combustion chamber walls. The rest of the equipment on the engine are typical for test cell installations and includes a cradle mounted electric dynamometer for motoring or absorbing power, a Hewlett-Packard electronic counter for measuring engine speed and a Honeywell-Brown electronik self-balancing potentiometer for measuring temperatures.

The timing marks are recorded every three degrees using a steel disc, 20 inches diameter, 1/8 inch thick which is mounted on the engine flywheel. The rim of the discs are slotted at 3° intervals, with deeper slots at 45° intervals. A magnetic pick up was mounted on the engine bedplate, with its pole close to the rim. The alternating

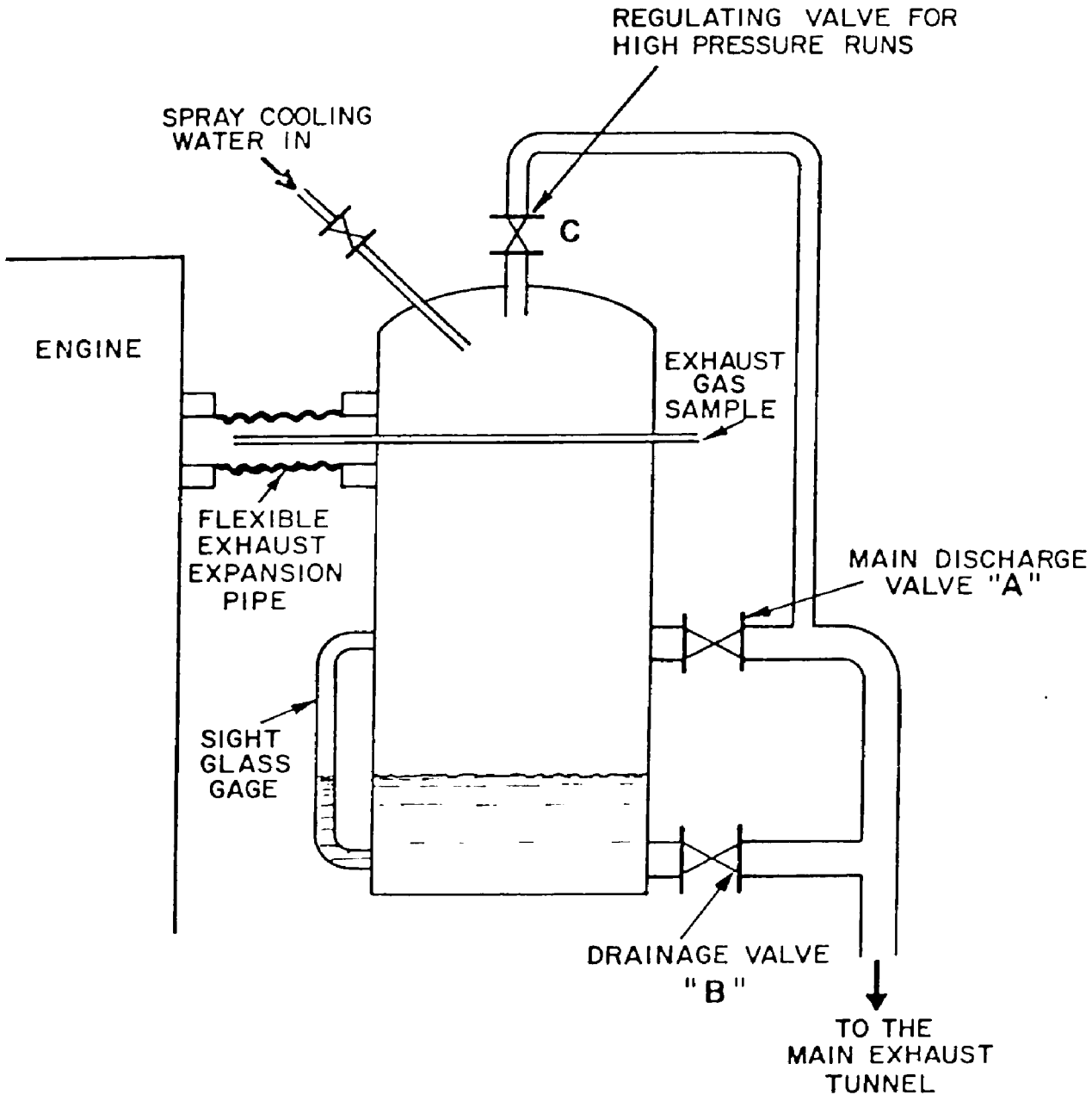


Figure 2.8 Details of Exhaust Surge Tank

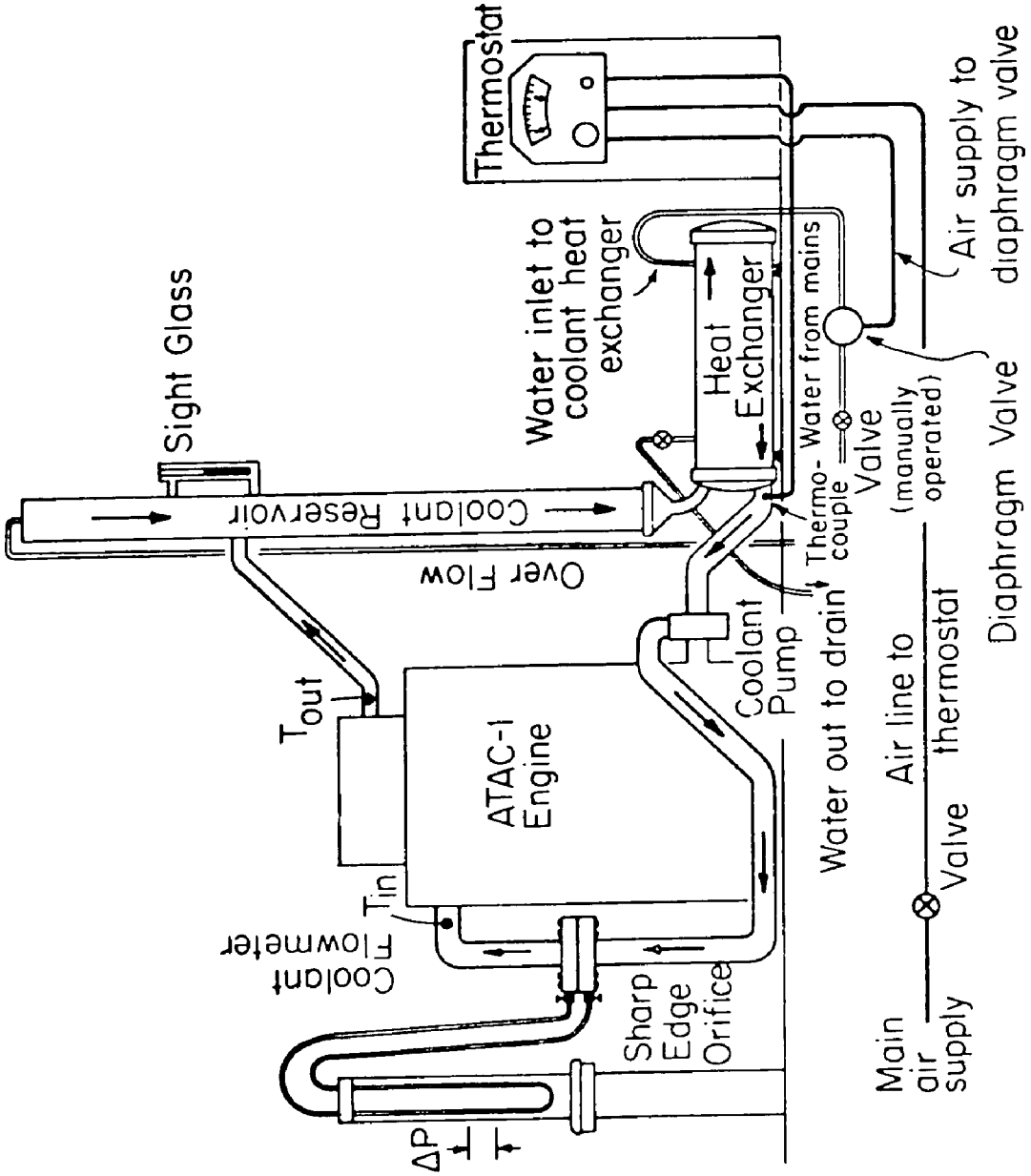


Figure 2.9 Closed Cooling System for Use of Ethylene-Glycol

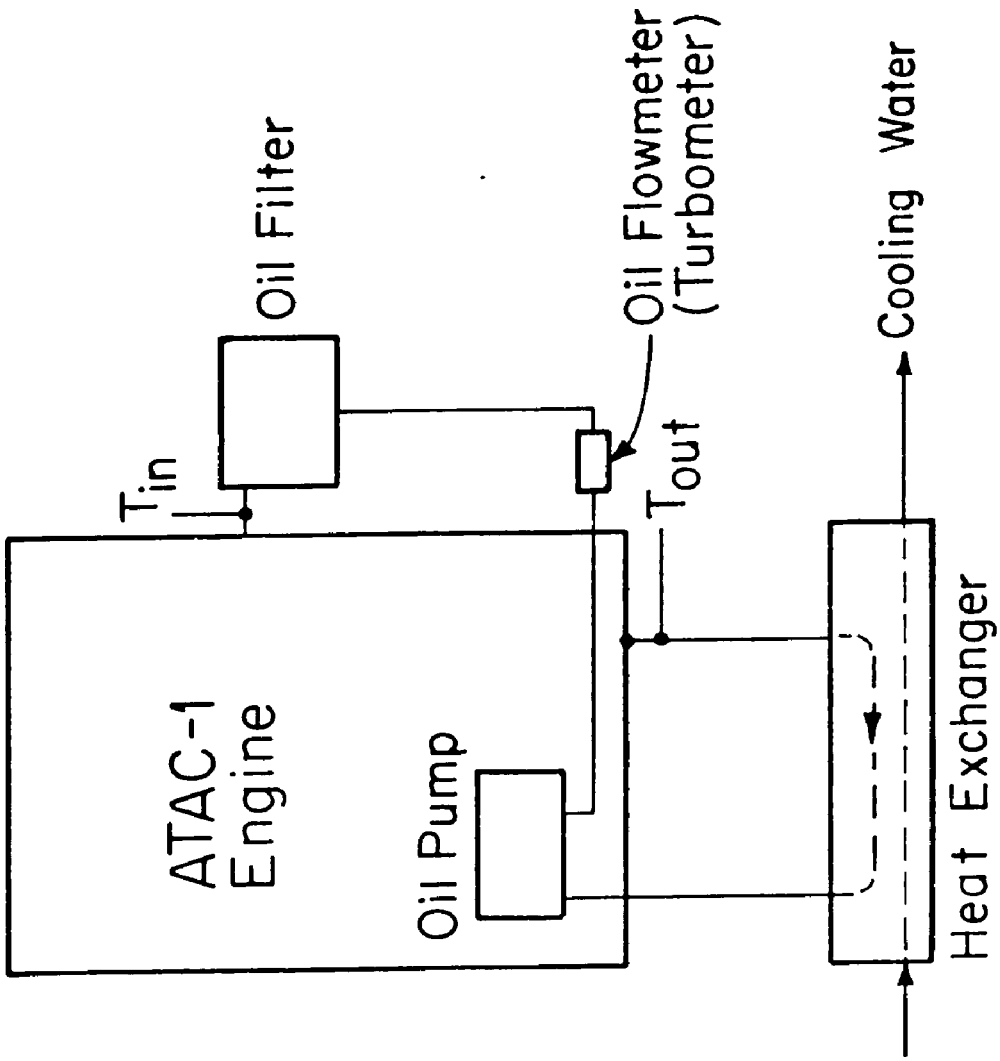


Figure 2.10 Lubricating Oil Cooling System

voltage generated when the disc rotates is applied to channel B of a dual beam oscilloscope. Little peaks are observed on the scope at 3° intervals with peaks corresponding to the deeper slots being higher than the others. One of the 45° slots was aligned at the T.D.C. and the crankangle position on the oscilloscope can then be easily determined. Figure 2.11 shows a schematic of the crank angle measuring system.

The fuel injection system is shown schematically in Figure 2.12. The injection system used for this work consists of an American Bosch APE1B type single plunger pump with a 10 mm plunger and a tangent cam; a high pressure pipe line of .082 inch inside diameter and 24 inches long; and an American Bosch ADB type injector with 4 injector holes each of .0118 inches in diameter. The injector opening pressure is set at 3000 psia. The fuel delivery is regulated by a fuel rack in the pump which is positioned by a micrometer. The micrometer setting is readily varied from 0 to 1 inch in increments of .001 inch. The 0 inch corresponds to maximum fuel delivery and the 1 inch setting corresponds to minimum fuel delivery. The fuel is supplied to the pump from a fuel beaker resting on a balance. A mercury switch, a standard electric clock and a relay system all attached to the balance provides for semiautomatic fuel weighing. The clock records the time it takes to withdraw a known weight of fuel from the beaker and this gives the average flow rate of the fuel through the injector.

2.3 Pressure and Needle Lift Measurements

Because of their utilization in the determination of rates of injection, pressure and needle lift measurements are two of the most

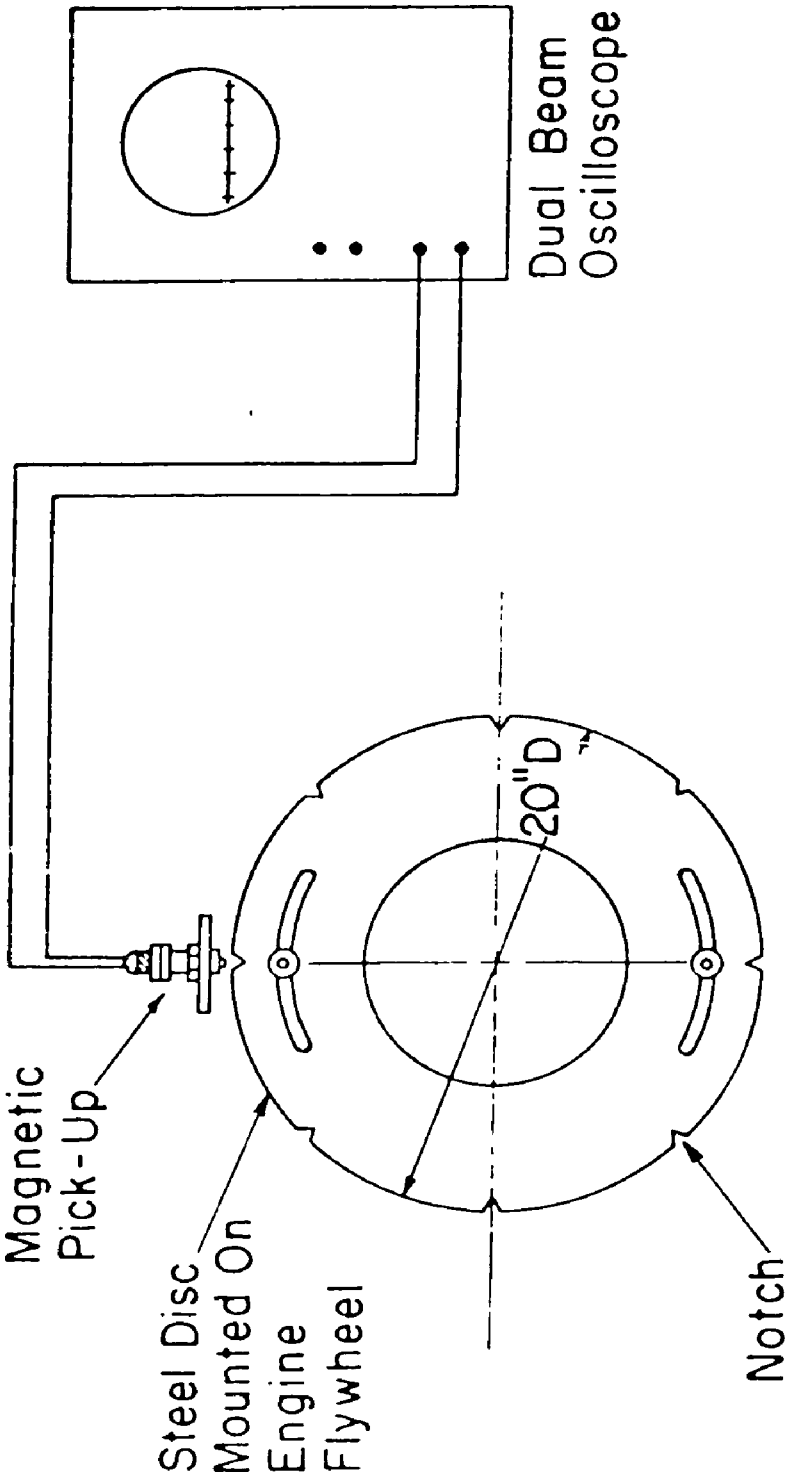


Figure 2.11 Details of Crank Angle Degrees Marking Unit

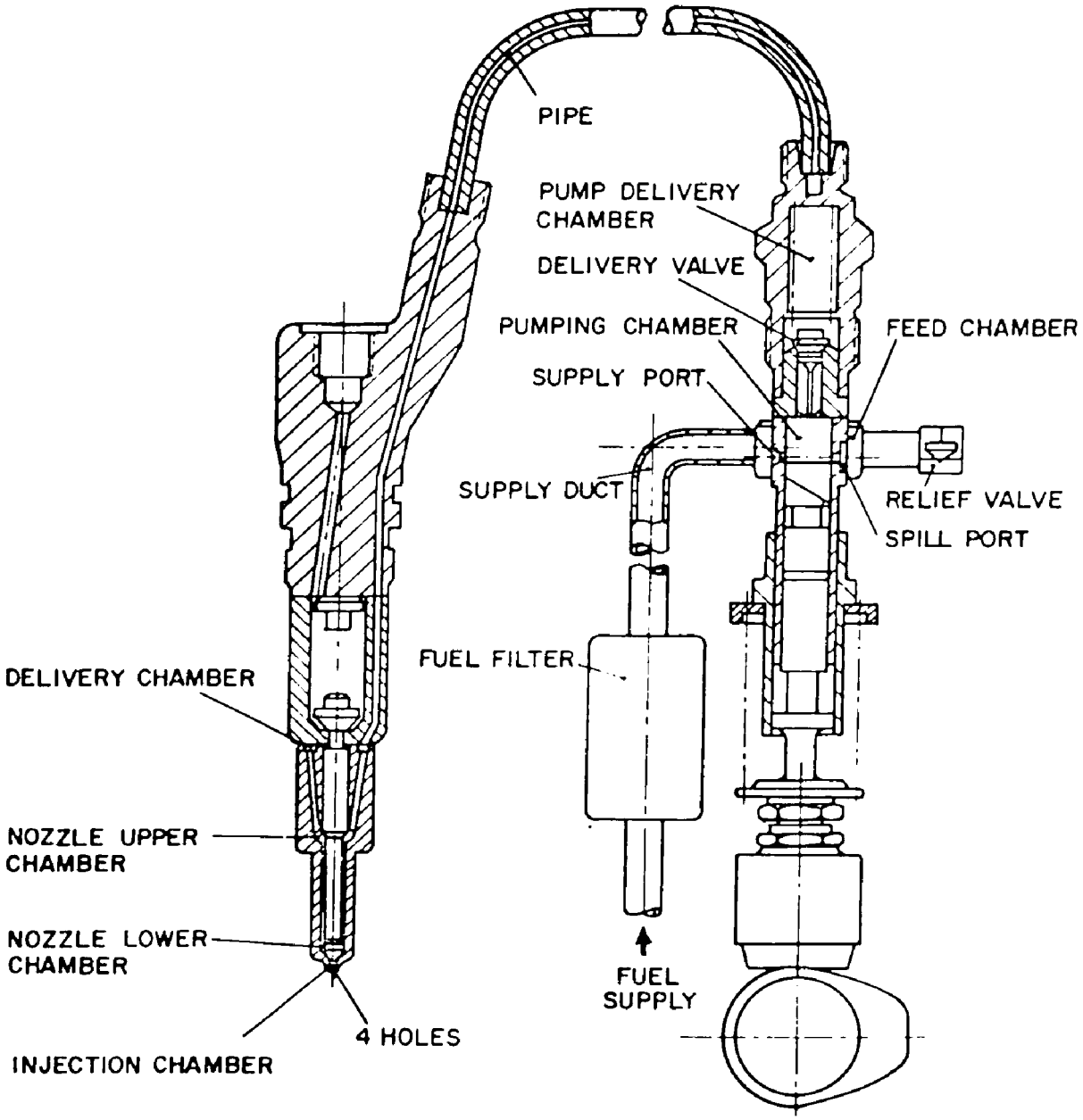


Figure 2.12 Schematic Representation of the Diesel Fuel Injection System

TABLE III

FUEL INJECTION SYSTEM SPECIFICATIONS

Injection Pump	American Bosch, Type APE1B with manual timing advance unit
Plunger Diameter	10 mm
Injection Line	30" x .082 I.D.
Injection Nozzle	American Bosch, Type ADB-150S
Number and Pattern of Injection Holes	4 holes spaced symmetrically on 150° apex angle cone
Size of Injection Holes	.0118 in Dia.
Nozzle Opening Pressure	3000 psi
Injector Sac Volume	.001 $in.^3$
Supply Pump Pressure	60 psi
Cam Profile	26/2X tangential

TABLE IV

FUEL SPECIFICATIONS

Fuel	Diesel Fuel VV-F-800 Grade II
Flash Point, F min.	165
Cloud Point, F max.	+4
Pour Point, F max.	-5
Kinematic Viscosity at 100 F, CS, min.	2.5
Water and Sediment, % by Vol; max.	nil
Sulfur, %	0.11
Ash, % max.	0.001
Corrosion, Cu strip 3 hr. at 122 ASTM No., max.	1.0
Distillation, °F	
50%	516
90%	590
End Point	604
Ignition Quality, Cetane No.	57.5
Gravity, deg. API	39.1

important measurements to be made for this work. Great care was therefore exercised in making pressure measurements in the cylinder as well as in the injector. Because of the transient nature of pressures involved, a pressure transducer with fast response time was needed. Piezoelectric quartz pressure transducers were found to be most suitable. This type of pressure transducer converts pressure force acting on it into an electric charge which is then amplified by a charge amplifier. The amplified electric signal can be monitored on an oscilloscope. Besides their very good frequency response, these transducers have the added advantage of high signal/noise ratio, and are available in small sizes which makes it easy to use them even in highly inaccessible places. Their main disadvantage is their susceptibility to thermal drift of the zero level, which for this investigation was negligible for all test runs.

Cylinder pressure is measured by Kistler pressure transducer type 401A together with a charge amplifier type 655, S/N 1194. The location of the pressure transducer in the engine for cylinder pressure measurement is shown in Figure 2.13.

The pressure in the injector is measured by a Kistler pressure transducer type 601H together with a charge amplifier type 503, S/N 359. Both pressure transducers and amplifiers were statically calibrated with a dead weight tester.

Most investigators use either a variable capacitance-type pick-up or a linear differential transformer to sense the motion of the injector needle. However, because of the problems of adapting to the injector, a Bently electro-mechanical distance detector system was used to detect and measure needle lift. The Bently system is capable

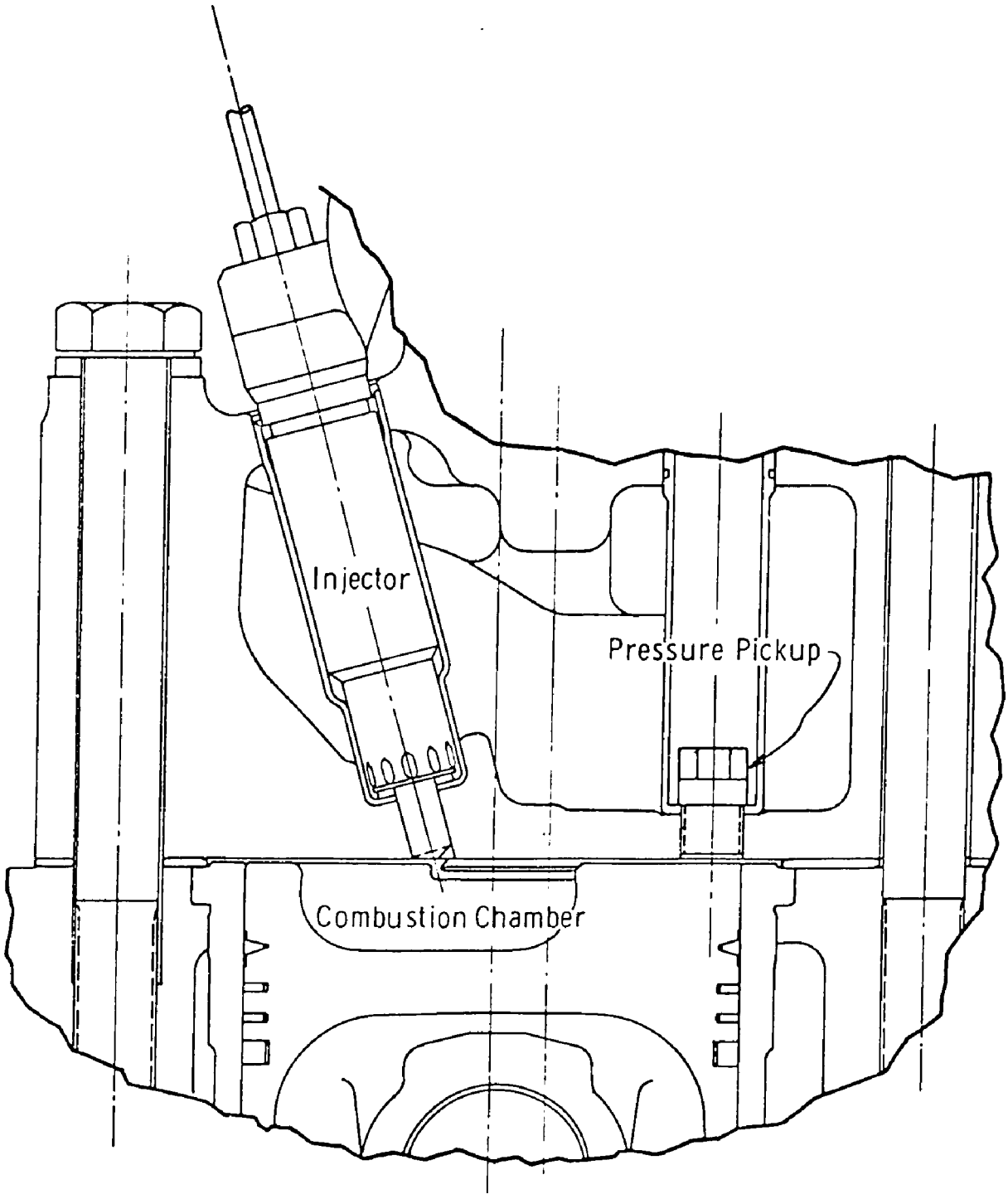


Figure 2.13 Open-Chamber Combustion System Showing Details of Pressure Pick-up and Injector Location

of electronically sensing distances from a conductive surface to its sensor head. The equipment consists essentially of a Model E-15 energizer, a Model D-152 distance detector and an appropriate sensor head. The sensor head contains the pick-off element and a connector lead to the detector. The distance detector contains the detection circuitry and an output to an oscilloscope as read out. The chief advantages of the Bently system include non-contacting measurement, high sensitivity, rapid response, very stable output and easy adaptability.

Figure 2.14 shows the modified nozzle holder, modified to accommodate the Bently system as well as for injector pressure measurement. Figure 2.15 shows the circuit connection for the Bently system.

2.4 Exhaust Gas Samping and Analysis

The exhaust system and exhaust sampling lines used in this investigation are shown in Figure 2.16. On leaving the engine through the exhaust valve, the exhaust gas flows through a 2 inch diameter, 12 inch long exhaust pipe, then through a mixing tank with baffles. The mixing tank has a volume of about seven times that of the engine displacement and this ensures proper mixing of the exhaust gases. The mixed exhaust gases then flow through a short 2 inch diameter pipe and into the exhaust surge tank. The gases are then exhausted into the laboratory exhaust line through a control gate valve. Three exhaust sampling probes and a smoke sampling line were initially installed. The first probe is located near the engine exhaust valve while the second is located close to the mixing tank entrance. The third probe is located after the mixing tank exit. The smoke sampling line is also located

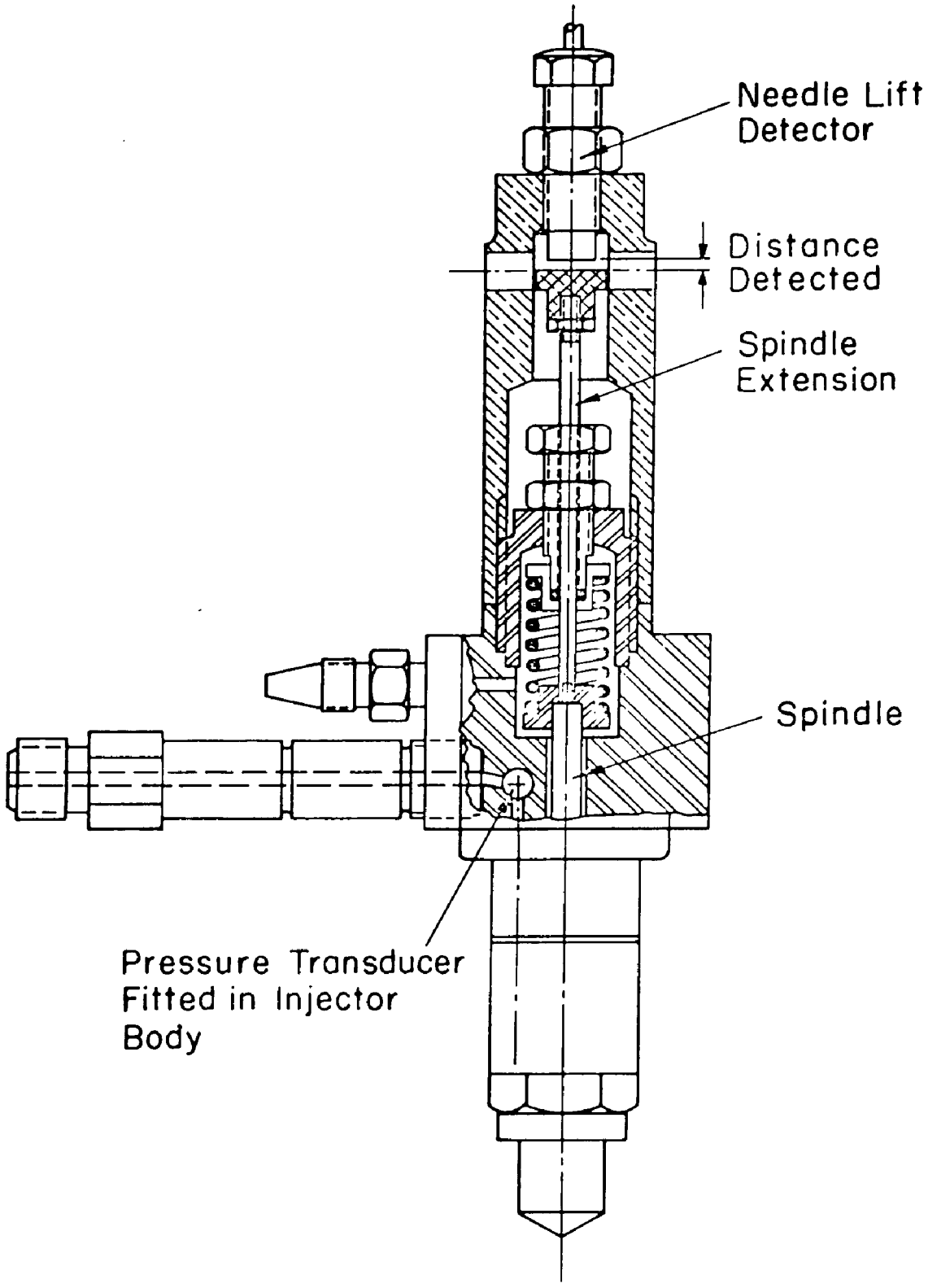


Figure 2.14 Fuel Injector Fitted with a Needle Lift Detector and a Pressure Transducer

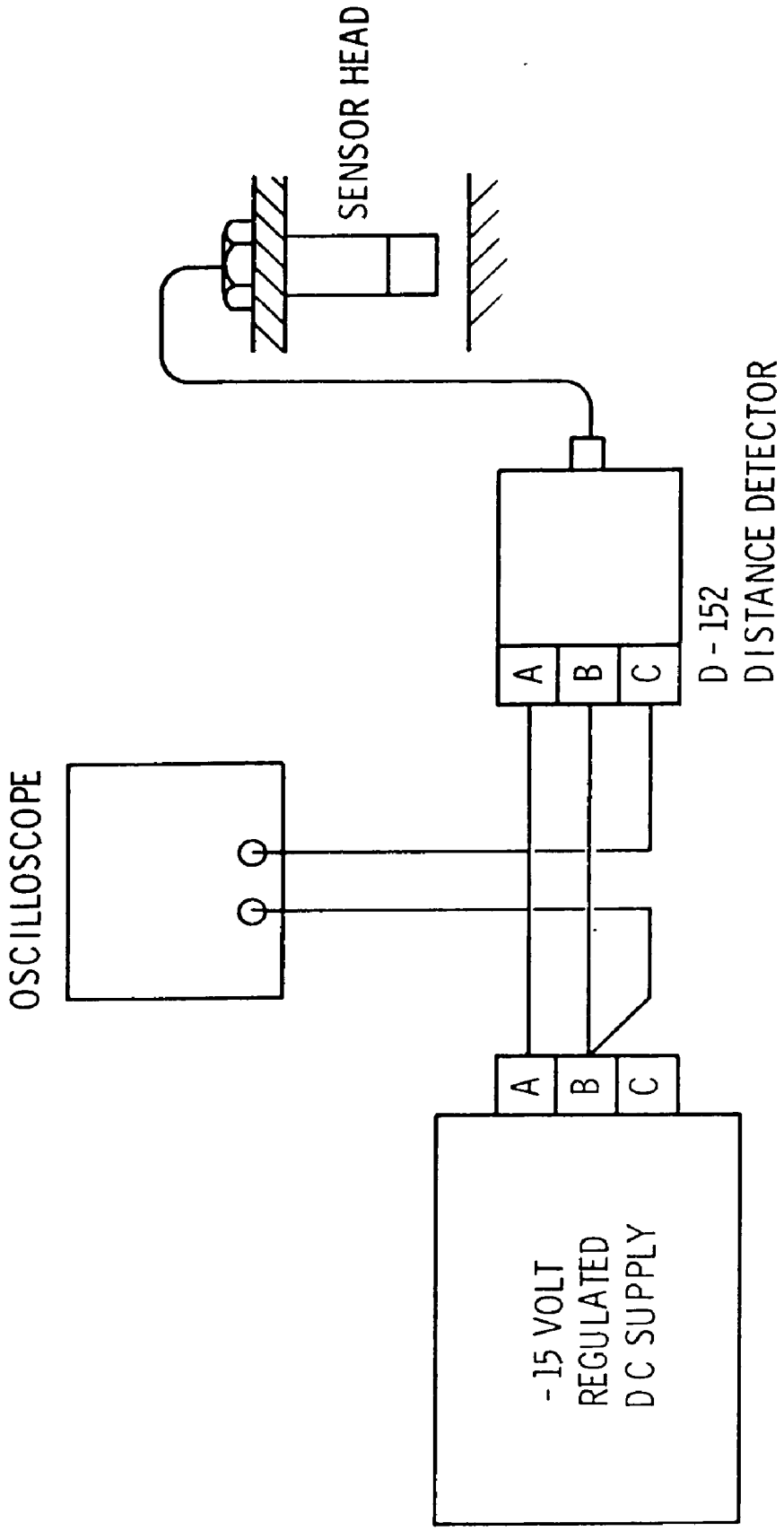


Figure 2.15 Circuitry for the Bently Distance Detector System

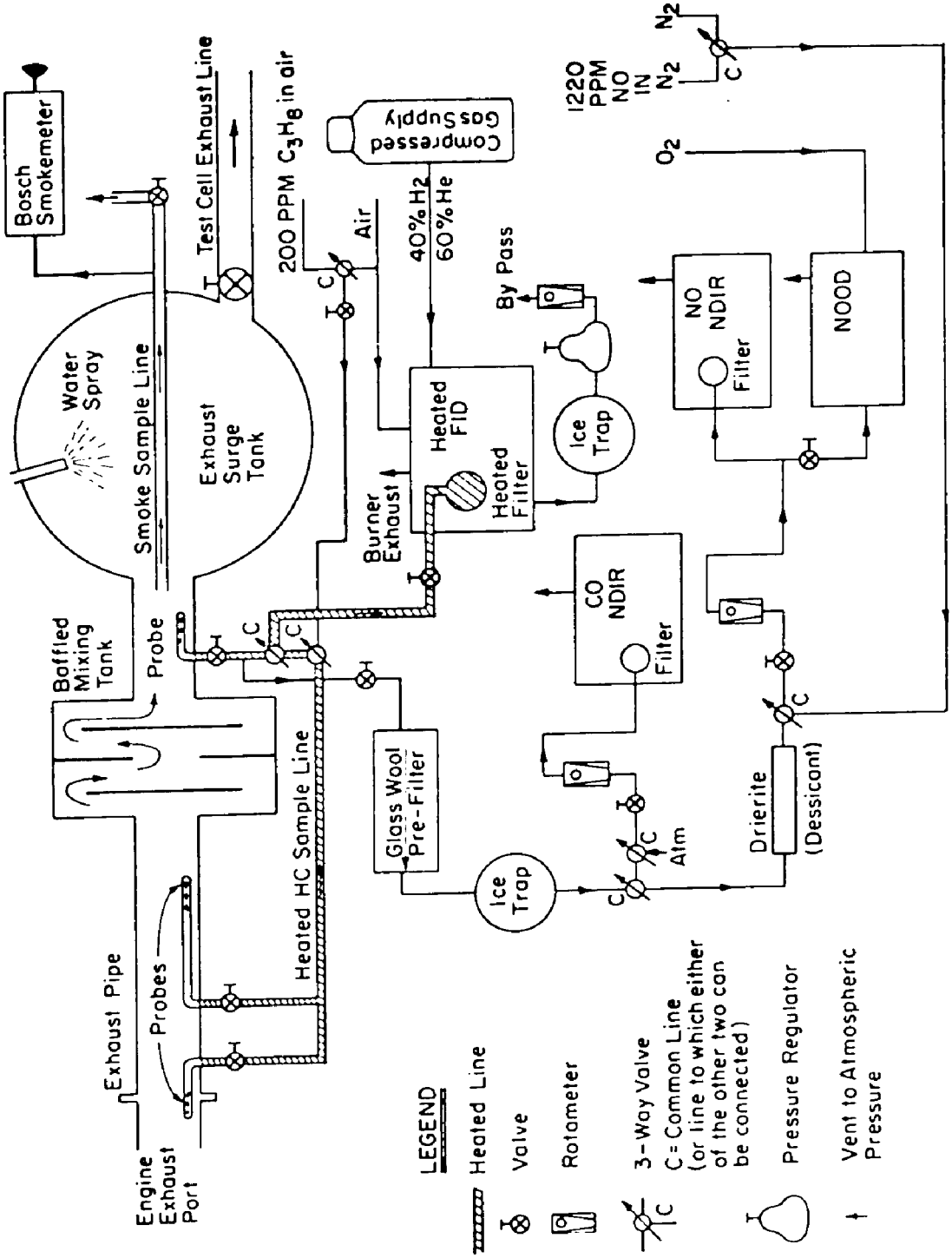


Figure 2.16 Exhaust Gas Sampling System

after the mixing tank exit.

The sampling systems, and measuring instruments for emission measurements (hydrocarbons, oxides of nitrogen, carbon monoxide and smoke) are given in the following subsections.

2.4.1 Sampling and Measurement of Hydrocarbons

The measurement of unburned hydrocarbons in the exhaust is done using a Beckman 402 heated Flame Ionization Detector (FID). An exhaust sample is drawn from one of the three probes through a heated teflon sampling line maintained at about 350°F. This temperature level is needed to prevent condensation of high molecular weight hydrocarbons commonly present in diesel engine exhaust. A metering valve located at the inlet of the FID regulates the exhaust flow rate into the detector. The detector system is completely enclosed by an oven which is maintained at 350°F. The exhaust sample, on entering the detector, flows through a glass fiber filter and is then divided into two streams, - a sample stream and a by-pass stream. The sample stream flows to the detector burner where the carbon atoms which are chemically bonded to hydrogen are ionized. The carbon ions are then counted. The number of the carbon ions is proportional to the hydrocarbon content of exhaust gas. The by-pass stream flows out of the oven through an ice trap, a pressure regulator, and a rotameter before being exhausted into the laboratory exhaust system. The pressure regulator is set for 5 psi gage pressure and the rotameter for a flow rate of 6 cu.ft. per hour. Figure 2.17 shows a schematic of the Beckman 402 FID detector. The detector burner uses a mixture of 40% hydrogen and 60% helium as the fuel and high purity air as the oxidant. Pure

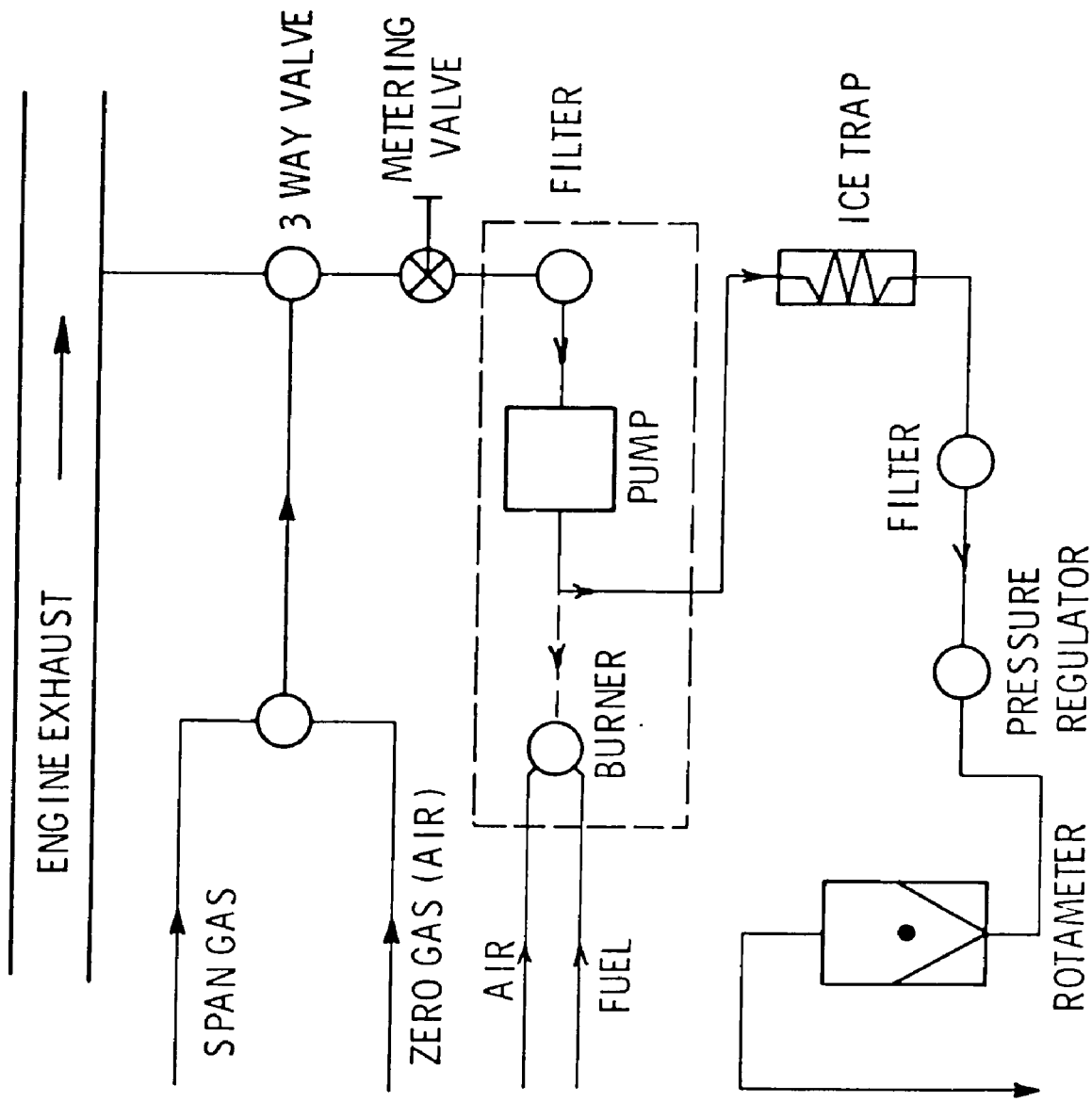


Figure 2.17 Schematic Representation of the FID Instrument

air is used to calibrate the instrument for the zero point, while a mixture of 186 parts per million propane in air is used for the span. To improve the accuracy of the calibration, the zero, the span, and the exhaust sample gases enter the detector from the same line. The effect therefore of any sample line contamination is then negated in the calibration.

Samples of unburned hydrocarbon were initially taken at three different locations from the three sample probes. Tests showed that, in general, the readings from the first and second probes were identical while readings from the third were always different from the other two. Figure 2.18 shows typical hydrocarbon measurements obtained using the first and third probes.

Two main observations could be made from these measurements. The hydrocarbon measurements using the third probe which is located after the mixing tank peaks at a fuel-air ratio of about .04 while those from the first probe located at the engine exhaust valve increase continuously with fuel-air ratio. The peak is believed to result from hydrocarbon oxidation in the mixing tank. This oxidation reaction is negligible at exhaust temperatures below 900°F, but at temperatures above 900°F, (which corresponds to fuel-air ratios of .04 and higher) the oxidation reaction is significant and results in a reading less than the actual value. The next observation is that the hydrocarbon readings from the first probe are in general less than those from the third probe. These two observations posed the problem of how does one get a representative sample of the exhaust.

Due to pulsating flow and uneven distribution of hydrocarbon concentration in the exhaust gas, it seems reasonable to expect

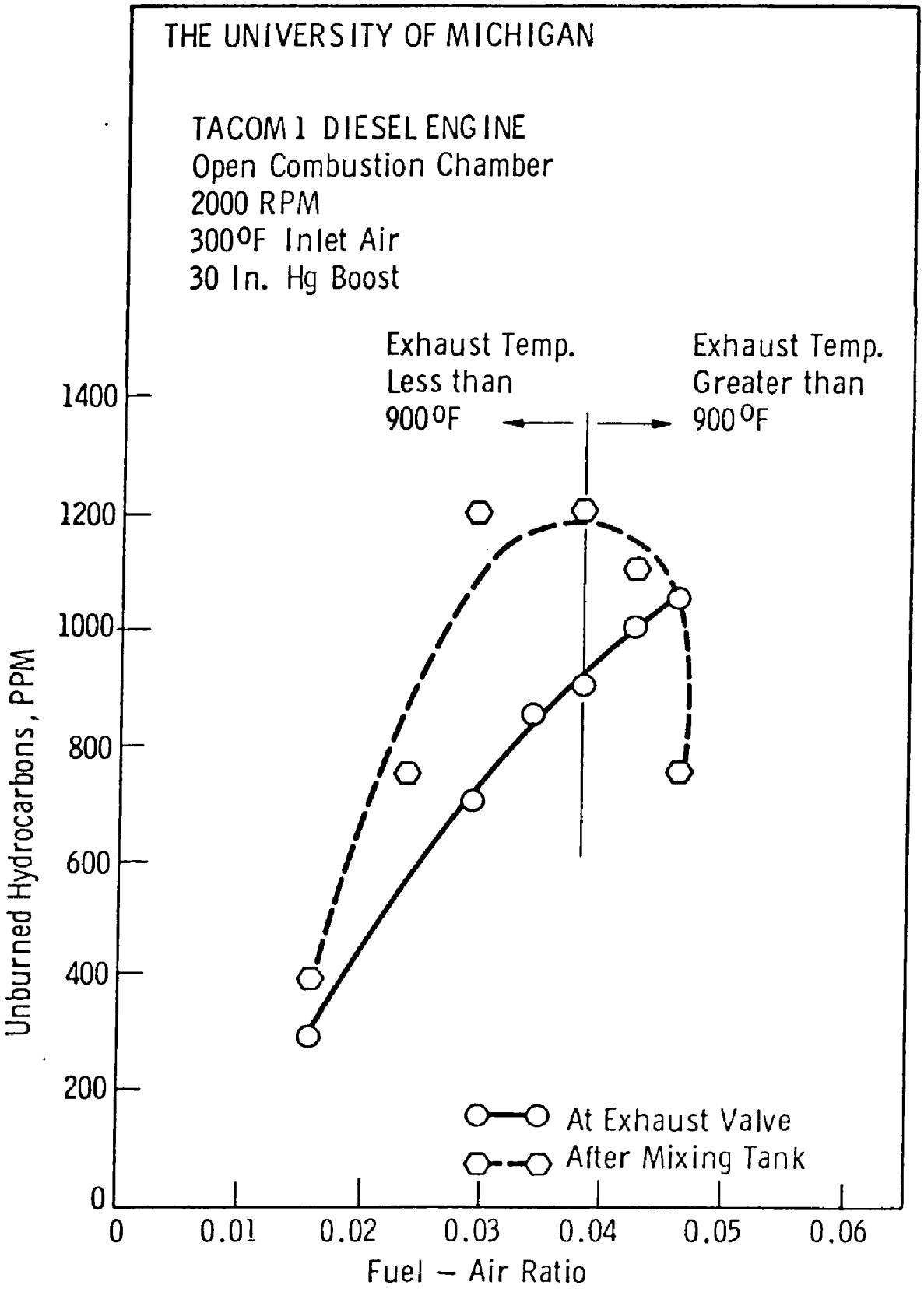


Figure 2.18 Effect of Sample Probe Location on Unburned Hydrocarbon Measurement

hydrocarbon concentration to vary along the length of the exhaust pipe as well as to vary with time or crank angle. Hence sampling from a single point in the exhaust system would not give a true or representative sample of the entire exhaust sample. One way of overcoming this problem is to insert probes all along the length of the exhaust pipe and obtain continuous hydrocarbon concentration at all the points over a period of one cycle. What one gets in essence is hydrocarbon concentration as a function of time and length from the exhaust ports, C(t,x). The representative hydrocarbon concentration is then obtained by graphical integration as follows.

$$C = \frac{\int_0^T \int_0^L C(t,x)\, dx\, dt}{T\, L}$$

where T is the time for one cycle, and L is the length of the exhaust pipe. The sample obtained after the mixing tank is in a way an integrated sample and so from the above considerations should be more representative of the exhaust sample than the sample from any other point in the exhaust pipe. For this reason, the hydrocarbon data presented in this thesis represent data obtained using the probe located at the exit of the mixing data.

2.4.2 Sampling and Measurement of Nitric Oxide

Two methods which permit a fast and accurate determination of nitric oxide in the diesel exhaust are the Nitric Oxide Optical Detector (NOOD) and the Non-Dispersive Infrared Analyzer (NDIR).

The basic design of the NOOD chemiluminescent system is given in Figure 2.19. The chemiluminescent detector utilizes the reaction of

ozone and nitric oxide.

$$NO + O_3 \longrightarrow NO_2 + O_2 + h\nu$$

When nitric oxide reacts with ozone, NO_2 and O_2 are produced. About 10 percent of the NO_2 is electronically excited and in its transition to the ground state, it yields a detectable light emission. To measure NO concentration, the gas sample to be analyzed is blended with O_3 in a flow reactor. The resulting chemiluminescence is monitored through an optical filter by a highly sensitive photomultiplier at the end of the reactor. The filter-photomultiplier combination responds to light in a narrow wave length band unique only to the above reaction and hence is not subject to interference or distortion. The output of the photomultiplier is linearly proportional to the NO concentration in the gas sample. The NOOD had a range of 0 to 3000 parts per million.

The design on the NDIR analyzer is given in Figure 2.20. The NDIR analyzer utilizes the differential absorption of infrared energy by two columns of gas in two cells with transparent windows. One cell contains a continuous stream, the sample gas to be analyzed and the other cell contains a reference gas. The reference gas is chosen for its minimal ability to absorb infrared energy of those wave lengths absorbed by the component of interest. For NO detection, the reference gas used is nitrogen. Two infrared energy sources are positioned one at the end of each cell, and energy detectors are positioned at the other end. The amount of energy through each cell is measured and the difference which is due to the absorption by the NO in the sample gas is proportional to the concentration of NO in the gas sample. The

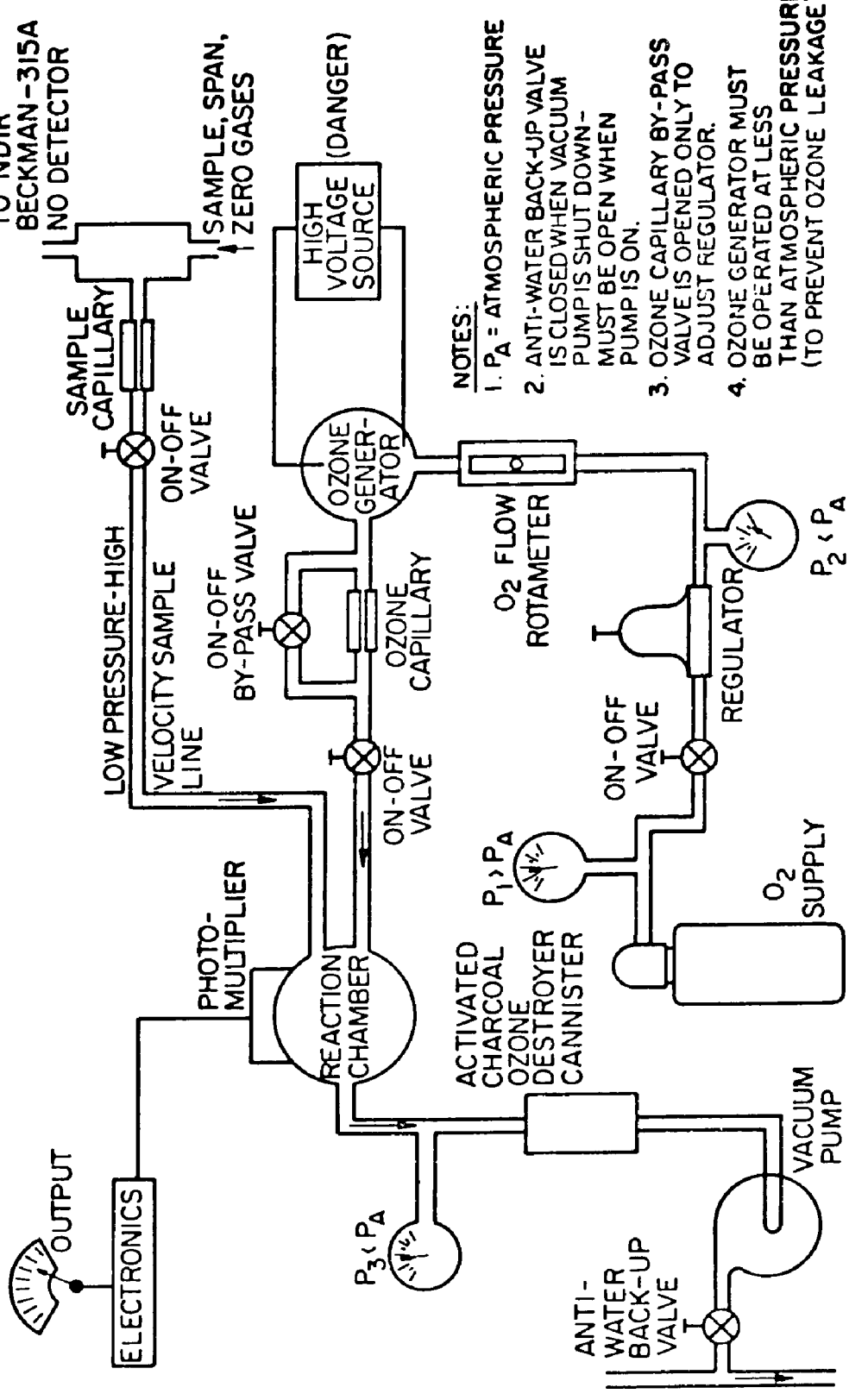


Figure 2.19 Schematic Representation of the NOOD Instrument

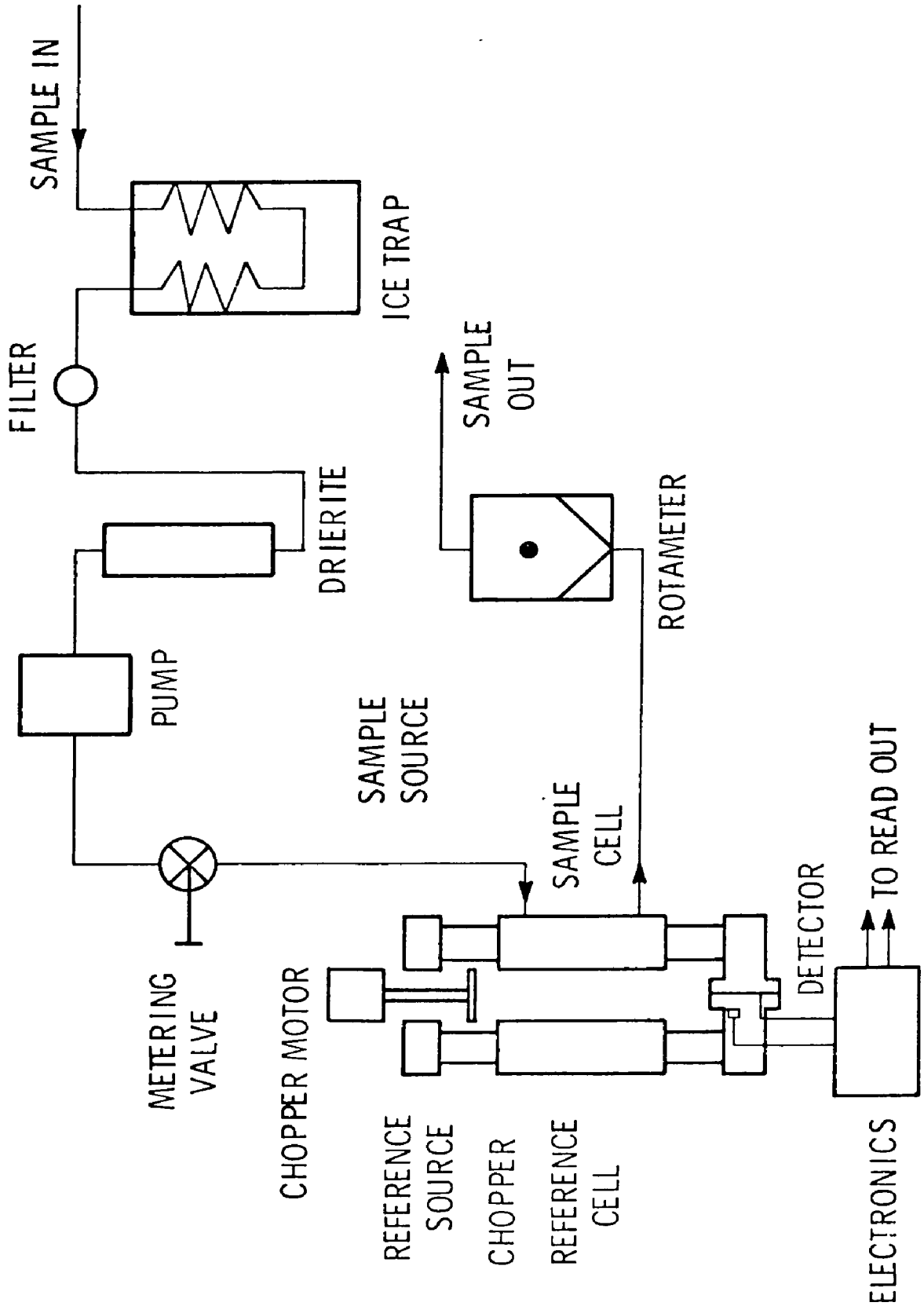


Figure 2.20 Schematic Representation of the NDIR Instrument

NDIR analyzer has a range of 0 to 4000 parts per million.

The exhaust gas samples for NO measurement are drawn from the probe downstream of the baffled mixing tank. The sample is passed through a stainless steel sample line to a glass wool packed filter of about 70 $in.^3$ volume. The filter helps keep the optical systems of the instruments as well as the capillary of the NOOD free of dirt which could affect instrument calibration. The sample is next passed through an ice trap to condense out the water in the sample. It is absolutely essential to remove all water from the exhaust sample because water vapor absorbs infrared light in the same frequency band as NO and therefore if present will cause errors in the NO reading of the NDIR instrument. Any NO_2 in the sample is removed by the water, however, since the trap is near the sample probe, there is very little NO_2 in the sample at this stage. From here, the sample is passed through a desiccant chamber filled with drierite to dry the gas. A metering valve and a rotameter allow the sample flow rate to both the NOOD and NDIR instruments to be set and maintained at a total flow rate of 5 cubic feet per hour. Dry span and zero gases of 1220 parts per million NO in nitrogen and pure nitrogen respectively are introduced upstream of the metering valve, and can be fed to the instruments in exactly the same manner as the exhaust sample gas. The span and zero gases are used to calibrate the instruments. NO readings from the exhaust were taken using the above two methods and it was observed that the readings obtained from both instruments varies with the flow rate of the exhaust gas through the instruments. A typical test result is shown in Figure 2.21. It was also observed that when NO in nitrogen span gas flowed through both instruments the response does not vary with flow rate. It was

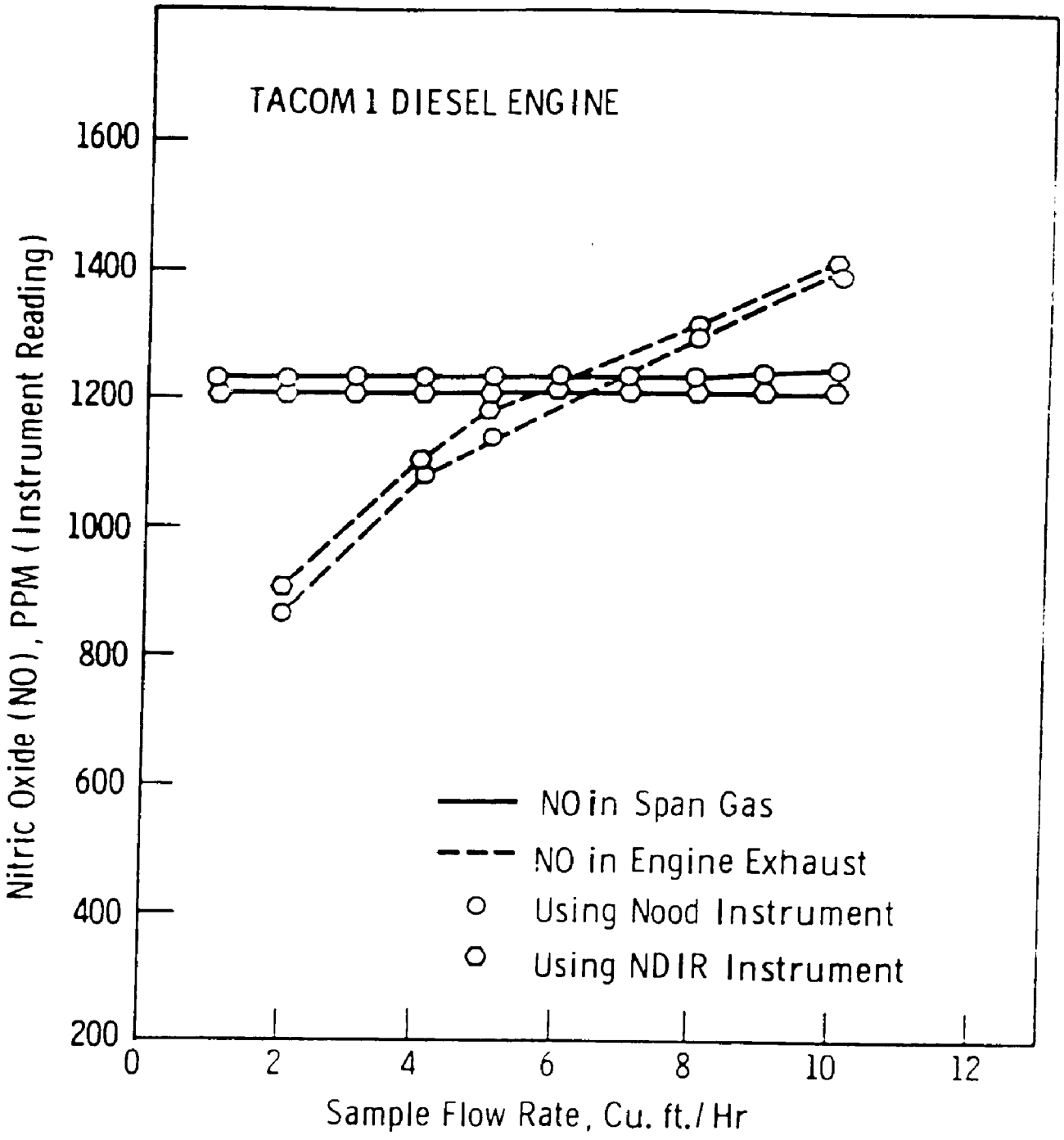


Figure 2.21 Effect of Sample Flow Rate on NO Measurement

therefore believed that the dependence of the NO reading on the flow rate is due to the oxidation of some of the NO in the exhaust sample line. Since there is always excess oxygen available in the diesel exhaust, a low flow rate would mean a long residence time for the exhaust gases in the sample line. For a sample flow rate of 5 cu. ft. per hour, the exhaust gas residence time in the exhaust line after it passes the ice trap is about 88 seconds. This time is much longer than the time required to reach equilibrum between NO, NO_2, O_2 and the other exhaust products at the low exhaust gas temperatures. Some NO will therefore be oxidized according to the following reaction:

$$NO + 1/2\ O_2 \longrightarrow NO_2$$

This will result in a low NO reading.

To detect NO_2 a thermal converter is needed to dissociate the NO_2 to NO by the bimolecular reaction, $2\ NO_2 \longrightarrow 2\ NO + O_2$. The total NO can then be measured in the NOOD.

The equilibrium ratio, for the $NO_2 \rightleftharpoons NO + 1/2\ O_2$ reaction is a function of both temperature and pressure. The reaction proceeds more to the right as temperature increases and as pressure decreases. It is known from studies by Breitenbach and Shelef (9), 1973, that at low pressures less than 5 torr, 98 percent conversion is achieved at about 900°F. With the aid of catalysts, such as stainless steels, molybdenum, and carbon, reasonably complete conversion can be achieved at slightly lower temperatures. Figure 2.22 shows percent conversion versus temperature at fixed pressure of 10 torr, using two different catalysts, stainless steel and molybdenum. Most thermal converters will also oxidize ammonia to NO by the following reaction: $4\ NH_3 + 5\ O_2 \longrightarrow 4\ NO + 6H_2O$ Since there is very little ammonia in diesel exhaust, this reaction

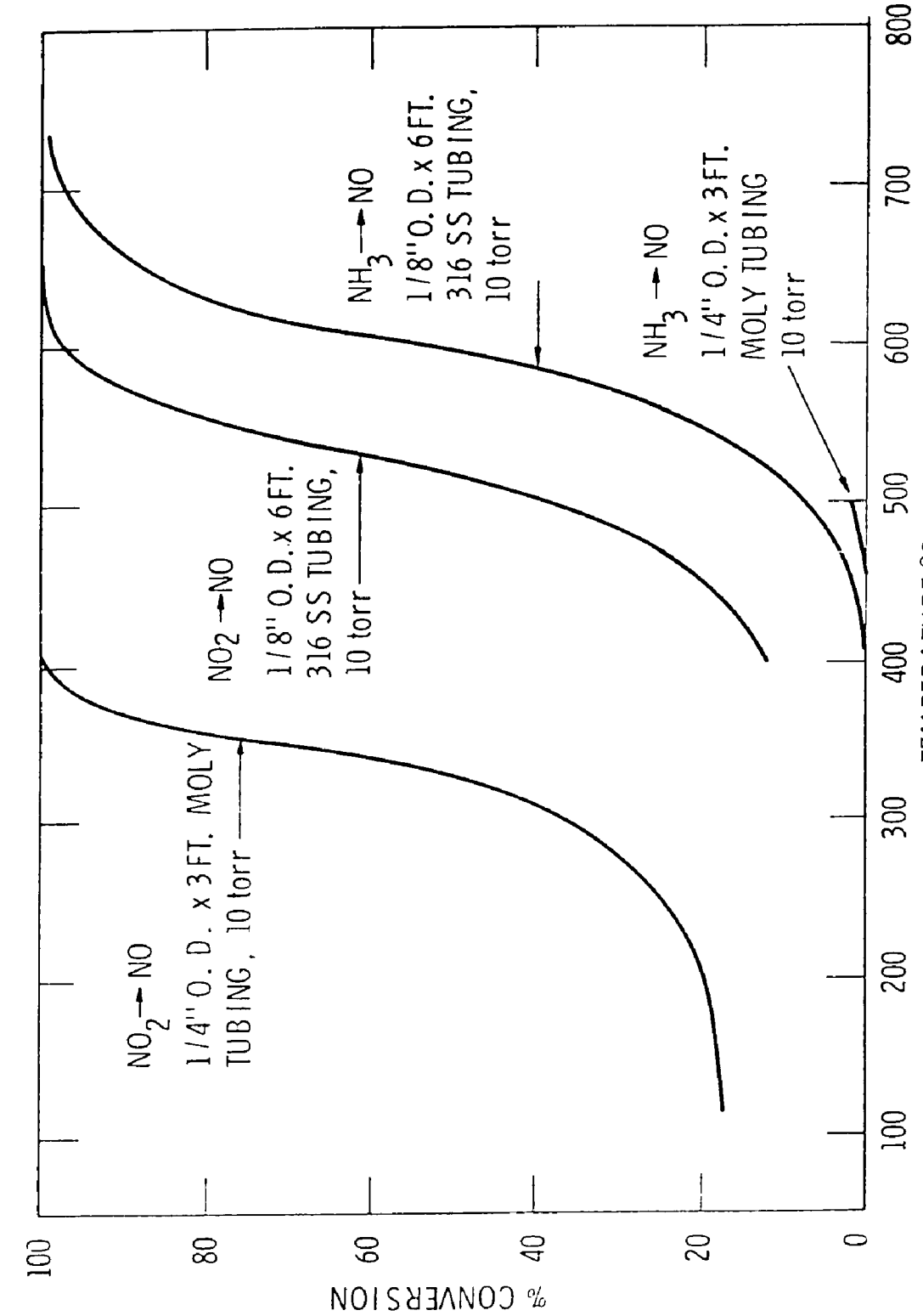


Figure 2.22 Effect of Temperature and Material on Percent Conversion of NO_2 to NO, and NH_3 to NO

will be neglected in this work.

The converter used for this study consists of a 6 foot long stainless steel tube of 1/4 inch outside diameter and 1/8 inch inside diameter which is electrically heated by a low voltage high current supply. The converter is used downstream of the NOOD capillary where the pressure is low. Figure 2,23 shows details of the converter.

2.4.3 Sampling and Measurement of Carbon Monoxide

Samples for the analysis of carbon monoxide are taken through the same line as the nitric oxide as described in the previous subsection. The flow rate for the carbon monoxide sampling is maintained at 5 cubic feet per hour, even though it was observed that the reading from the instrument does not vary significantly with sample flow rate.

The instrument used for the CO analysis is a Horiba Model MEXA-122 NDIR CO analyzer with a range of 0 to 5% CO. Calibration is accomplished by using atmospheric air as zero gas, and pressurized cans of 5% CO in N_2 as span gas.

2.4.4 Smoke Sampling and Measurement

The smoke in the exhaust sample is measured using a Robert Bosch smoke meter. It consists of a sampling probe, a pump model EFAW65A and an optical measuring instrument model EFA68A. The smoke sample is taken by drawing a constant volume of exhaust gas through a paper filter disk. This is accomplished by pneumatically releasing a spring loaded piston in the pump unit. The volume of the sample drawn is always equal to the displacement of the pump piston. The filter disk, darkened by trapped carbon particles from the exhaust gas which passed through it, is then optically analyzed by photo-

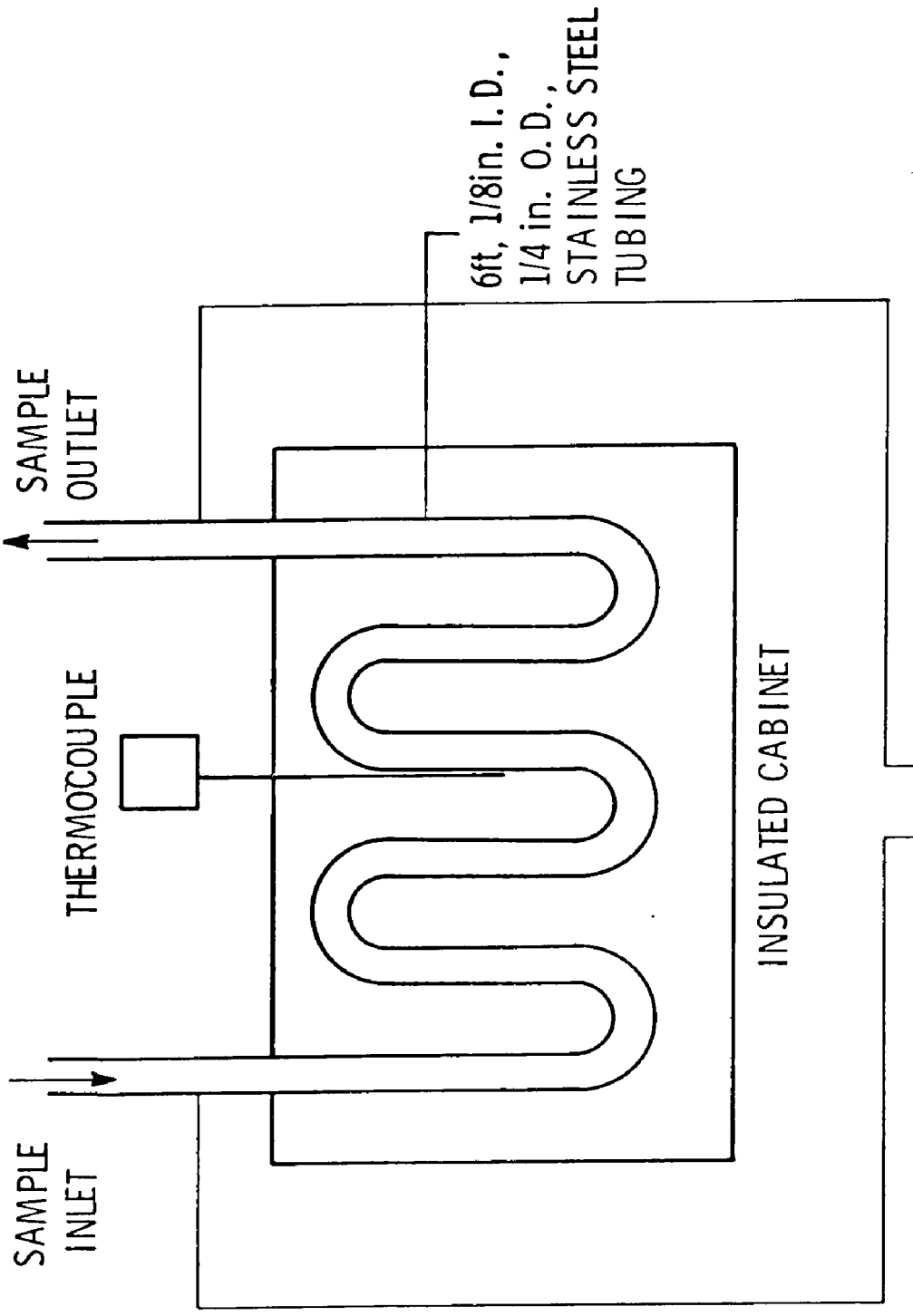


Figure 2.23 Details of the NO Converter

electrically measuring the degree of darkening of the filter. The smoke level is read from a microammeter which is calibrated from 0 to 10. The 0 corresponds to an absolute white disk while 10 corresponds to a completely blackened disk from very high smoke. Smoke readings obtained were very reproducible. Schematic representatives of the exhaust smoke sample system and smoke probe are found in Figures 2.24 and 2.25.

The following procedure was used in taking smoke readings.

a. The sample probe is cleaned and high-pressure exhaust gas sample is blown through the sample pipe in order to minimize the effect of carbon deposits left in the sample line.
b. The sample probe is placed in position
c. The valve in the sample pipe is regulated to give a small positive exhaust gas pressure at the probe
d. A clean filter disk is placed in the pump and a sample is drawn by squeezing the bulb
e. The sample valve is closed and the filter is removed and analyzed.

The smoke readings obtained using this procedure were repeatable in most cases. This is in contrast to the previously used Hartridge smoke meter which had a tendency to lose its calibration as carbon deposits accumulated in the sample cell and optical instruments.

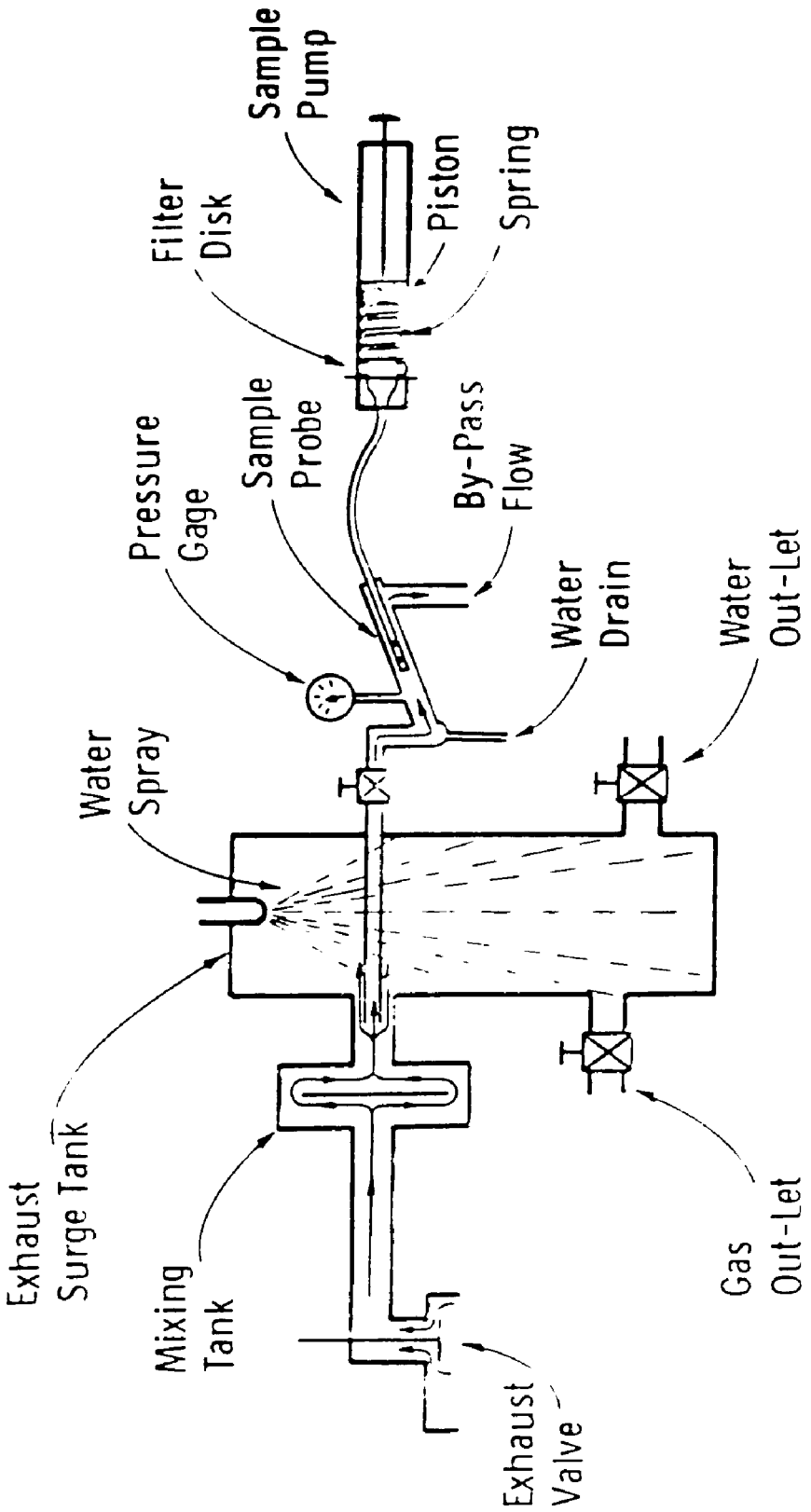


Figure 2.24 Schematic Representation of Smoke Sampling System

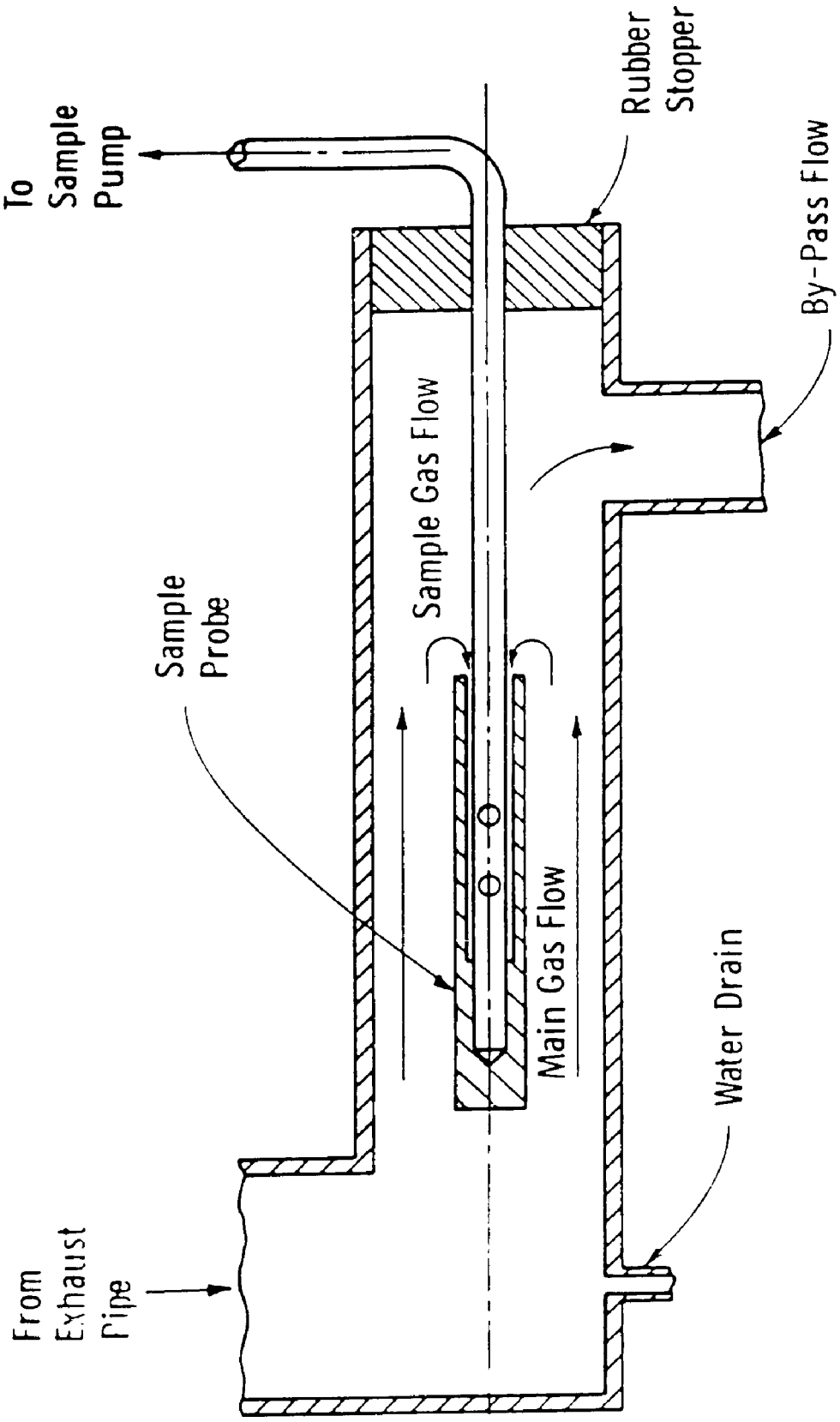


Figure 2.25 Schematic Representation of Smoke Sample Probe

CHAPTER III

EXPERIMENTAL RESULTS - FUEL INJECTION

3.1 Computation of the Rate of Injection

Careful consideration was given to the computation of rate of injection because for this study, it is critical to know how much fuel is injected as secondary injection, and how much fuel is injected during the main injection period. The rate of injection is computed from experimental measurements of transient pressures at the injector nozzle and combustion chamber, and measurements of the injector needle lift. The flow area consists of the needle seat orifice and the injector nozzle holes, both being separated by the nozzle sac. The flow area is therefore considered as two orifices in series. The area of the needle seat orifice and volume of the nozzle sac are both functions of needle lift and consequently the effective or equivalent flow area of the system is a function of this needle lift.

Figure 3.1 shows the actual configuration of the needle, injection body, needle seat, nozzle sac, and nozzle holes. Because of the volumes involved, for flow calculations, both the combustion chamber and injector delivery chamber are considered as infinite reservoirs while the nozzle sac is considered as a finite reservoir. The rate of injection and effective flow area are then calculated as follows for the prevalent unsteady flows.

Bernoulli's equation at a path along the needle seat orifice gives

$$\frac{V_n^2}{2} + L_n \frac{dV_n}{dt} = \frac{P_f}{\rho} - \frac{P_s}{\rho}$$

Therefore

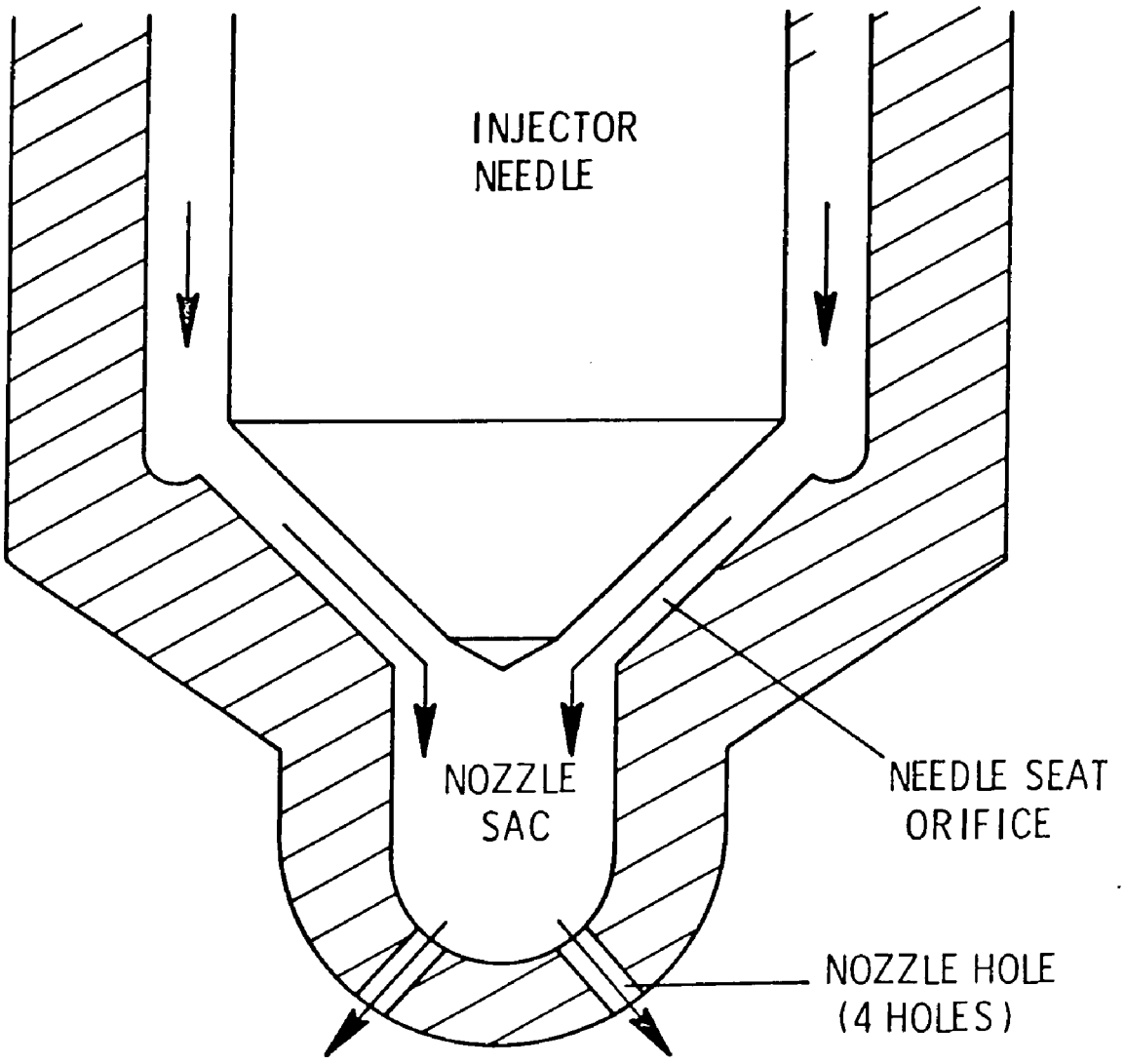


Figure 3.1 Needle Seat and Injector Holes Orifices

$$V_n = \left[2(P_f - P_s)/\rho - 2L_n \frac{dV_n}{dt} \right]^{1/2} \tag{3.1}$$

flow through needle seat orifice is

$$Q_n = C_{c_n} A_n V_n = C_{d_n} A_n \left[2(P_f - P_s)/\rho - 2L_n \frac{dV_n}{dt} \right]^{1/2} \tag{3.2}$$

Bernoulli's equation at the path along the nozzle holes is

$$\frac{V_h^2}{2} + L_h \frac{dV_h}{dt} - \frac{V_s^2}{2} = \frac{P_s}{\rho} - \frac{P_g}{\rho}$$

Therefore

$$V_h = \left[2(P_s - P_g)/\rho + V_s^2 - 2L_h \frac{dV_h}{dt} \right]^{1/2} \tag{3.3}$$

flow through nozzle holes is

$$Q_h = C_{c_h} A_h V_h = C_{d_h} A_h \left[2(P_s - P_g)/\rho + V_s^2 - 2L_h \frac{dV_h}{dt} \right]^{1/2} \tag{3.4}$$

Continuity equation at the nozzle sac is

$$\frac{V}{E} \frac{dP_s}{dt} = -\frac{dV}{dt} + Q_h - Q_n \tag{3.5}$$

flow through nozzle sac is

$$Q_s = A_s V_s \tag{3.6}$$

Assuming equal contractions in flow equations for both orifices, no time varying accumulations in the nozzle sac, the equations simplify to

$$Q_n = C_d A_n \left[2(P_f - P_s)/\rho \right]^{1/2} \tag{3.7}$$

$$Q_h = C_d A_h \left[2(P_s - P_g)/\rho + V_s^2 \right]^{1/2} \tag{3.8}$$

$$Q_h = Q_n = Q_s = A_s V_s \tag{3.9}$$

Eliminate V_s and P_s from equations (3.7), (3.8) and (3.9) to get

$$Q = C_d A_{equiv} [2(P_f - P_g)/\rho]^{1/2}$$

where

$$(1/A_{equiv})^2 = (\frac{1}{A_n})^2 + (\frac{1}{A_h})^2 - (C_d/A_s)^2$$

A coefficient of mass flow discharge is assumed and the computed cumulative flow per cycle is compared with the experimentally measured flow. Any discrepancy between these two valves is corrected for by adjusting the coefficient of discharge.

The nozzle seat area is computed as the area of revolution of the circular arc normal to both the needle and seat. This is

$$A_n = \pi \ell \sin\beta [d - \ell \sin\beta \cos\beta]$$

where

2β = tip angle of needle seat

d = nozzle sac hole diameter

ℓ = needle lift

The equivalent area of fuel flow as calculated using a discharge coefficient of .7 is shown in Figure 3.2. Typical histories of fuel pressures, needle lift and combustion chamber pressures are shown in Figures 3.3 and 3.4. Figures 3.5 and 3.6 show typical computed fuel injection schedule or rate or injection.

3.2 The Secondary Injection Survey

3.2.1 Region of Operation in Which Secondary Injection Occurs

Bradbury (8) presented a zone on a speed fuel delivery plane, Figure 1.1, which shows the region of operation in which secondary injection occurs. He defined a point X as the ideal or syster

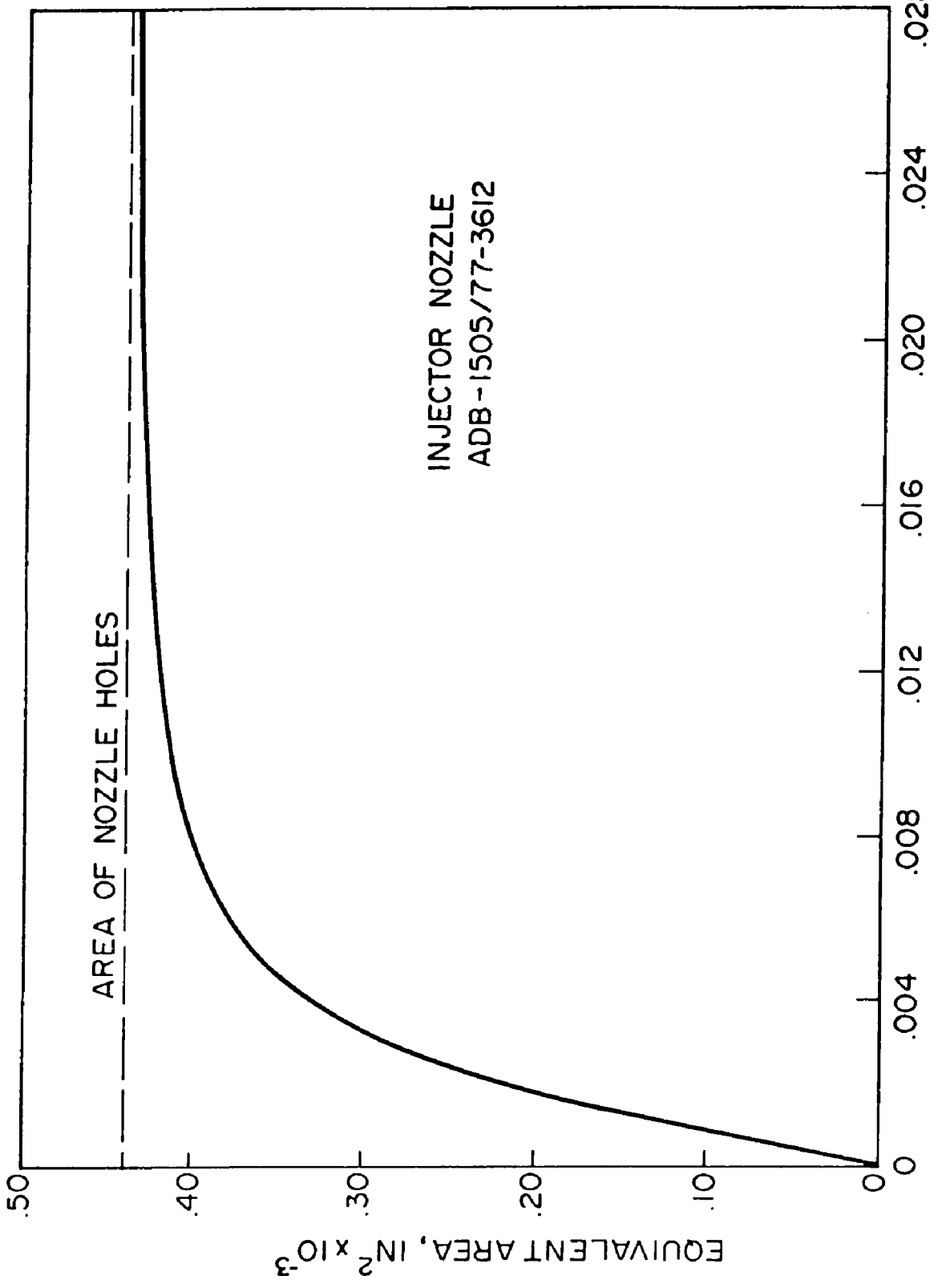


Figure 3.2 Equivalent Area for Fuel Flow Through Nozzle Orifices as a Function of Needle Lift

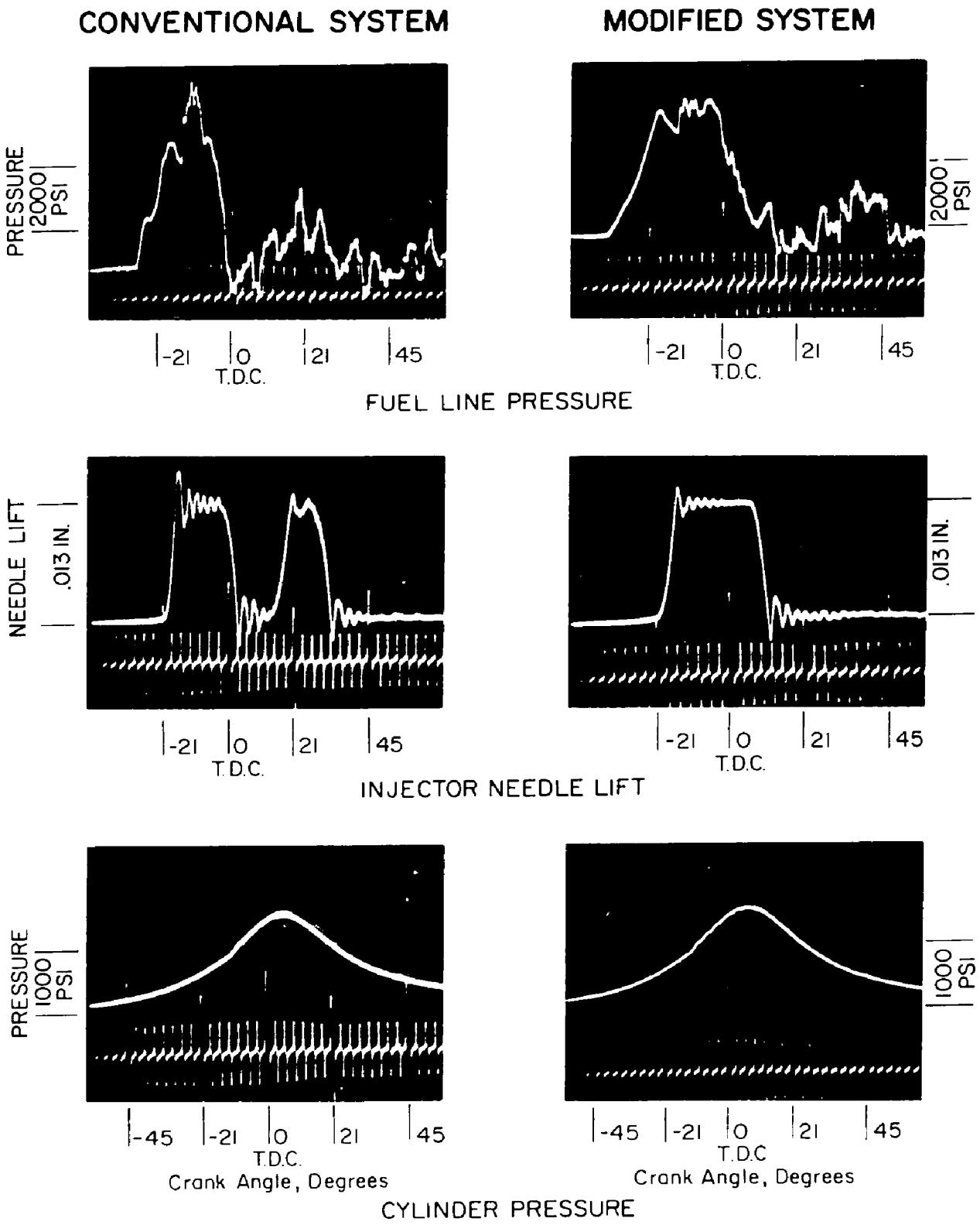


Figure 3.3 Oscilloscope Records of Transient Fuel Line Pressure, Needle Lift, and Cylinder Pressure at Engine Speed of 1800 rpm and Total Fuel-Air Ratio of .0506

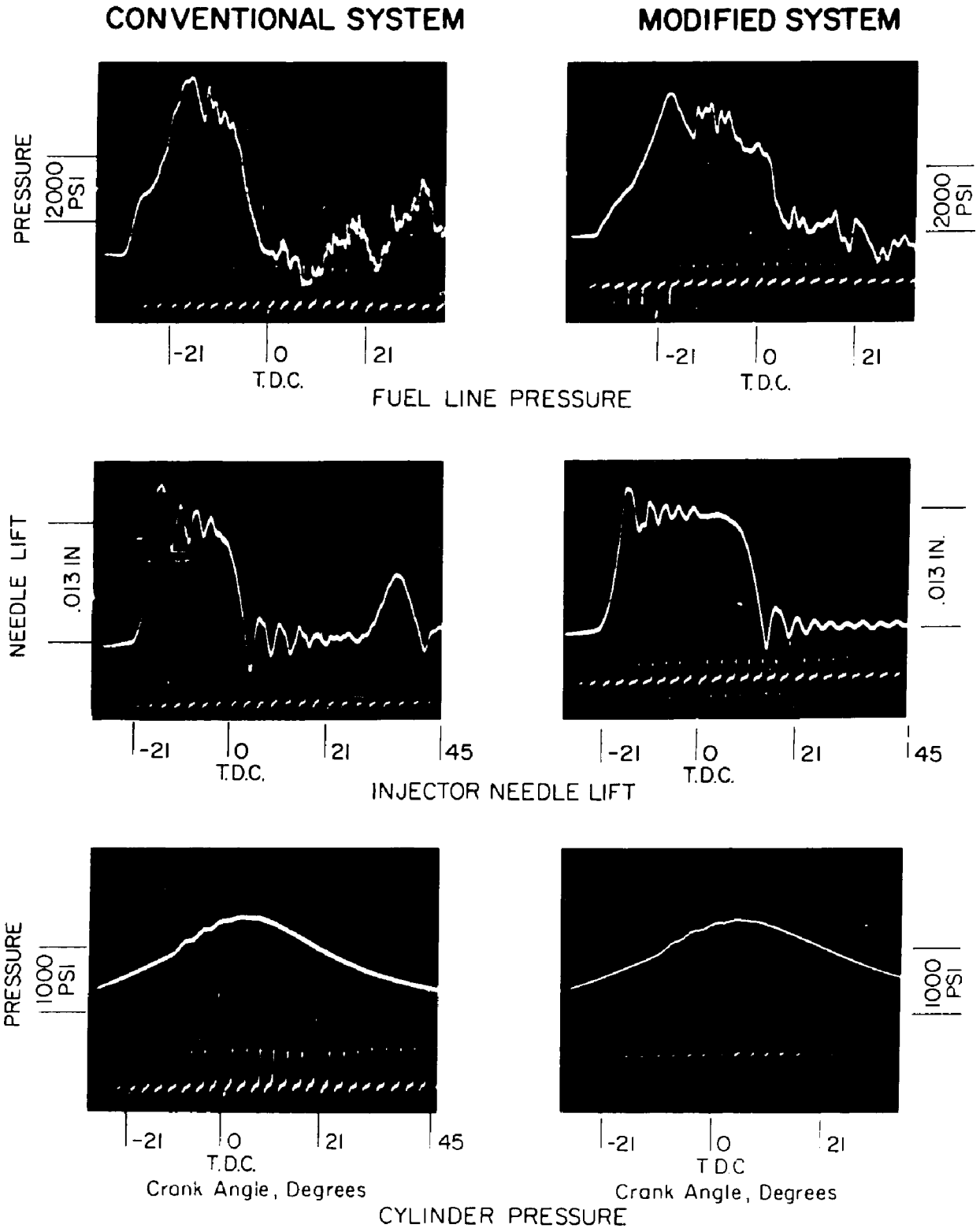


Figure 3.4 Oscilloscope Records of Transient Fuel Line Pressure, Needle Lift, and Cylinder Pressure at Engine Speed of 2400 rpm and Total Fuel-Air Ratio of .040

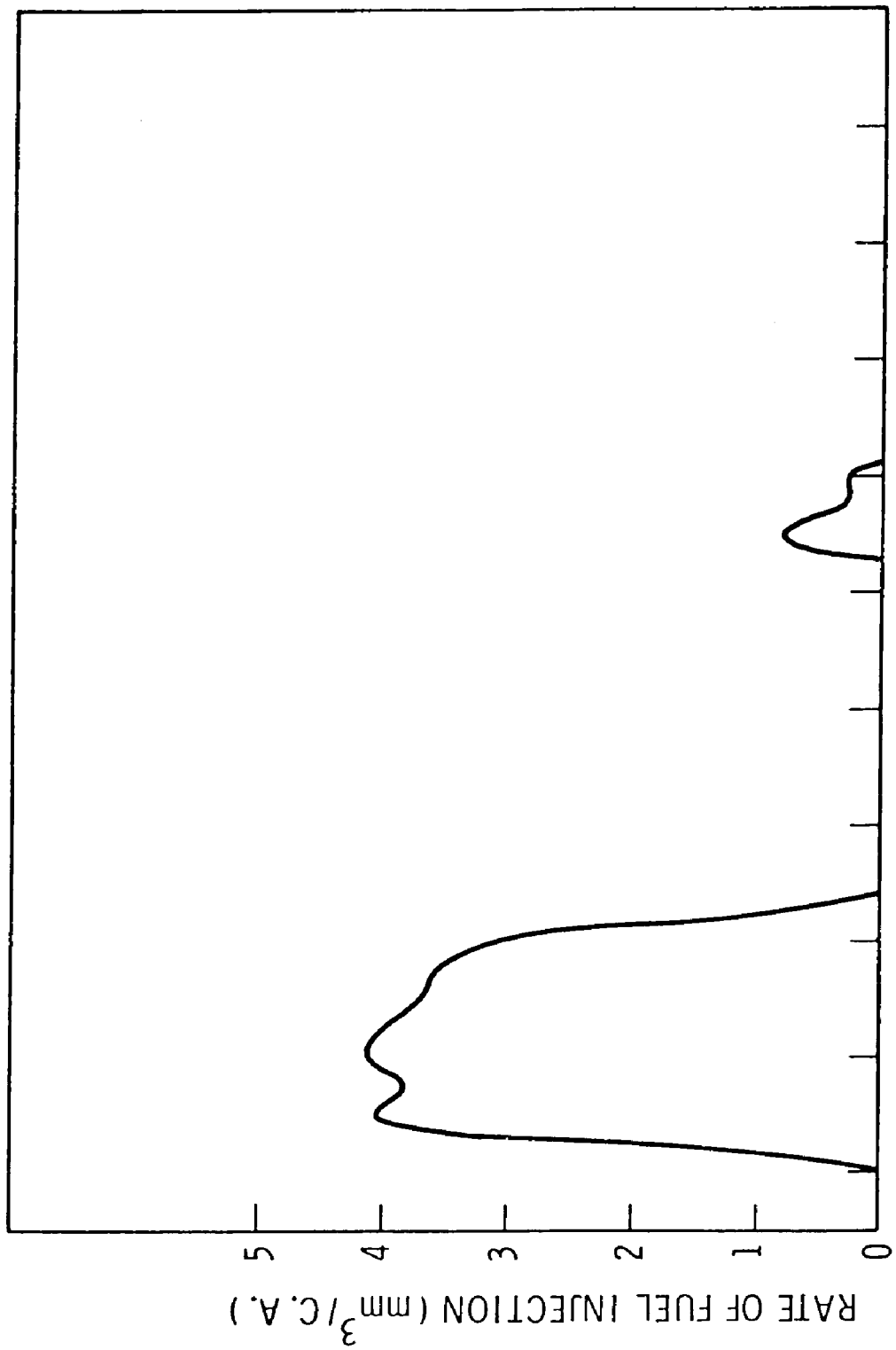


Figure 3.5 Fuel Injection Schedule for Conventional Injection System, at Engine Speed of 1200 rpm, and Total Fuel-Air Ratio of .0294.

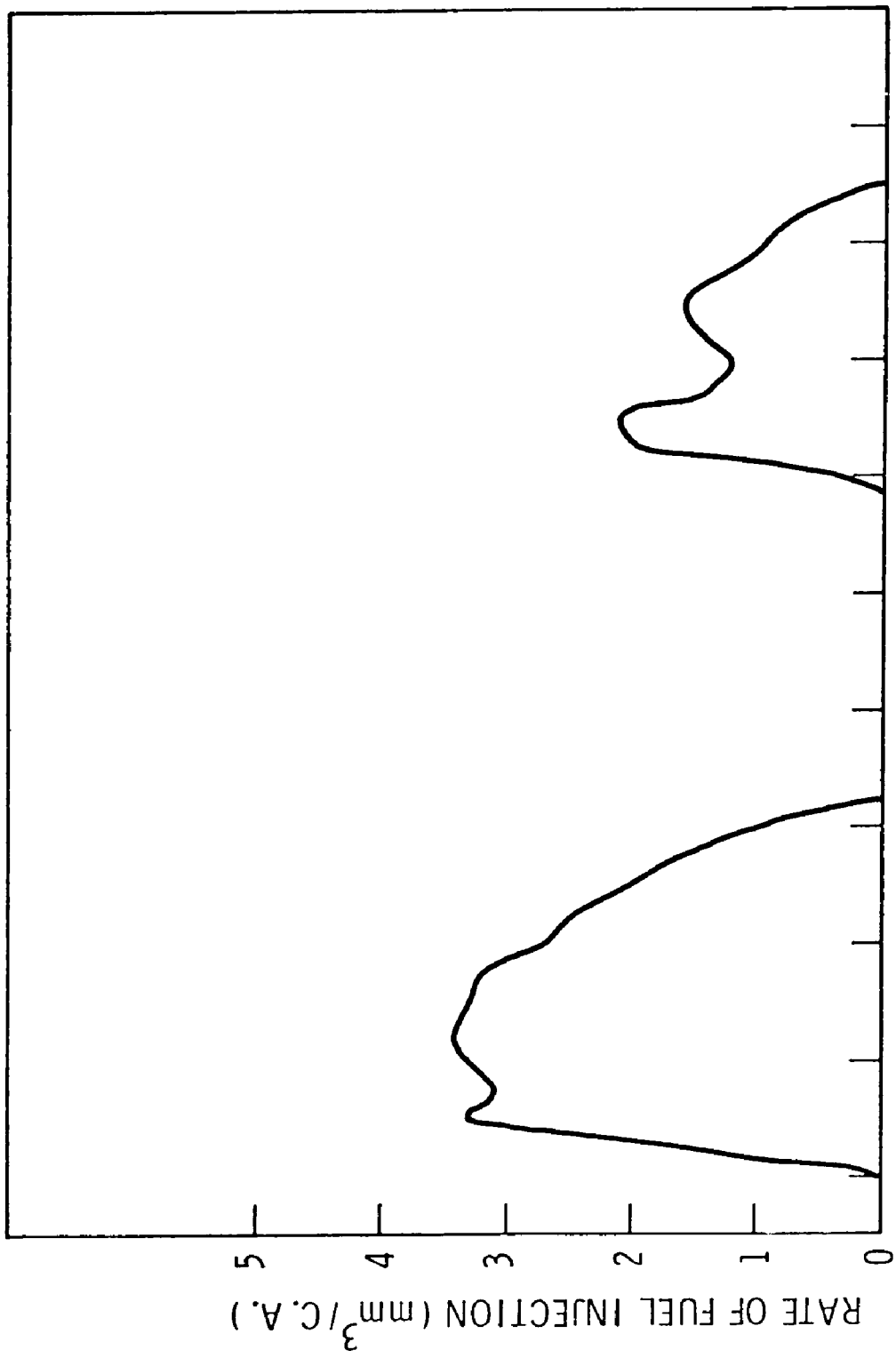


Figure 3.6 Fuel Injection Schedule for Conventional Injection System, at Engine Speed of 1800 RPM, and Total fuel-Air Ratio of .0407.

design point at which the particular fuel injection system should be operated and this point is outside the zone of secondary injection. This zone of secondary injection can be moved to right (decreased) by increasing the area of nozzle holes or to the left (increased) by decreasing the area of the nozzle holes. This same zone of secondary injection is shown in Figure 3.7 for the conventional fuel injection system used in this study. It shows that there is only a very small range of speed and load for which secondary injection does not occur. The figure also shows that for high speeds secondary injection starts occurring at low loads.

3.2.2 Magnitude of Secondary Injection and its Variation with Speed and Load

The relationship between total fuel injected over a whole cycle and fuel-air ratio is shown in Figure 3.8. It shows that the total fuel injected per cycle is a linear function of fuel-air ratio for any constant speed. We can also deduce from this figure that the total fuel injected per cycle does not vary much with speed for any constant fuel-air ratio.

The main injected fuel is defined as the fuel injected during the first needle opening and its first closing in a cycle. Figure 3.9 shows the relationship between fuel-air ratio and the quantity of fuel injected during the main injection period of one cycle. The main injected fuel is seen to increase as fuel-air ratio increases. It is of interest to note that for a fixed fuel-air ratio, the main injected fuel decreases as the speed is increased from 1200 rpm to 1800 rpm but increases as the speed is increased from 1800 rpm to 2400 rpm.

Figure 3.10 shows the relationship between fuel-air ratio and the

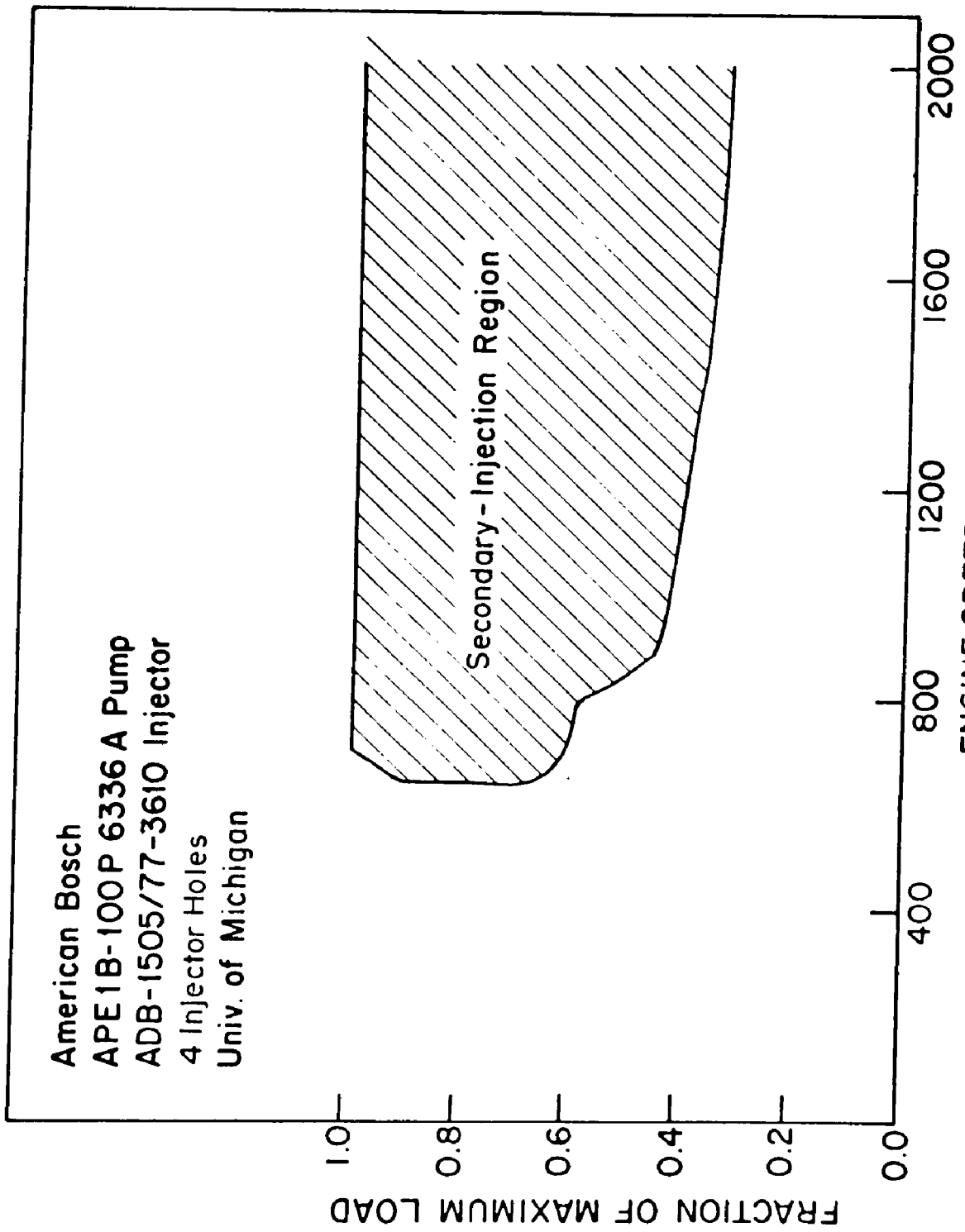


Figure 3.7 Zone of Secondary Injection in a Load, Speed Plane

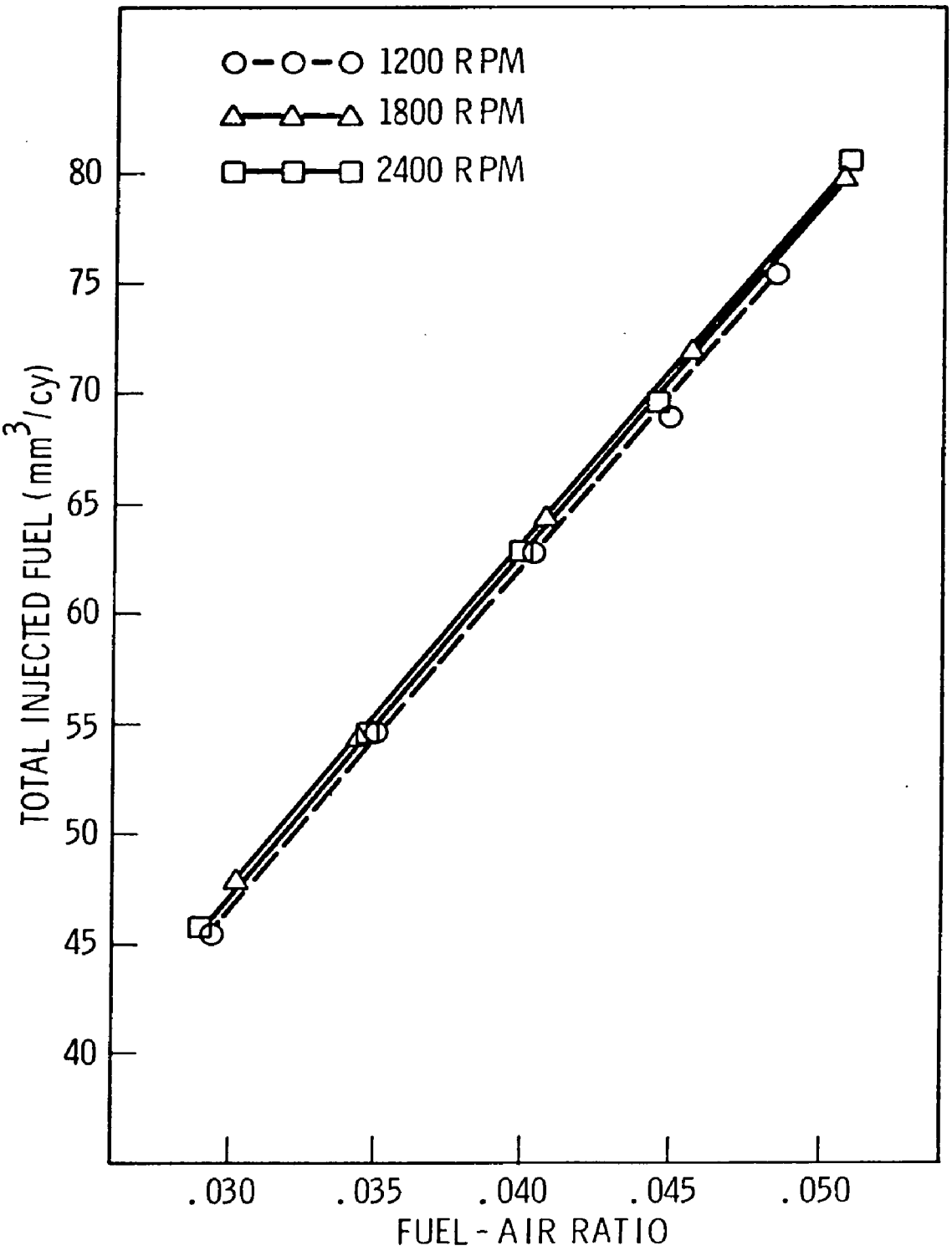


Figure 3.8 Relationship Between Total Fuel-Air Ratio and Total Fuel Injected per Cycle for Various Engine Speeds

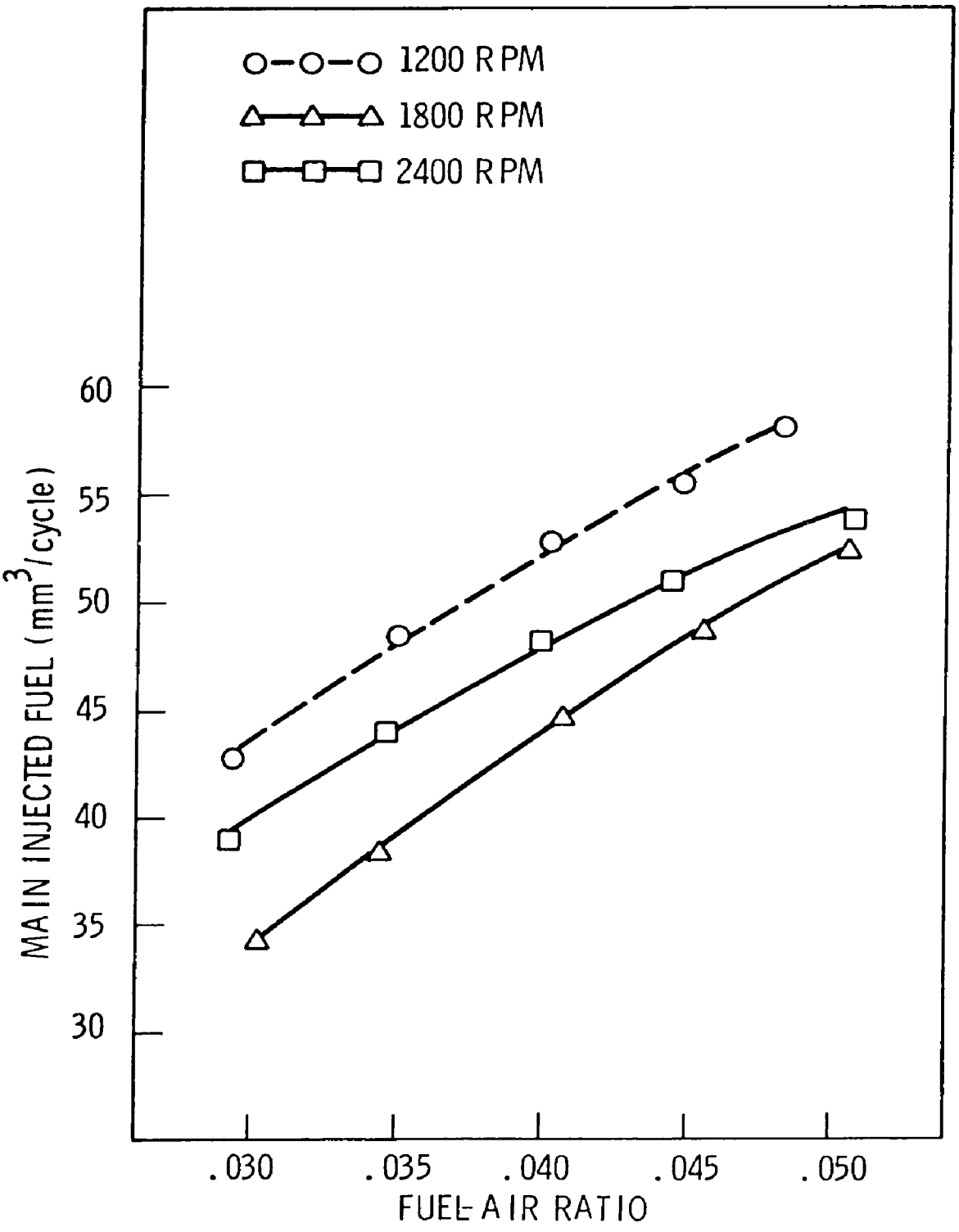


Figure 3.9 Relationship Between Total Fuel-Air Ratio and Main Injected Fuel per Cycle for Various Engine Speeds

quantity of secondary injected fuel at constant speeds of 1200 rpm, 1800 rpm, and 2400 rpm. It shows that for any constant speed, secondary injection increases with increasing fuel-air ratio. It also shows the interesting result that for a fixed fuel-air ratio, secondary injection increases as the speed is increased from 1200 rpm to 1800 rpm, but decreases as the speed is increased from 1800 rpm to 2400 rpm. This suggests that for any given fuel-air ratio, there is an optimum speed for which the secondary injected fuel per cycle is maximum.

Figure 3.11 illustrates the variation of percent secondary injection with fuel-air ratio for the constant speeds of 1200 rpm, 1800 rpm and 2400 rpm. The trends are essentially the same as those for the quantity of secondary injected fuel.

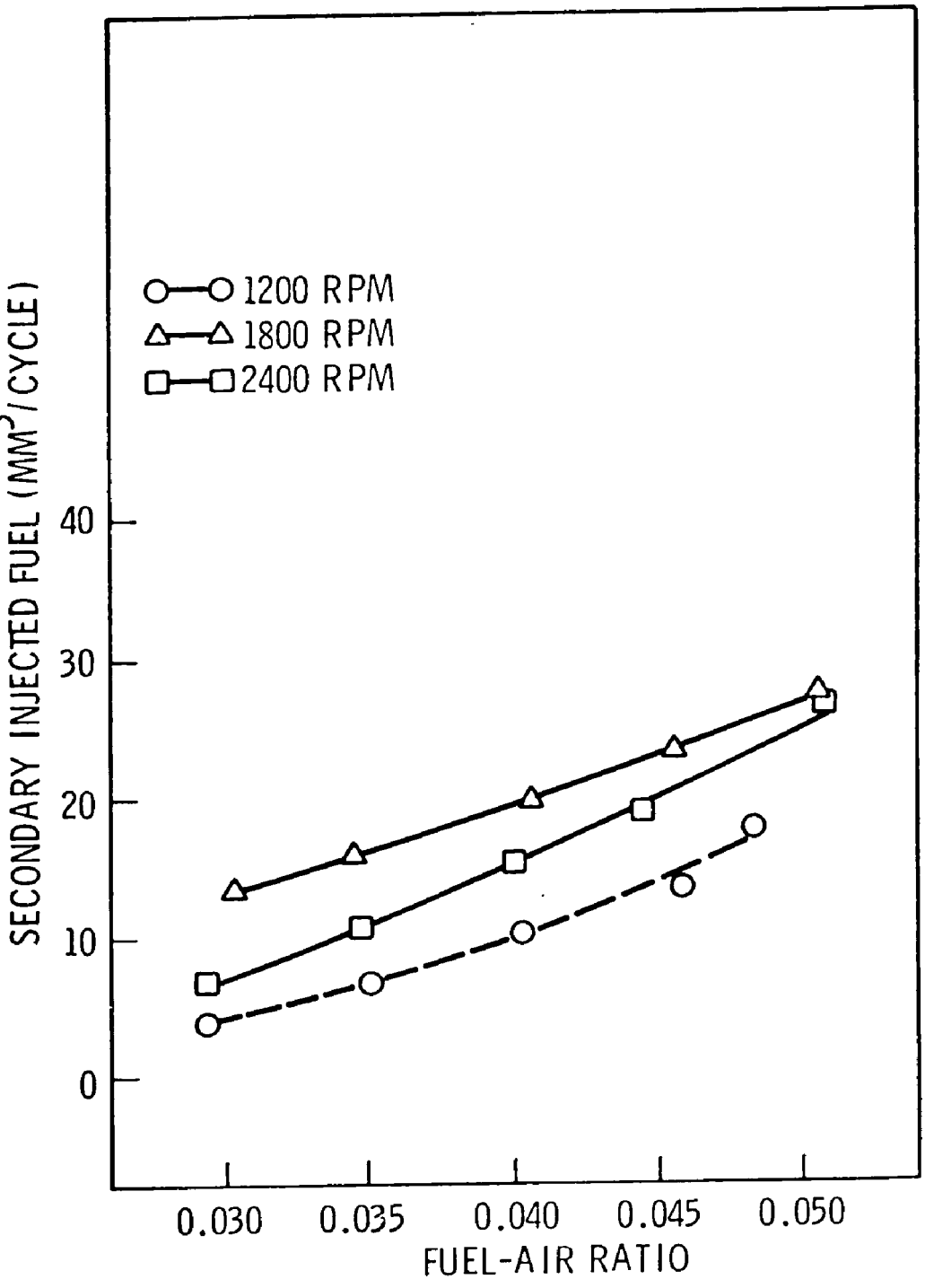


Figure 3.10 Relationship Between Total Fuel-Air Ratio and Secondary Injected Fuel per Cycle for Various Engine Speeds

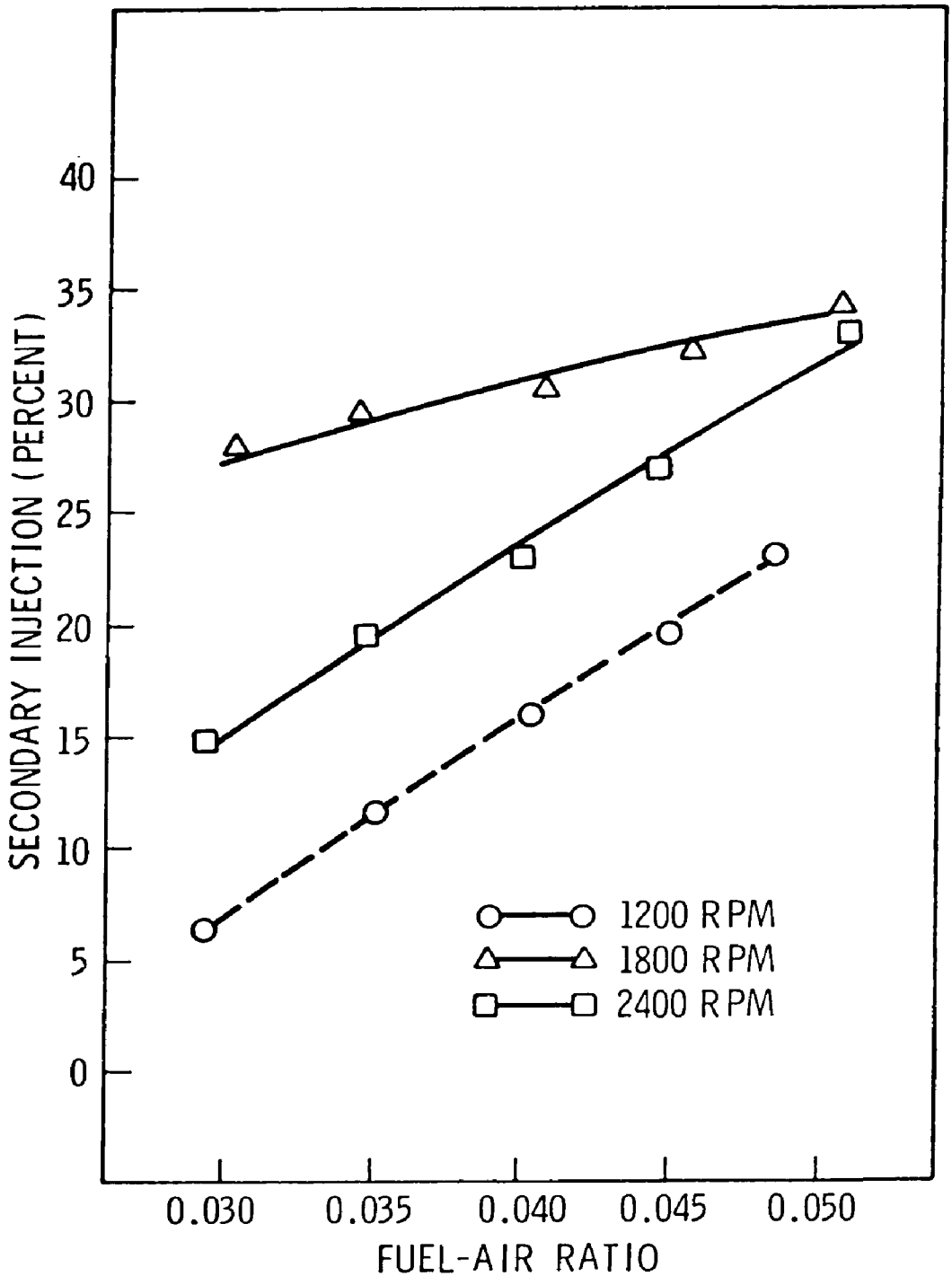


Figure 3.11 Relationship Between Total Fuel-Air Ratio and Percent Secondary Injection for Various Engine Speeds

CHAPTER IV

DIESEL ENGINE COMBUSTION PROCESS

In order to make any reasonable deductions from this investigation, it will be appropriate at this point to briefly introduce the theory of combustion in the diesel engine.

From earlier studies of a large number of high-speed photographs of diesel fuel spray, it is believed that fuel leaves the nozzle holes as a ligament which immediately breaks down into different size droplets, due to surface tension, as soon as it enters the combustion chamber. The leading droplets exchange their kinetic energy with the surrounding air causing a retardation in their motion and are then pushed aside by the subsequent spray. The droplets that have lost their energy and velocity tend to form a cloud suspended around the core of the spray. Appreciable heat transfer also takes place between the droplets and the air in the combustion chamber. The droplets therefore lose their mass by diffusion and vaporization into the air and the rate of this mass diffusion is a function of the droplet size and velocity. The smaller droplets give up more mass, vaporize faster, and travel shorter distance than larger ones.

The wet-bulb temperature corresponding to the conditions present in the cylinder is finally attained by each droplet at equilibrium, after a certain time interval. At some place in the combustion chamber, a combustible mixture of air and fuel vapor is formed which is near stoichiometric and this is where ignition begins at some elevated pressure and temperature. For the ignited fuel, the rate of burning and completeness of combustion is controlled by the chemical kinetics

of oxidation of the hydrocarbon fuel and the availability of oxygen. Each charge of fuel experiences all these phases in its combustion process. Combustion in diesel engines is therefore governed by such factors as atomization of liquid fuel, fuel spray penetration, diffusion, evaporation, chemical kinetics of hydrocarbon oxidation and availability of oxygen.

In this context, it is reasonable to picture what happens to a secondary injected fuel. During secondary injection, the average injection pressure is lower than that for main injection. The fuel droplets are therefore large with a small surface to volume ratio. Heat transfer and mass diffusion are therefore very poor. The spray penetration of the secondary injected fuel is also small because of the low injection pressure. The secondary injected fuel is injected fairly late in the expansion part of the cycle. The consequences of all these are that the ratio of oxygen to the secondary injected fuel is small, the degree to which the secondary injected fuel and oxygen are mixed and distributed is poor, the secondary injected fuel is injected too late in the cycle, and so does not have enough time to burn completely and have any effect on engine output and efficiency. The performance and emission results can be explained in terms of these conditions.

CHAPTER V

EXPERIMENTAL RESULTS - PERFORMANCE AND EMISSIONS

Performance and emission results obtained from experimental data using both the conventional (secondary injecting) fuel injection system, and the modified fuel injection system are presented and discussed in this chapter. An attempt is made to compare the results obtained with the two systems while keeping all engine variables constant and the difference between the two systems is attributed only to secondary injection. This comparison is done over a range of fuel-air ratios from about .03 to about .05, and speeds of 1200 rpm, 1800 rpm, and 2400 rpm. The lower limit of fuel-air ratio is chosen because it is about the point at which secondary injection begins for the 1200 rpm tests. The upper limit of fuel-air ratio is chosen because of an arbitrary limitation of 1200°F which the exhaust temperature should not exceed in order to avoid cylinder head cracking. The engine variables held constant for all runs are as follows:

Inlet Air Temperature = 300°F

Inlet Air Pressure = 15 in.Hg.G.

Exhaust Gas Pressure = 15 in.Hg.G.

Injection Timing = 21 degrees B.T.D.C.

Coolant Temperature = 185°F

5.1 BRAKE MEAN EFFECTIVE PRESSURE (B.M.E.P)

The effect of fuel-air ratio and injection system on brake mean effective pressure is shown in Figures 5.1, 5.2, and 5.3. At all three speeds and for each injection system, the effect of fuel-air ratio on BMEP is similar. BMEP increases with increasing fuel-air

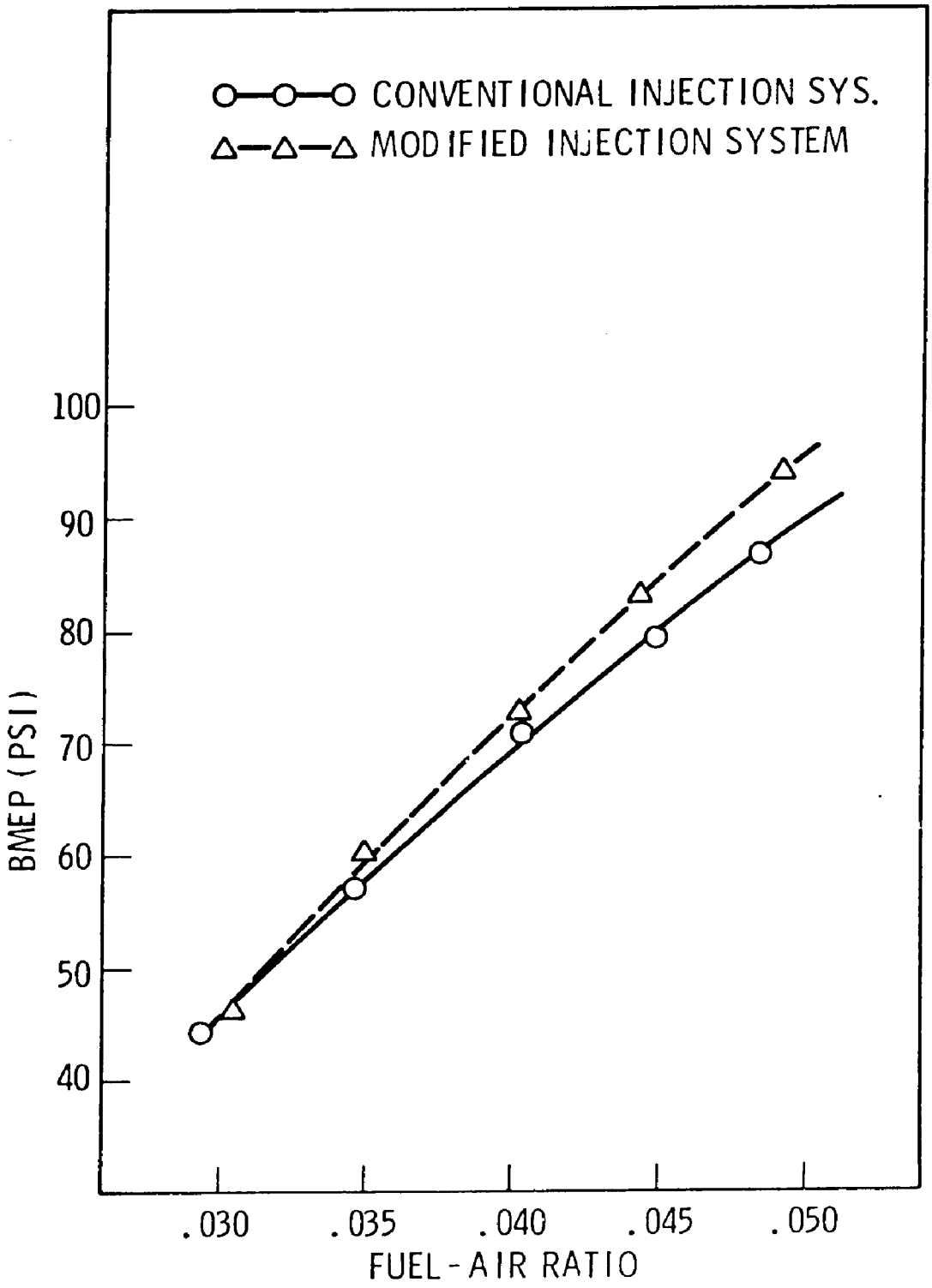


Figure 5.1 Effect of Total Fuel-Air Ratio and Injection System on BMEP for Engine Speed of 1200 rpm.

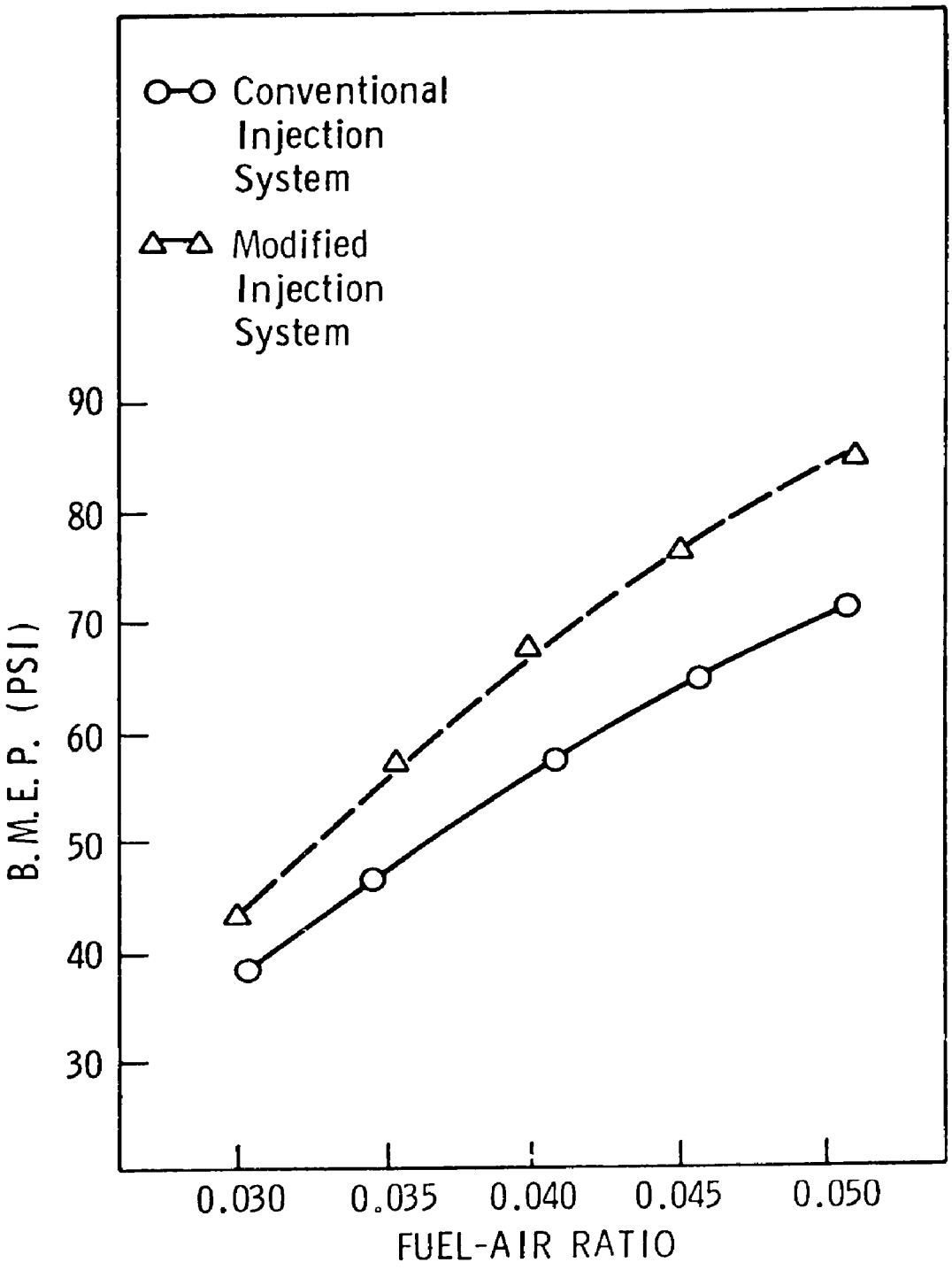


Figure 5.2 Effect of Total Fuel-Air Ratio and Injection System on BMEP for Engine Speed of 1800 rpm

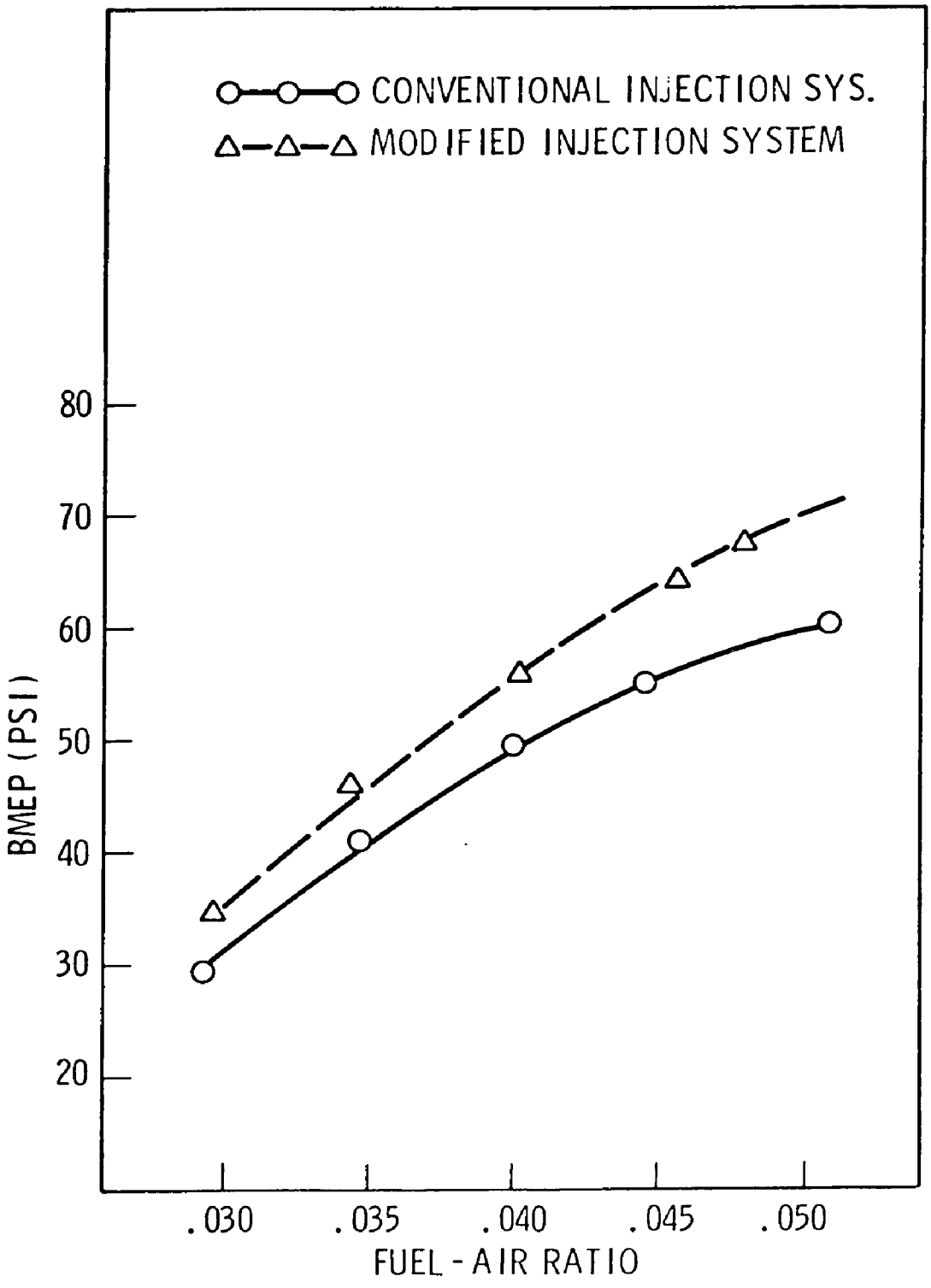


Figure 5.3 Effect of Total Fuel-Air Ratio and Injection System on BMEP for Engine Speed of 2400 rpm

ratio and the rate of increase is highest for the lowest speed and lowest for the highest speed. The curves also show that BMEP for the modified system is higher than BMEP for the conventional (secondary injecting) injection system, and they start approaching each other at low fuel-air ratios where secondary injection is getting smaller.

Increasing fuel-air ratio has a number of effects on the injection system which affect BMEP differently. First, increasing fuel-air ratio increases the total fuel injected per cycle and this goes entirely to increasing BMEP. Secondly, increasing fuel-air ratio extends the main injection period into the expansion stroke of the cycle and this reduces the rate of increase of BMEP. Thirdly, increasing fuel-air ratio increases the secondary injected fuel per cycle and this reduces the rate of increase of BMEP.

5.2 BRAKE SPECIFIC FUEL CONSUMPTION (B.S.F.C.)

The effect of fuel-air ratio and injection system on brake specific fuel consumption is shown in Figures 5.4, 5.5, and 5.6. For all three speeds and both injection systems, as the fuel-air ratio is increased, the brake specific fuel consumption decreases to a minimum valve and then begins to increase. This minimum value varies with speed and injection system. This BSFC trend is explained by the fact that at low fuel-air ratio, increase in fuel-air ratio results in an increase in mechanical efficiency and hence causes a decrease in BSFC. However, as fuel-air ratio becomes high, increasing fuel-air ratio causes more and more fuel to be injected in the expansion stroke and mechanical efficiency does not increase as much as before and this reduces the rate of decrease of BSFC. Also for the conventional system,

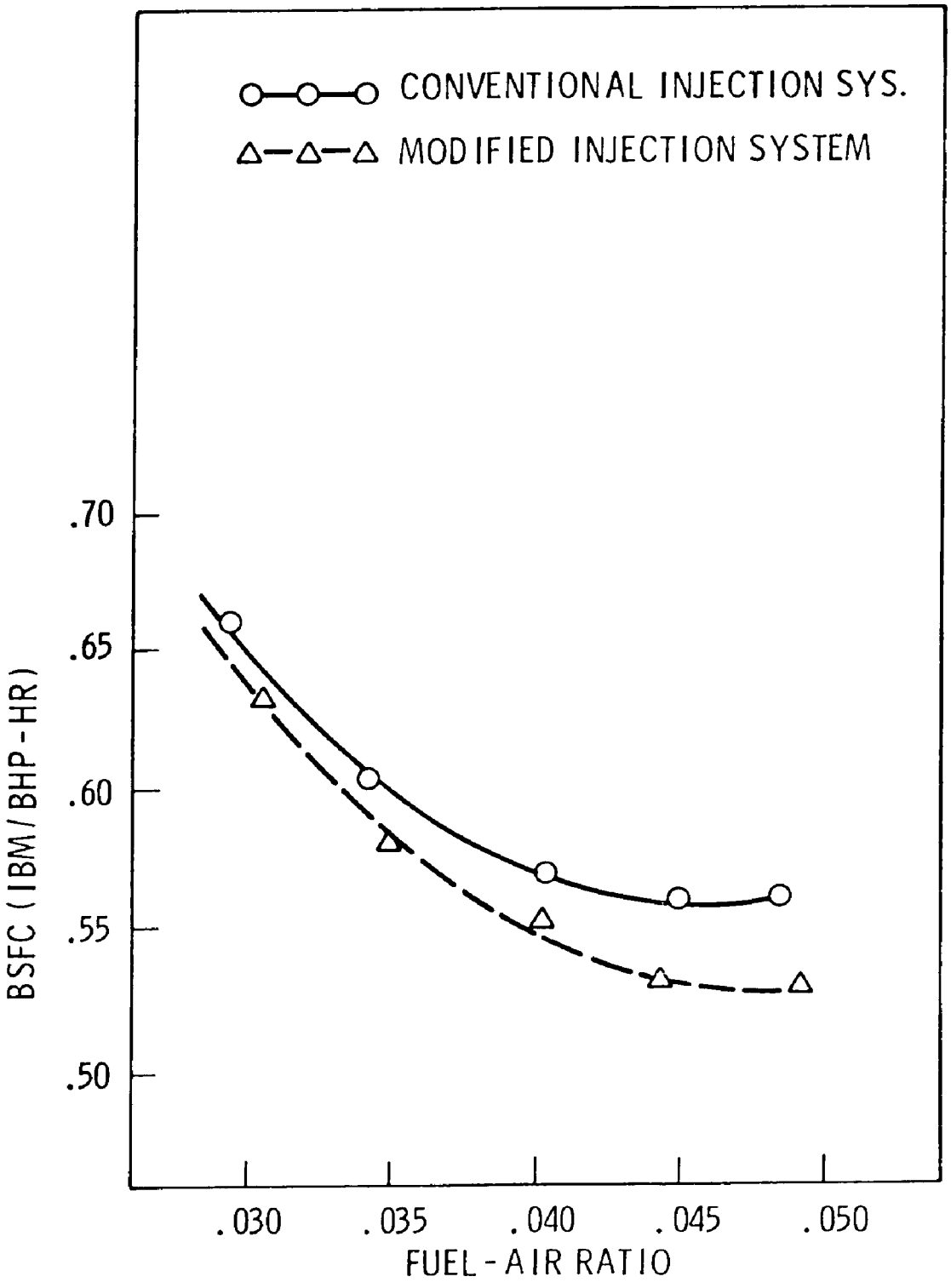


Figure 5.4 Effect of Total Fuel-Air Ratio and Injection System on BSFC for Engine Speed of 1200 rpm

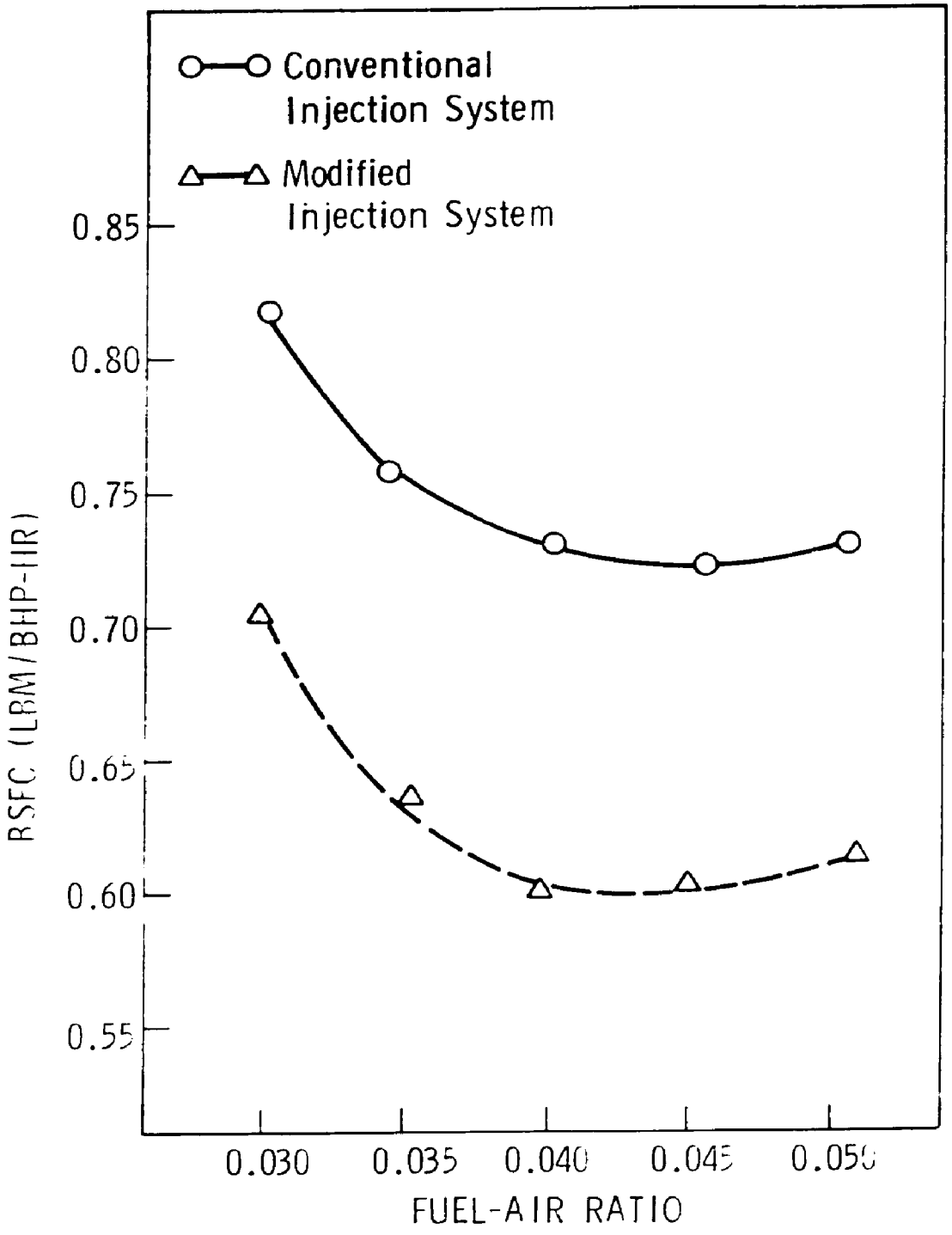


Figure 5.5 Effect of Total Fuel-Air Ratio and Injection System on BSFC for Engine Speed of 1800 rpm

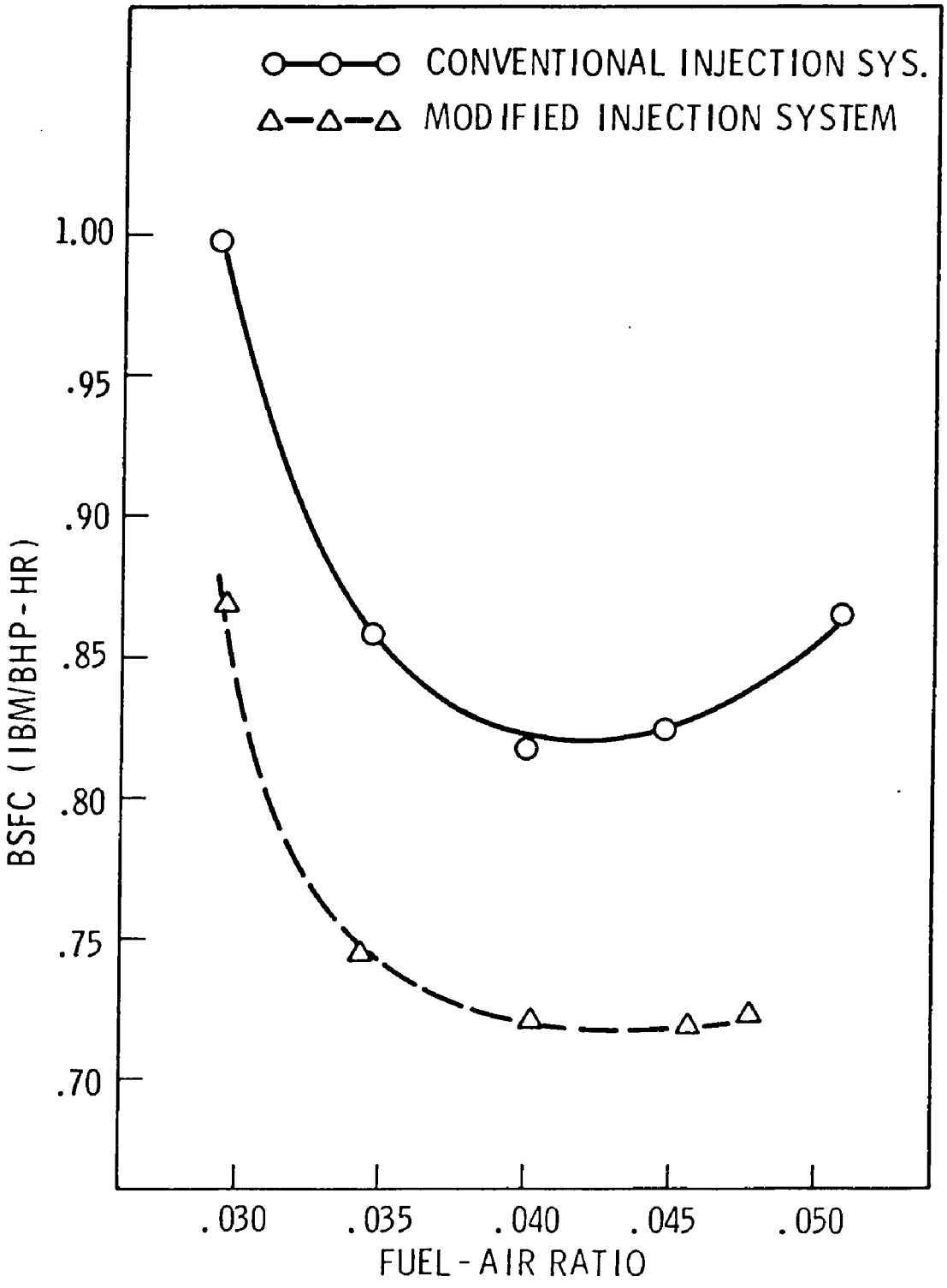


Figure 5.6 Effect of Total Fuel-Air Ratio and Injection System on BSFC for Engine Speed of 2400 rpm

secondary injection becomes appreciable at high fuel-air ratios causing a further decrease of BSFC.

A comparison between the modified system and conventional system shows that for all three speeds, the modified system has a lower BSFC than the conventional system. This difference can only be attributed to the occurence of secondary injection.

5.3 Smoke

Black smoke from diesel engines consists essentially of agglomerated fine particles of carbon. Earlier studies (20), (21), and (26) have shown that smoke in a diesel exhaust is controlled by the mechanism of carbon formation and carbon combustion or consumption in the combustion chamber. Carbon is formed during the combustion process in the diesel engine by the pyrolysis of unreacted hydrocarbon fuel. The reaction takes place when local temperature is high enough to decompose the fuel in an area of the combustion chamber where there is insufficient oxygen. In the engine the premixed fuel burns rapidly while the fuel injected after the ignition delay burns as it mixes as a diffusion flame and this is the main source of carbon formation. Smoke formation is therefore a function of the amount of diffusion burning in the engine. Carbon that is formed early in the combustion process, can be burnt later as it mixes with air at the end of the heat release period resulting in smoke reduction. The amount of carbon consumption depends on the region into which these particles move, the availability of oxygen or oxygen containing substances like H_2O, CO_2, and a high enough temperature.

Figures 5.7, 5.8, and 5.9, show the effect of fuel-air ratio and

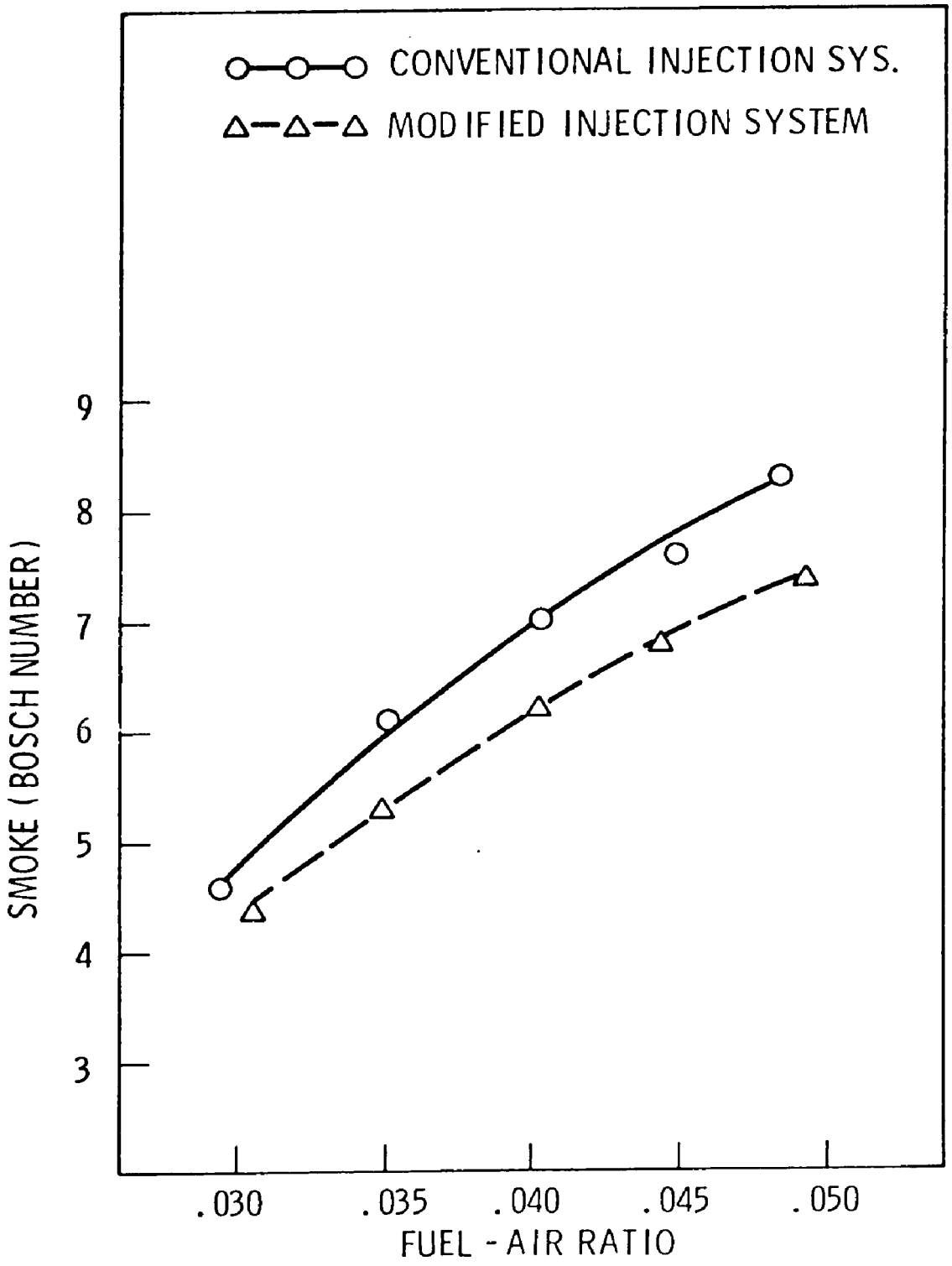


Figure 5.7 Effect of Total Fuel-Air Ratio and Injection System on Smoke for Engine Speed of 1200 rpm

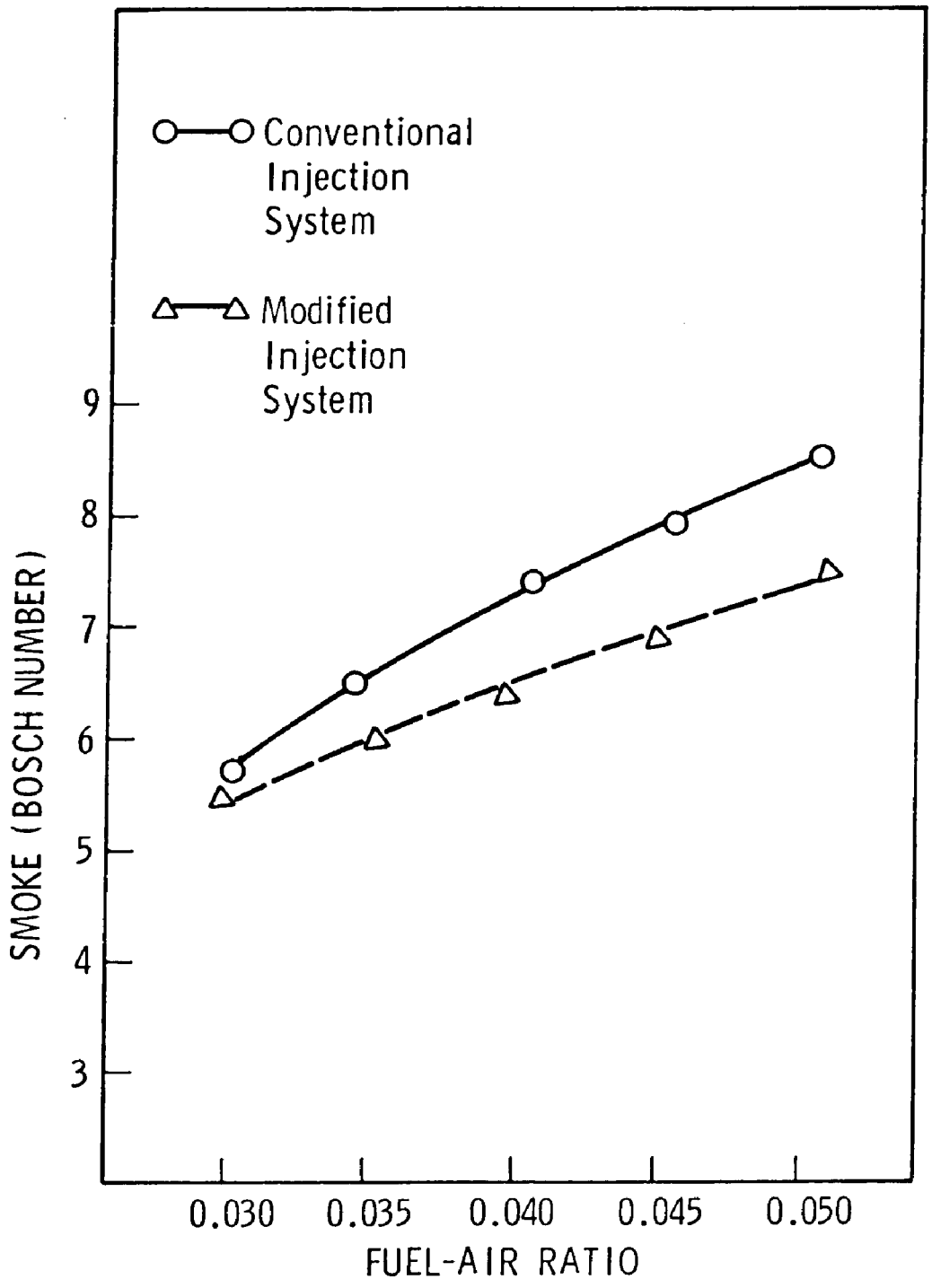


Figure 5.8 Effect of Total Fuel-Air Ratio and Injection System on Smoke for Engine Speed of 1800 rpm

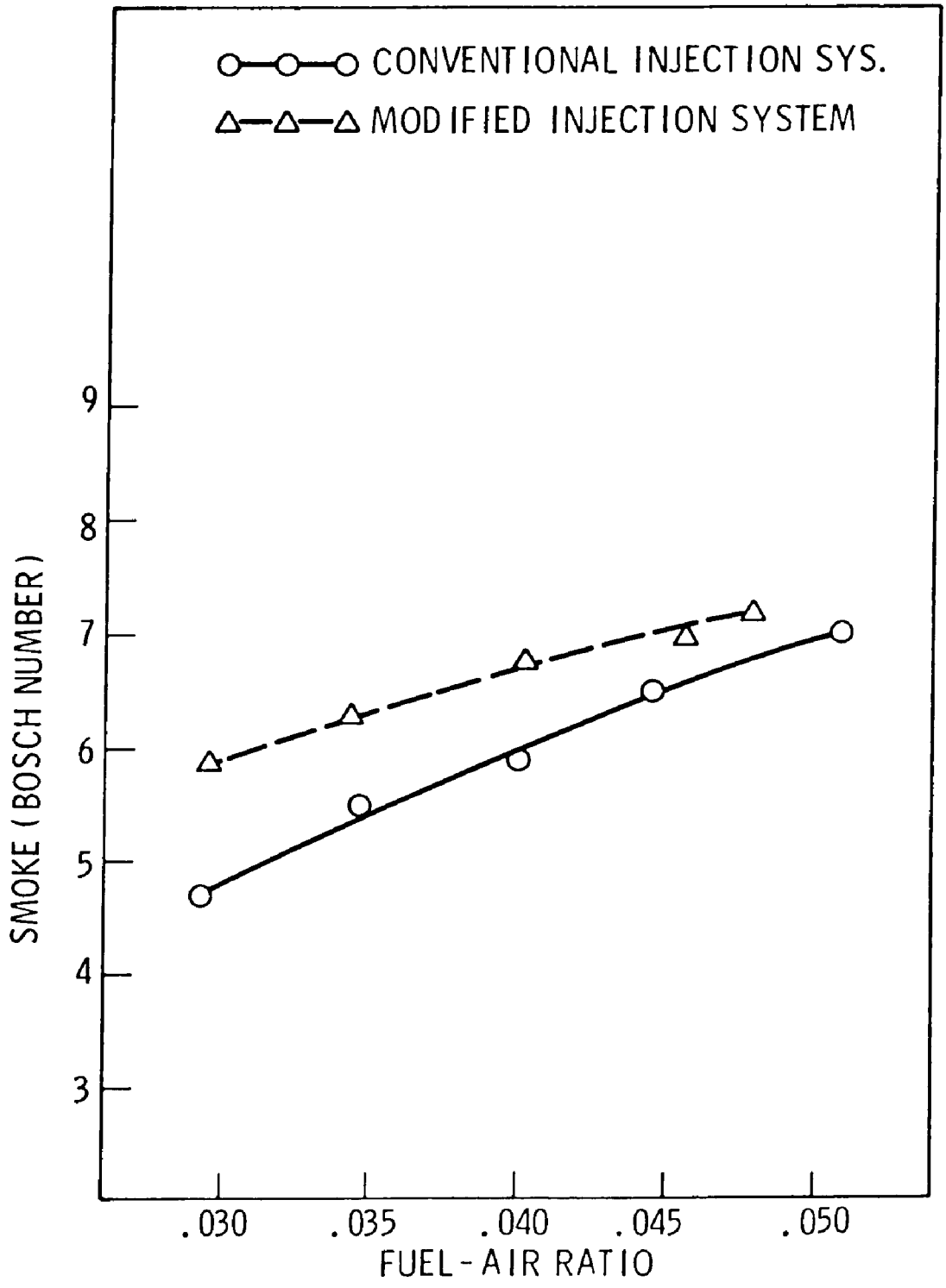


Figure 5.9 Effect of Total Fuel-Air Ratio and Injection System on Smoke for Engine Speed of 2400 rpm

injection system on smoke. For all the speeds, and injection system it can be observed that exhaust smoke increased with increase of fuel-air ratio. This is in keeping with the discussion in section 4.3.1 because the amount of diffusion burning increases with fuel-air ratio. The figures also show as expected that secondary injection causes an increase in diesel exhaust smoke. The large secondary injected droplets with slow evaporation, mixing and burning characteristics, also intensively cool various zones of the flame all resulting in smoke increase.

5.4 Unburned Hydrocarbons

Hydrocarbons from diesel exhaust consist of original, decomposed, and recombined intermediate hydrocarbons. Most unburned hydrocarbons originate from (a) large droplets injected late in the cycle whose oxidation are limited by lack of oxygen and lack of time for oxidation, (b) fuel impingement on the piston and cylinder walls.

Figures 5.10, 5.11, and 5.12 show the effects of fuel-air ratio and injection system on unburned hydrocarbon concentration in the exhaust. As fuel-air ratio is increased, the availability of oxygen is reduced and late burning is increased and hydrocarbon concentration goes up as shown in the figures. However, as fuel-air ratio increases, the exhaust temperatures also increase to a point where oxidation of unburned hydrocarbons in the exhaust mixing tank becomes significant. At exhaust temperatures above 850°F, this effect dominates the formation effect and the overall hydrocarbon content starts decreasing. The figures also show that the conventional system has higher hydrocarbon concentrations in the exhaust than the modified system mainly

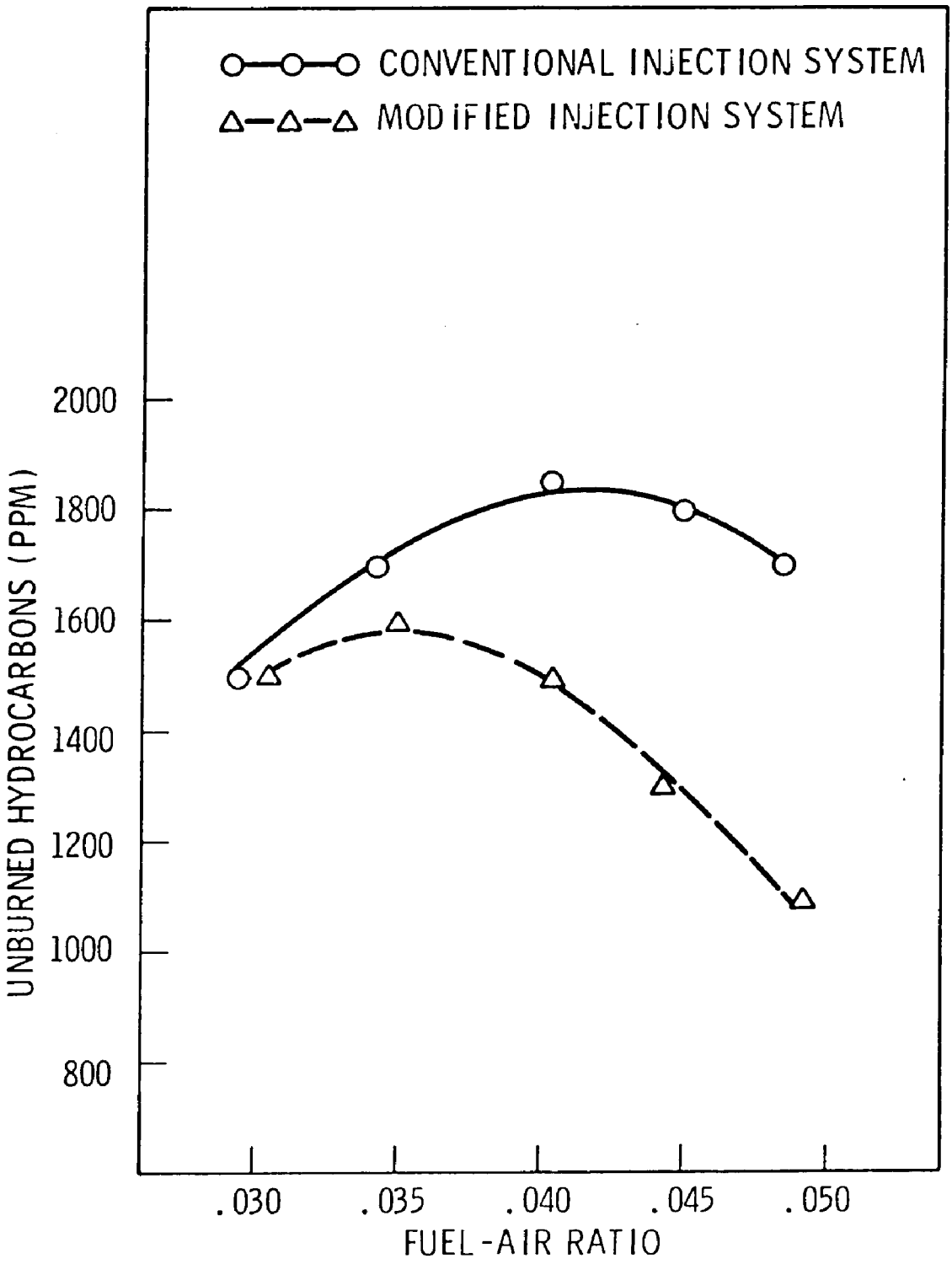


Figure 5.10 Effect of Total Fuel-Air Ratio and Injection System on Unburned Hydrocarbons for Engine Speed of 1200 rpm

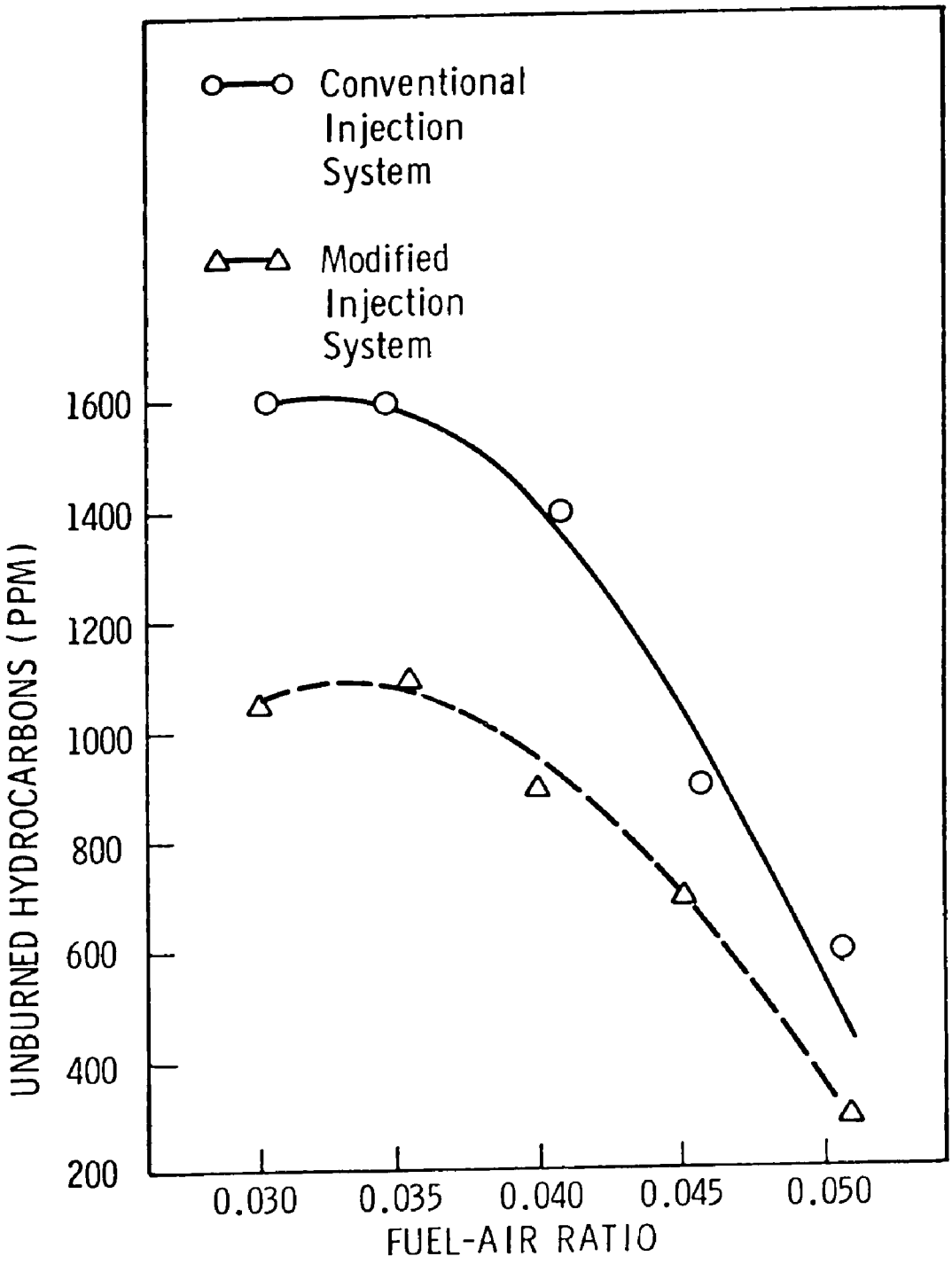


Figure 5.11 Effect of Total Fuel-Air Ratio and Injection System on Unburned Hydrocarbons for Engine Speed of 1800 rpm

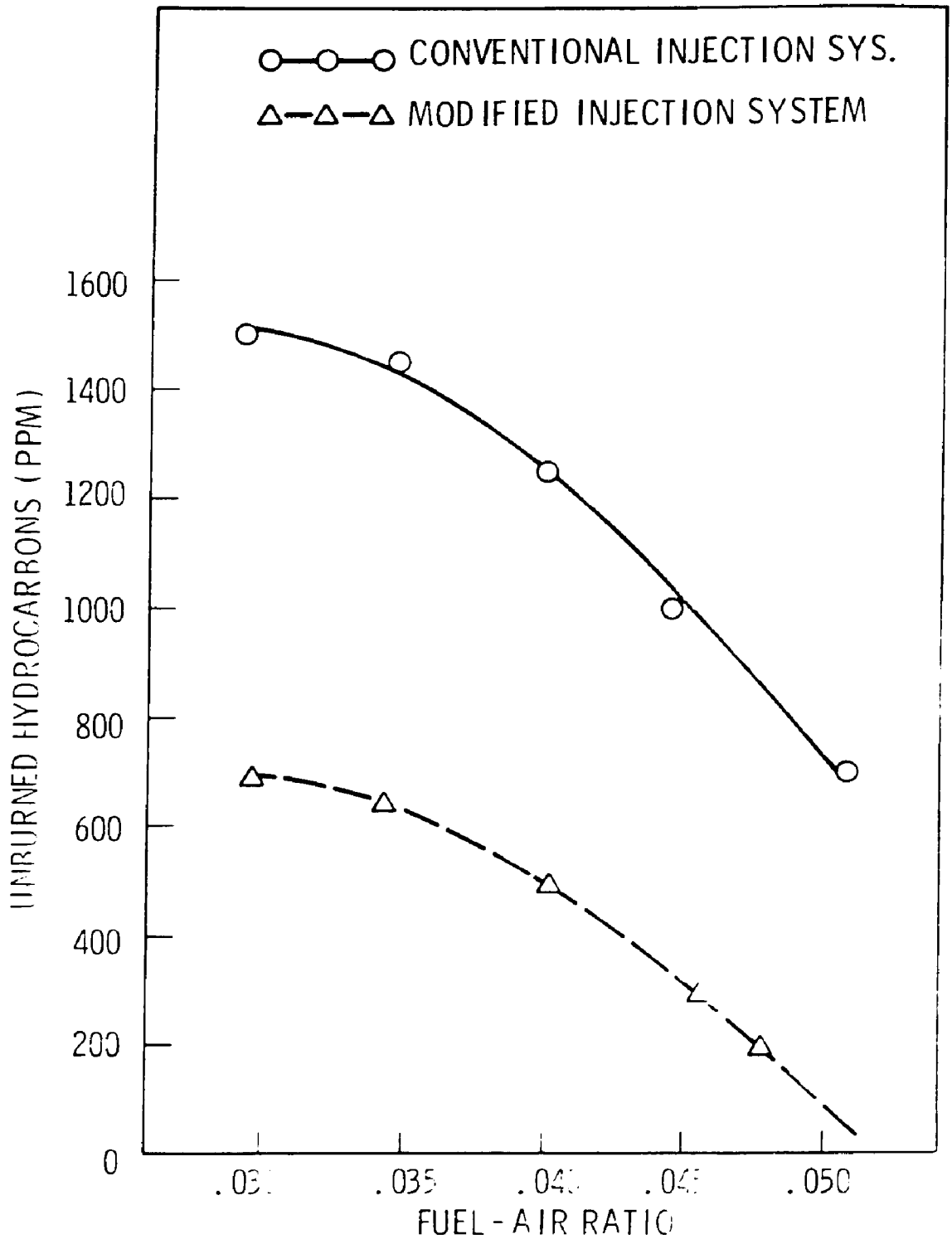


Figure 5.12 Effect of Total fuel-Air Ratio and Injection System on Unburned Hydrocarbons for Engine Speed of 2400 RPM

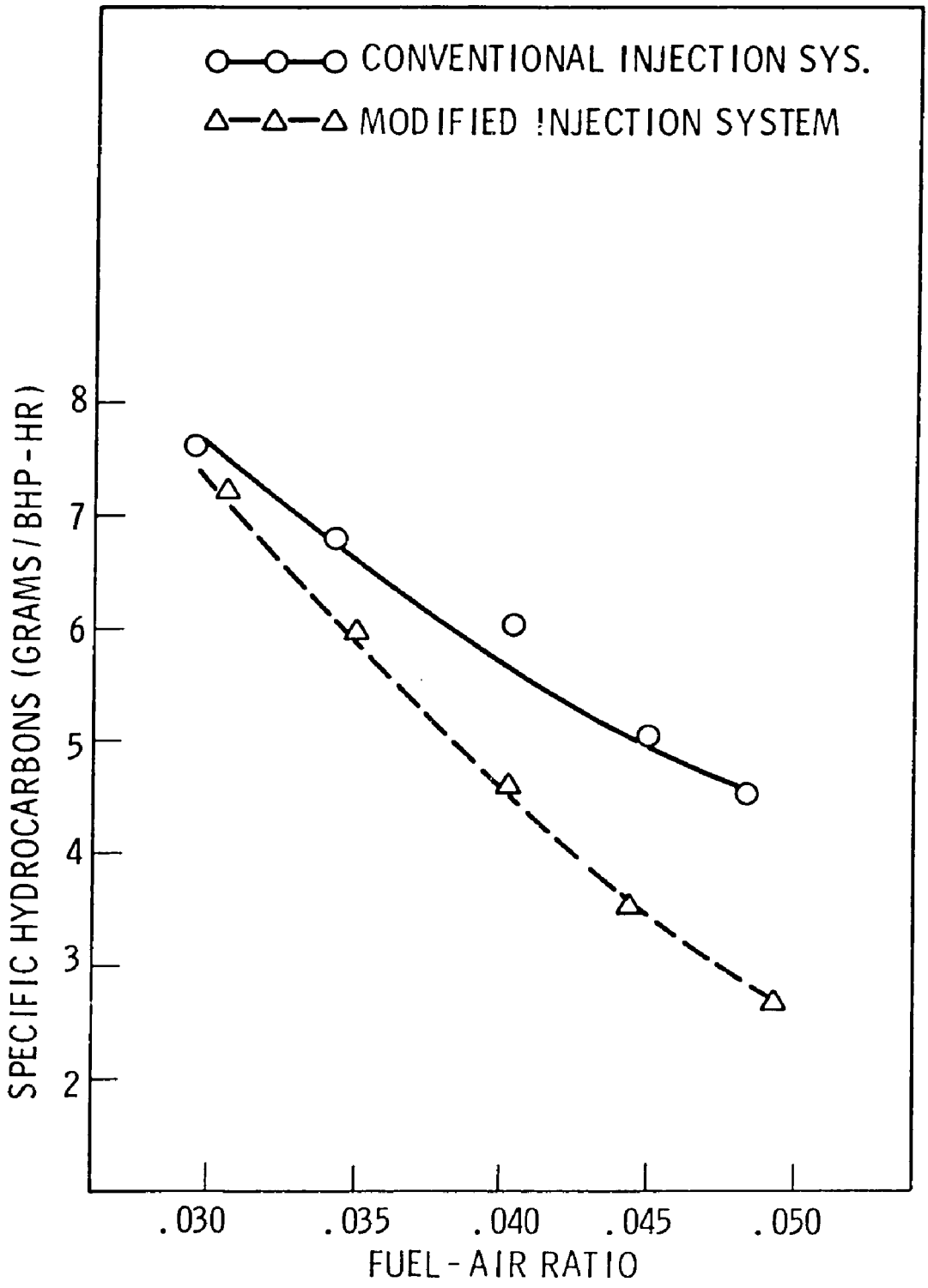


Figure 5.13 Effect of Total Fuel-Air Ratio and Injection System on Specific Hydrocarbon Emission for Engine Speed of 1200 rpm

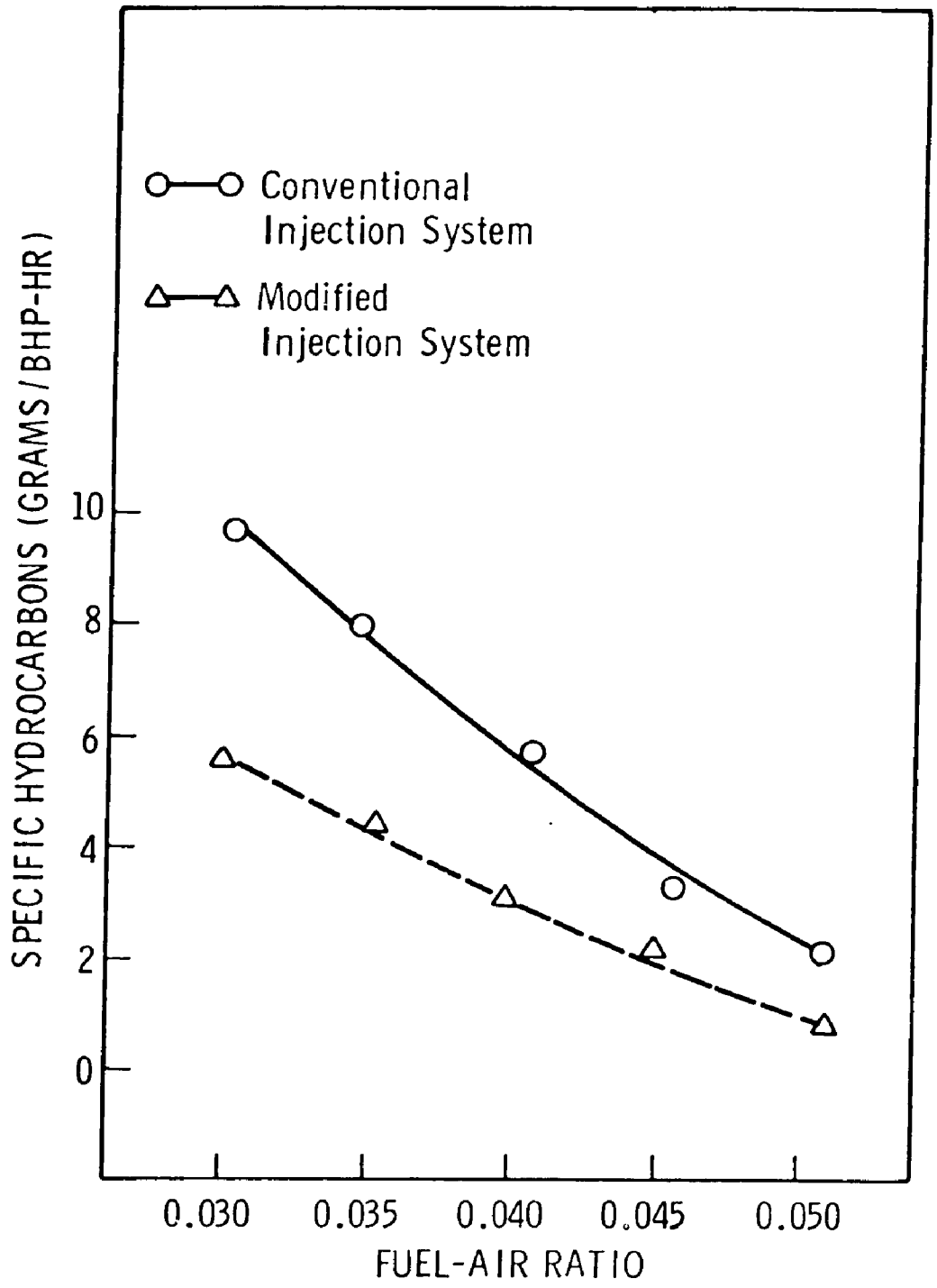


Figure 5.14 Effect of Total Fuel-Air Ratio and Injection System on Specific Hydrocarbon Emission for Engine Speed of 1800 rpm

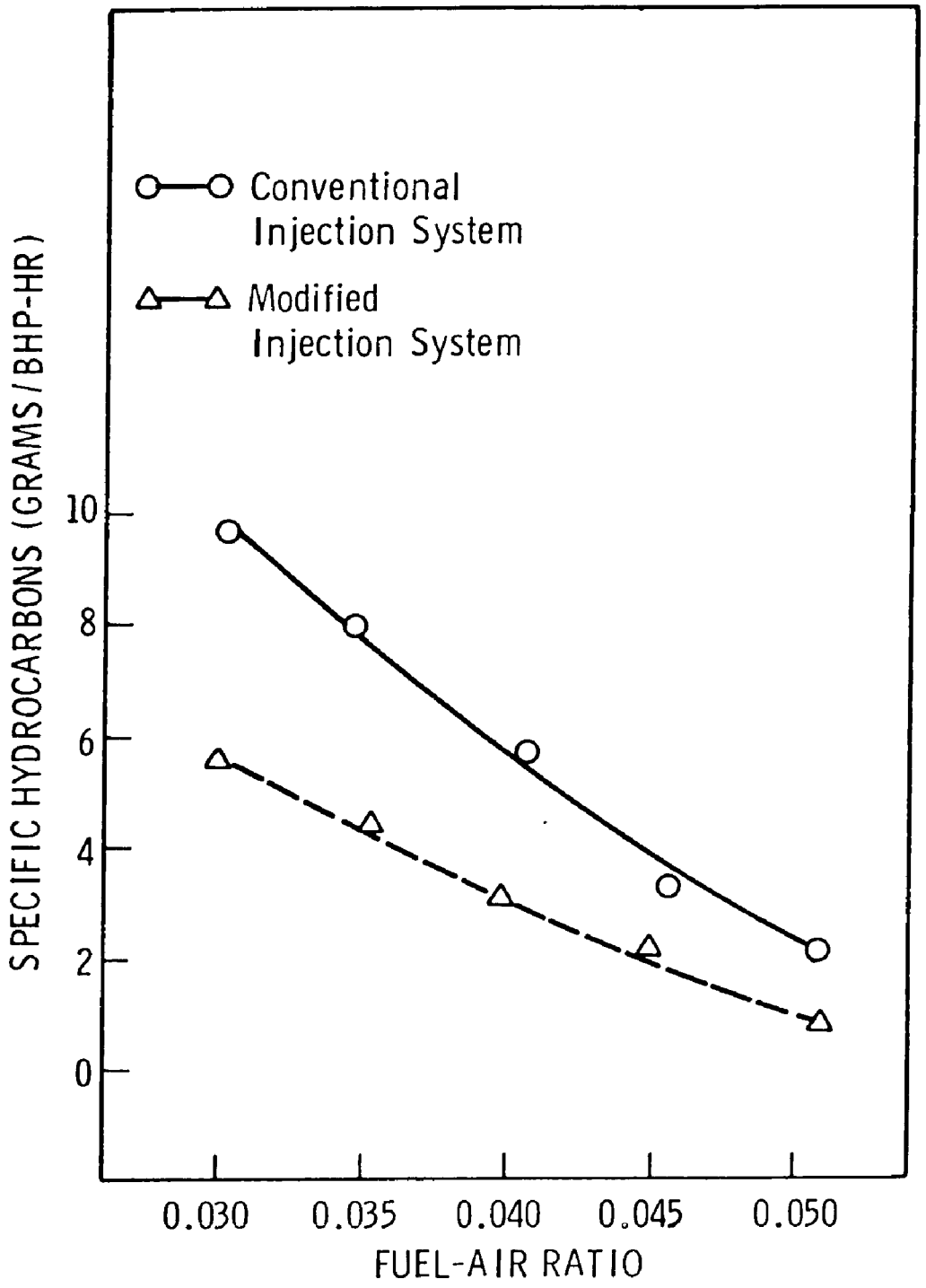


Figure 5.14 Effect of Total Fuel-Air Ratio and Injection System on Specific Hydrocarbon Emission for Engine Speed of 1800 rpm

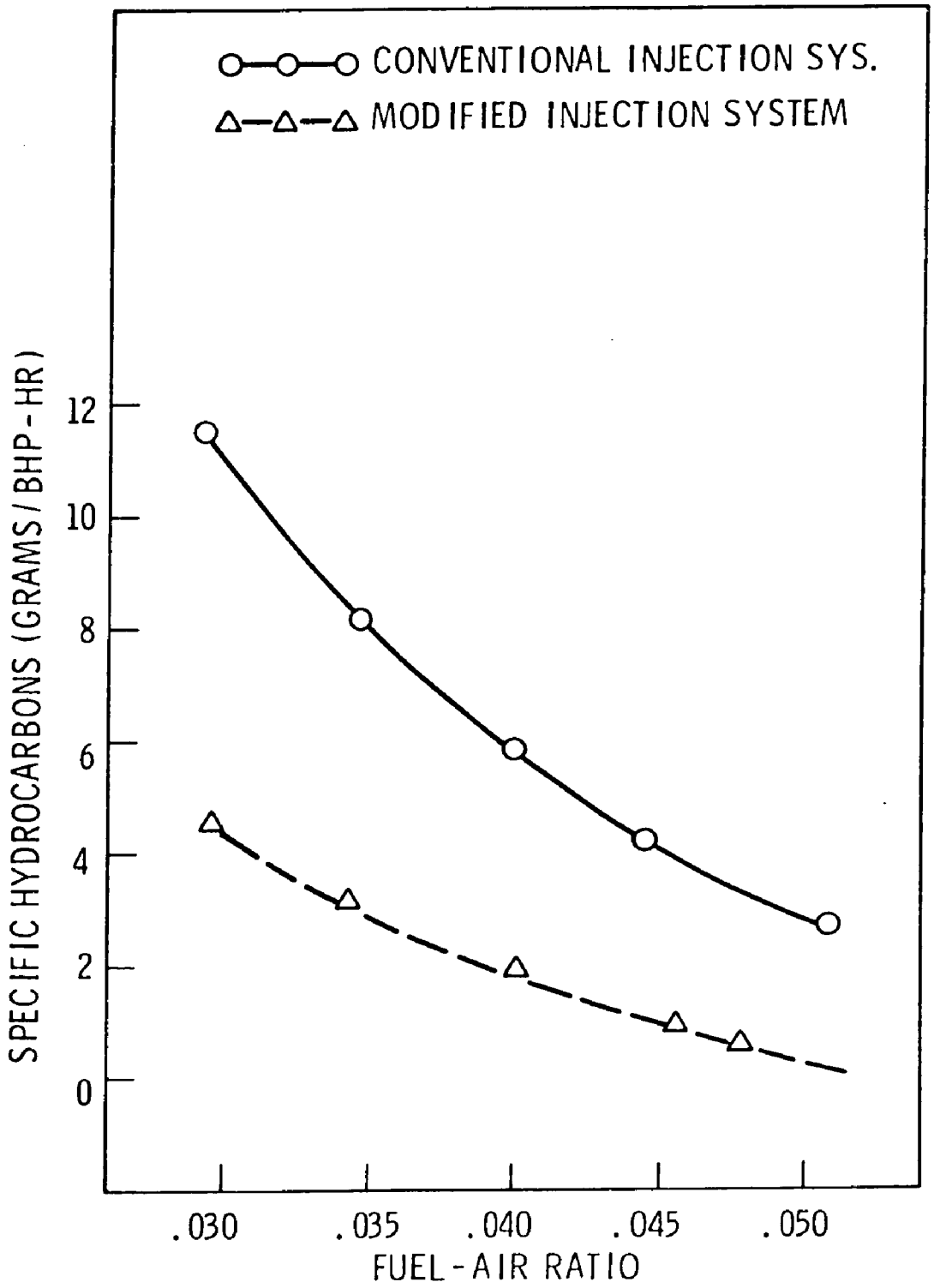


Figure 5.15 Effect of Total Fuel-Air Ratio and Injection System on Specific Hydrocarbon Emission for Engine Speed of 2400 rpm

because of secondary injections.

Figures 5.13, 5.14, and 5.15 show the specific hydrocarbons emissions and these decrease steadily with increasing fuel-air ratio as a result of the increase in brake horsepower.

5.5 Oxides of Nitrogen (NO_x)

The NO_x concentration in any part of the combustion chamber is a function of the local peak temperature and the time available for reaction to take place. NO formation rate is known to be relatively slow in comparison with the main energy release reactions and so all NO formation takes place in the burned gas side of the flame where temperatures are highest.

Figures 5.16, 5.17, and 5.18 show the effect of fuel-air ratio and injection system on NO_x. It shows that increasing fuel-air ratio increases NO_x concentration. This is as expected because of the resulting increase in exhaust temperature. The rate of increase, however, is less at higher fuel-air ratios because of the reduced reaction time for the subsequent late injected fuel.

All the curves show that for both injection systems, the NO_x is essentially the same. This result corroborates the results obtained for temperature, which showed that secondary injection had little or no observable effect on exhaust temperature. It also implies that a lack of oxygen at the end of combustion or events at the end of combustion do not affect NO_x.

This result differs from the results of McConnell (33) in which he found that by using a fuel pump with one cam rate, he was able to produce secondary injection and the NO_x concentration was 1400 ppm. On changing to a pump with a different cam profile (faster cam rate),

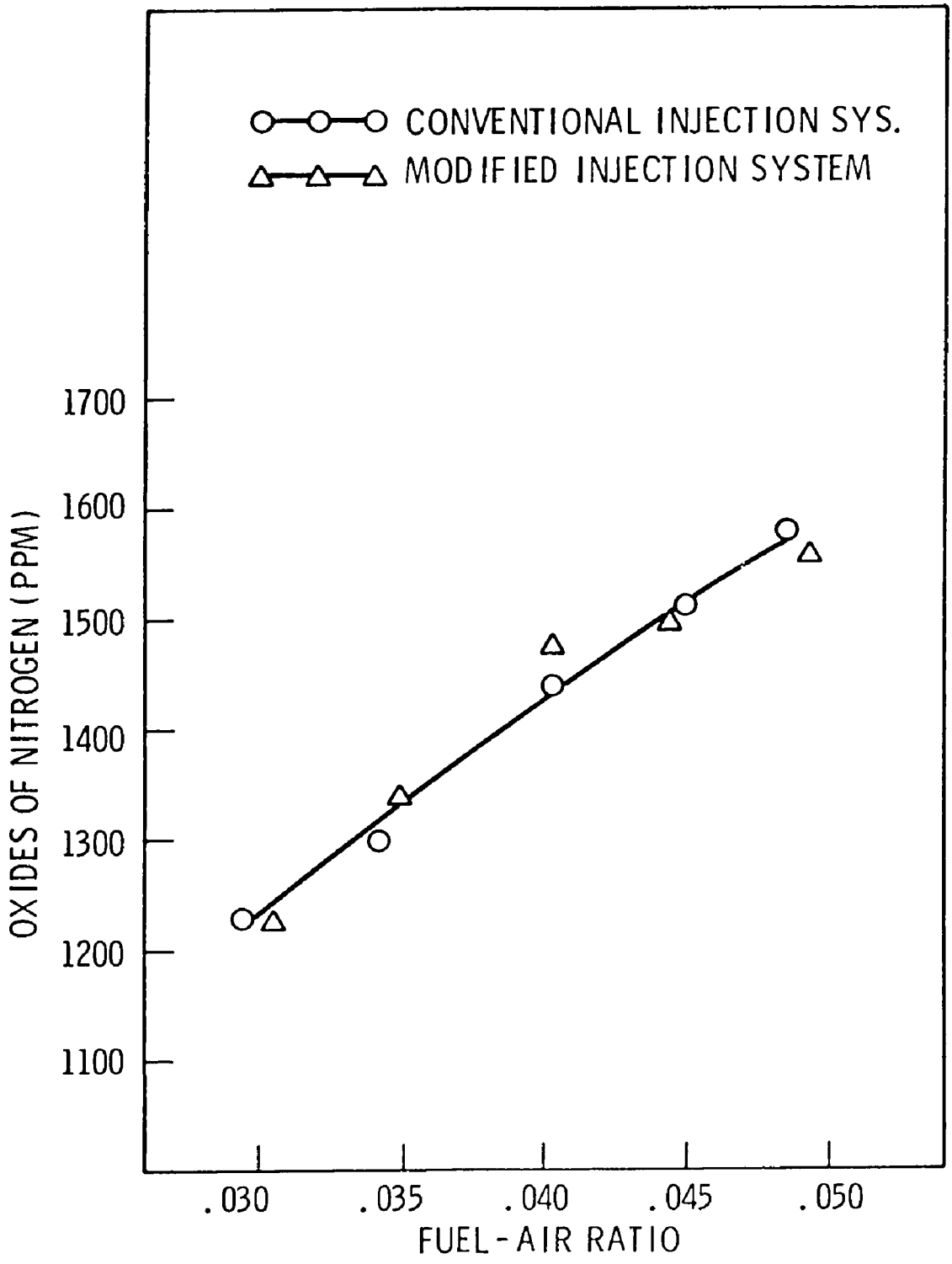


Figure 5.16 Effect of Total Fuel-Air Ratio and Injection System on Oxides of Nitrogen for Engine Speed of 1200 rpm

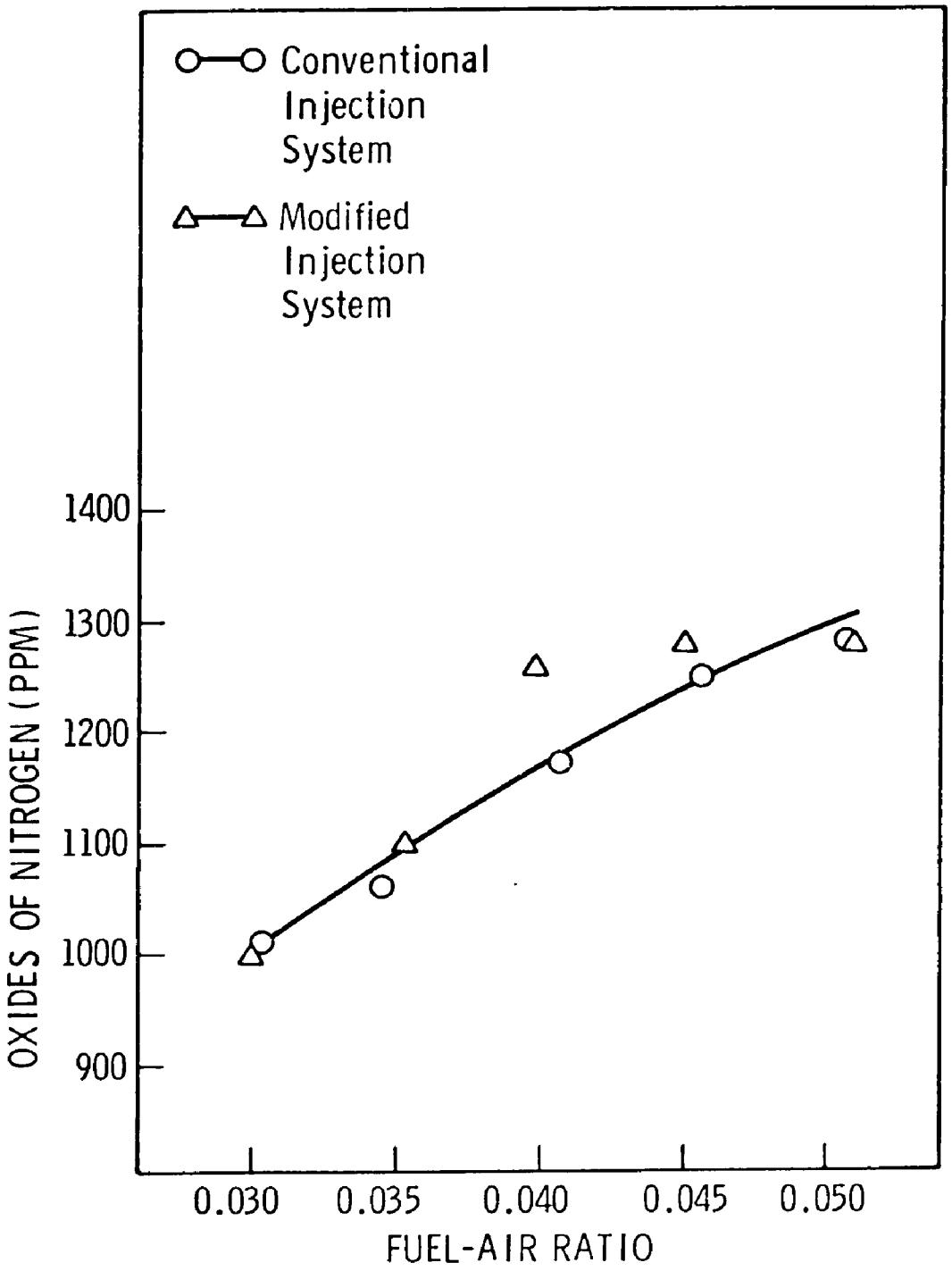


Figure 5.17 Effect of Total Fuel-Air Ratio and Injection System on Oxides of Nitrogen for Engine Speed of 1800 rpm

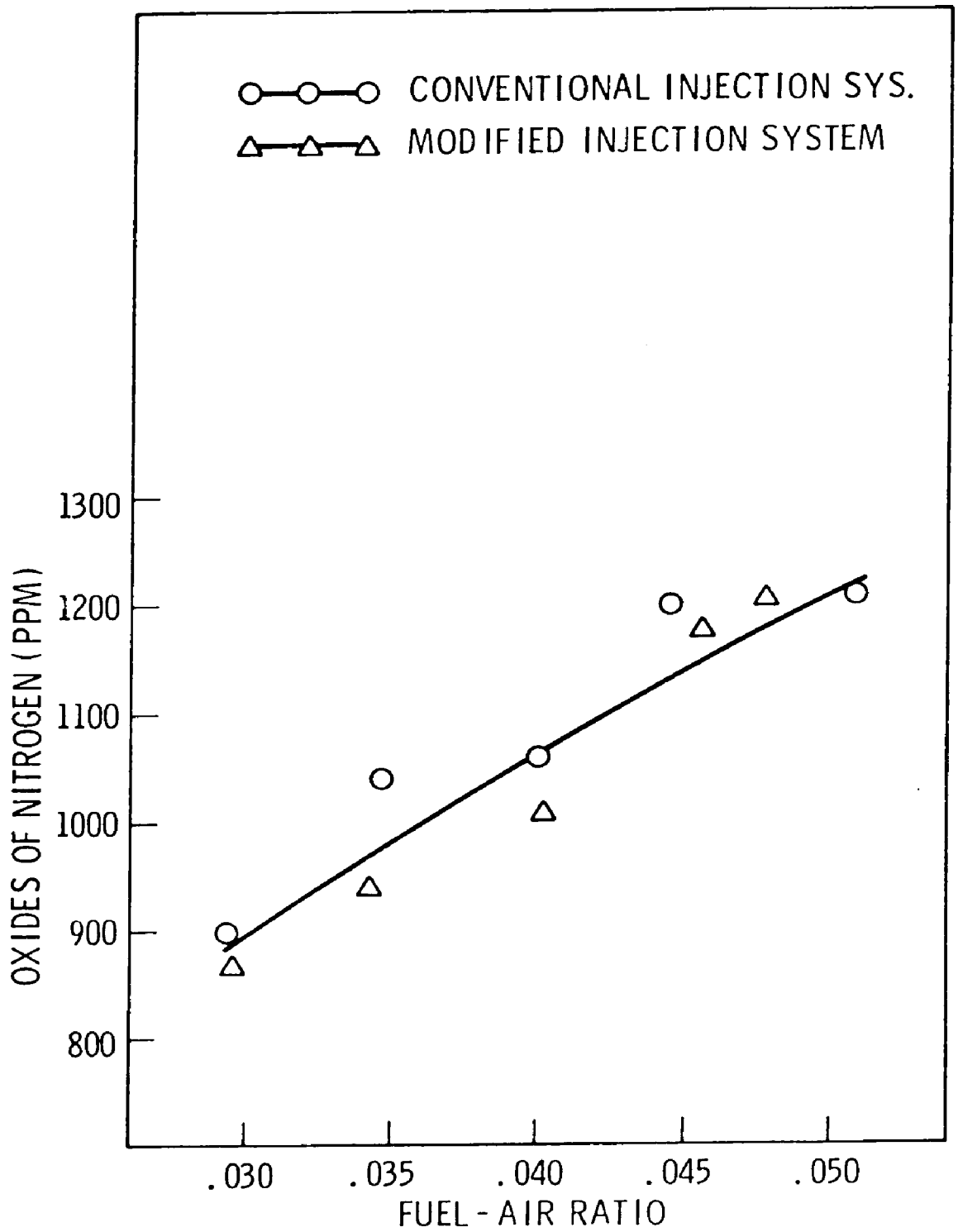


Figure 5.18 Effect of Total Fuel-Air Ratio and Injection System on Oxides of Nitrogen for Engine Speed of 2400 rpm

he was able to inject the same amount of fuel as before but without secondary injection and the NO_x concentration was 3100 ppm, an increase of 120 percent. The difference between his work and this work is that by using a different cam profile, the rate of injection is completely altered and it is possible to alter it so much that almost all the fuel is injected before top dead center and this of course will cause considerable peak temperature and NO_x differences.

5.6 Exhaust Temperature

Figures 5.19, 5.20, and 5.21 show the effects of fuel-air ratio and injection system characteristics on exhaust temperature measured at the exhaust valve for three different engine speeds. The results indicate that exhaust temperature for a given engine speed increases almost linearly as fuel-air ratio is increased. This increase is due to the increase in fuel flow and extended combustion periods at high fuel-air ratios. The results also show that for both injection systems the exhaust temperatures are about the same for a given fuel-air ratio and engine speed. The conclusion from this is that secondary injection has little or no observable effect on exhaust temperature.

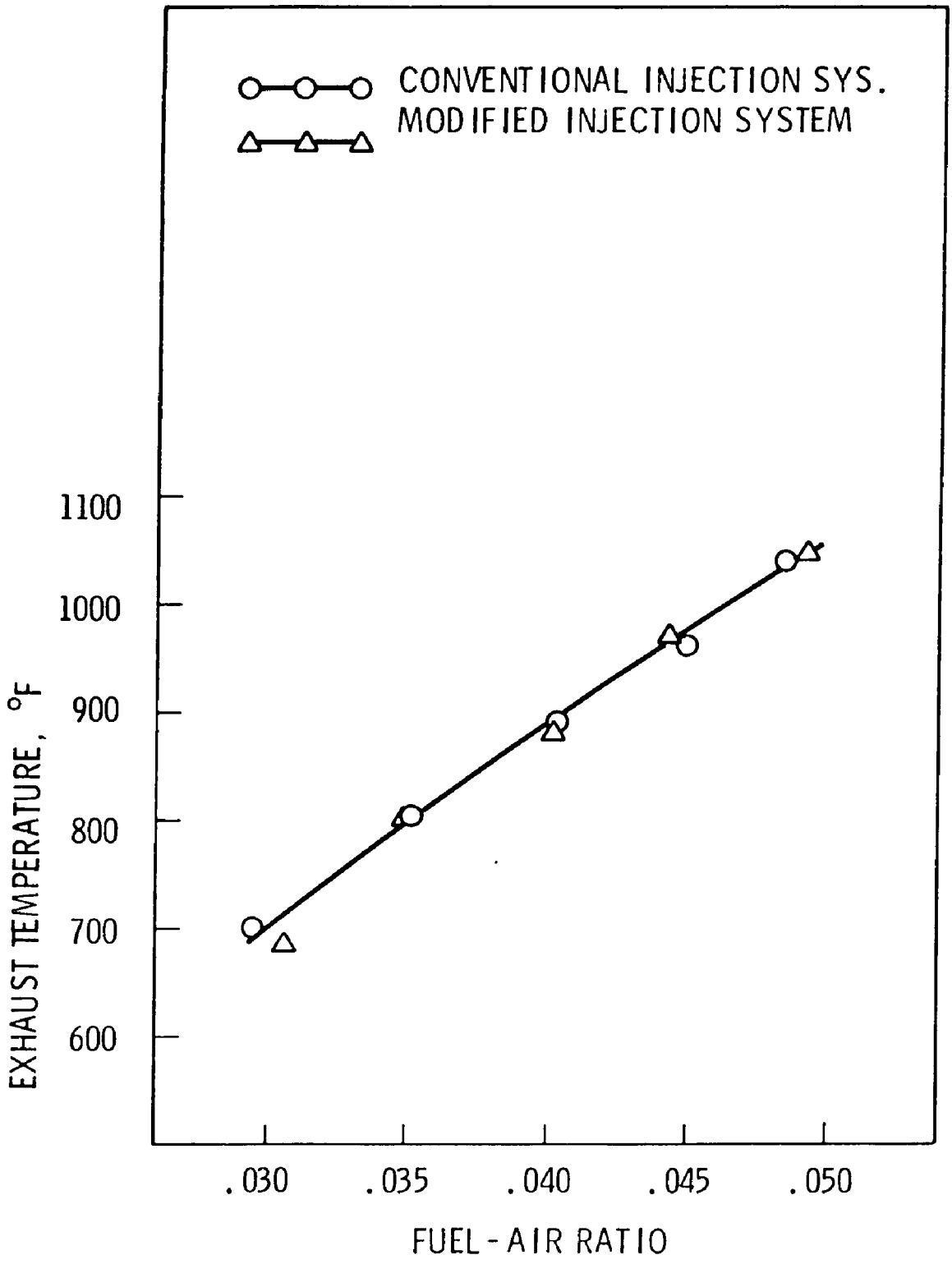


Figure 5.19 Effect of Total Fuel-Air Ratio and Injection System on Exhaust Temperature for Engine Speed of 1200 rpm

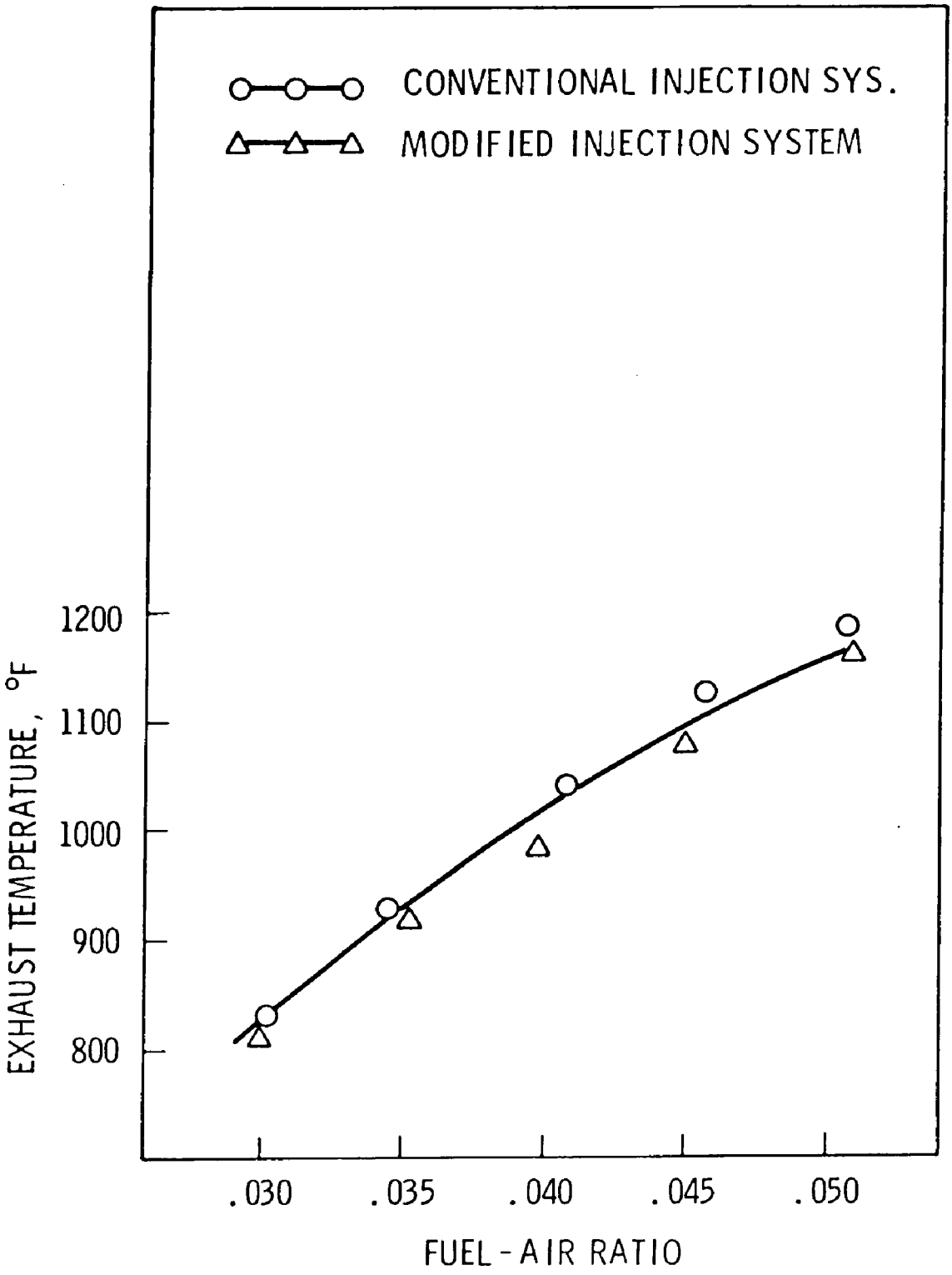


Figure 5.20 Effect of Total Fuel-Air Ratio and Injection System on Exhaust Temperature for Engine Speed of 1800 rpm

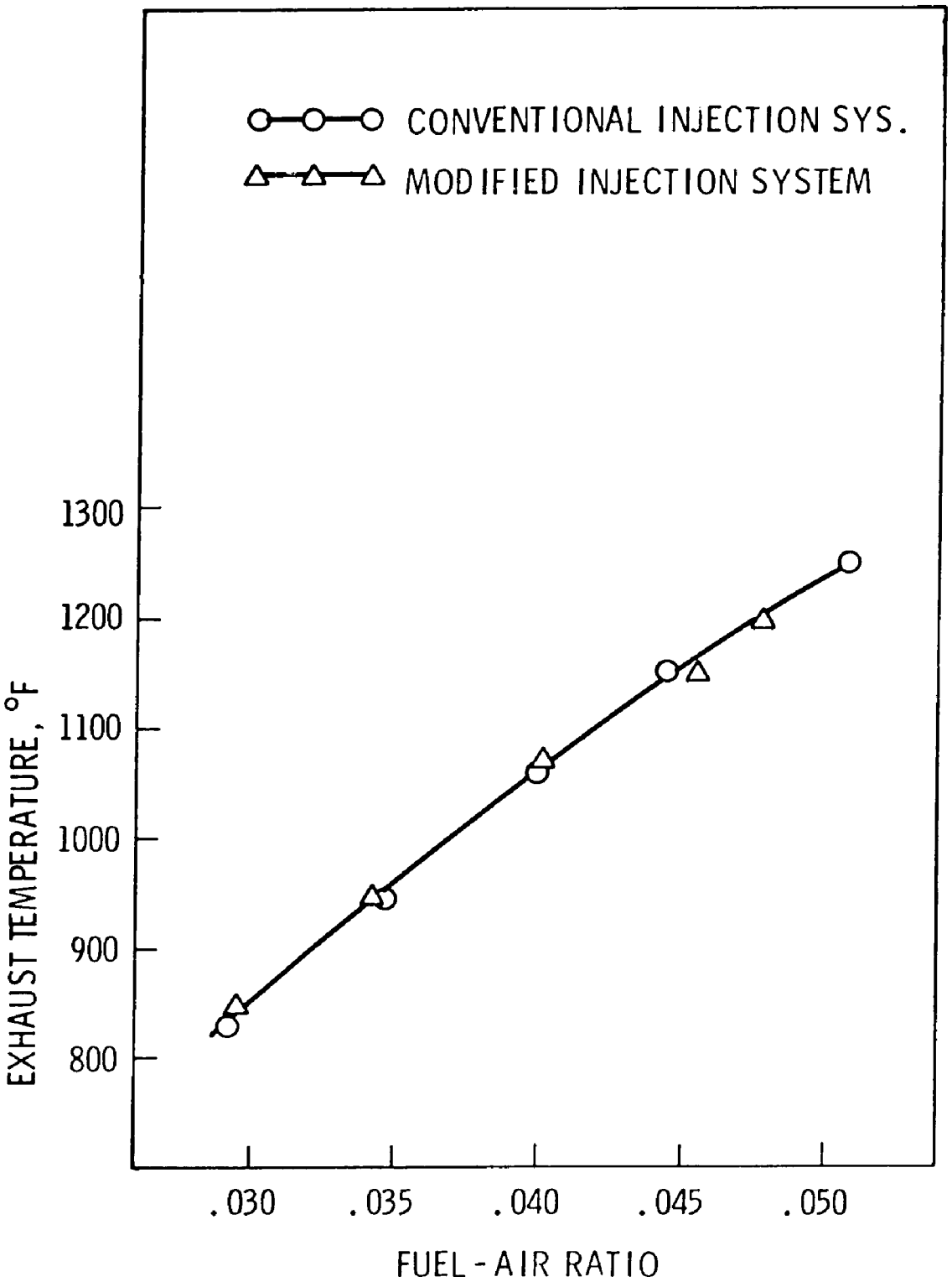


Figure 5.21 Effect of Total Fuel-Air Ratio and Injection System on Exhaust Temperature for Engine Speed of 2400 rpm

CHAPTER VI

CORRELATION BETWEEN SECONDARY INJECTION, ENGINE PERFORMANCE, AND EMISSIONS

In this chapter an attempt will be made to correlate the diesel engine performance emissions with secondary injection. It is expected that a relationship of this nature, if it exists, will be useful to diesel engine and fuel injection system designers. Because of the uncontrollable nature of most of the variables that define secondary injection, it is extremely difficult to isolate the effect of secondary injection alone on diesel engine performance and emissions. Some of these variables as stated in chapter one are: timing of the secondary injected fuel, duration of the secondary injection, distribution and size of the secondary injection process. It is observed, however, that for the conventional fuel injection system, keeping engine speed constant also keeps the beginning or timing of secondary injection about constant with a maximum deviation of $\pm$ 2.5°. For the experimental test run speeds of 1200 rpm, 1800 rpm, and 2400 rpm, the timings of secondary injection can be taken as -9°BTDC, -14°BTDC, and -29°BTDC respectively.

The directly controllable variable which indirectly encompasses most of the factors that define secondary injection is the quantity of fuel injected as secondary injection. The quantity of fuel injected as secondary injection is a direct function of the duration and rate or shape of the secondary injection process, while the distribution and size of the nozzle sprays have been correlated to flow rates (28). The only secondary injection variable not related to quantity of

secondary injected fuel is the time of the secondary injection, but as stated earlier, it was observed that this variable remained about constant for a given engine speed. It is therefore convenient to use the quantity of secondary injected fuel as the dependent variable in the correlation between secondary injection and diesel engine performance and emissions. For a better understanding of the total effects of secondary jection, the following two extreme cases have been considered.

The first case is the situation in which test runs for the conventional system (Series I) are compared with test runs for the modified system (Series II) on a total fuel-air ratio basis. In this case, test runs for Series I have the same total fuel-air ratio (and same total injection per cycle) as the corresponding test runs for Series II. The difference between the two test run series is that part of the fuel in Series I is injected as secondary injection.

The second case is the situation in which test runs for the conventional system (Series I) are compared with test runs for the modified system (Series III) on a main injection per cycle basis. In this case, test runs for Series I have the same main injection per cycle (and same main fuel-air ratio) as corresponding test runs for Series III. The difference between the two series is that Series I test runs have an accompanying secondary injection making them have total fuel-air ratios greater than their corresponding Series III test runs. Typical fuel injection rates used for test runs Series I, II and III are shown in Figures 6.1 through 6.4. In analyzing the performance and emissions results for the two cases, the results of test run Series I have been used as the reference points only because they are the test

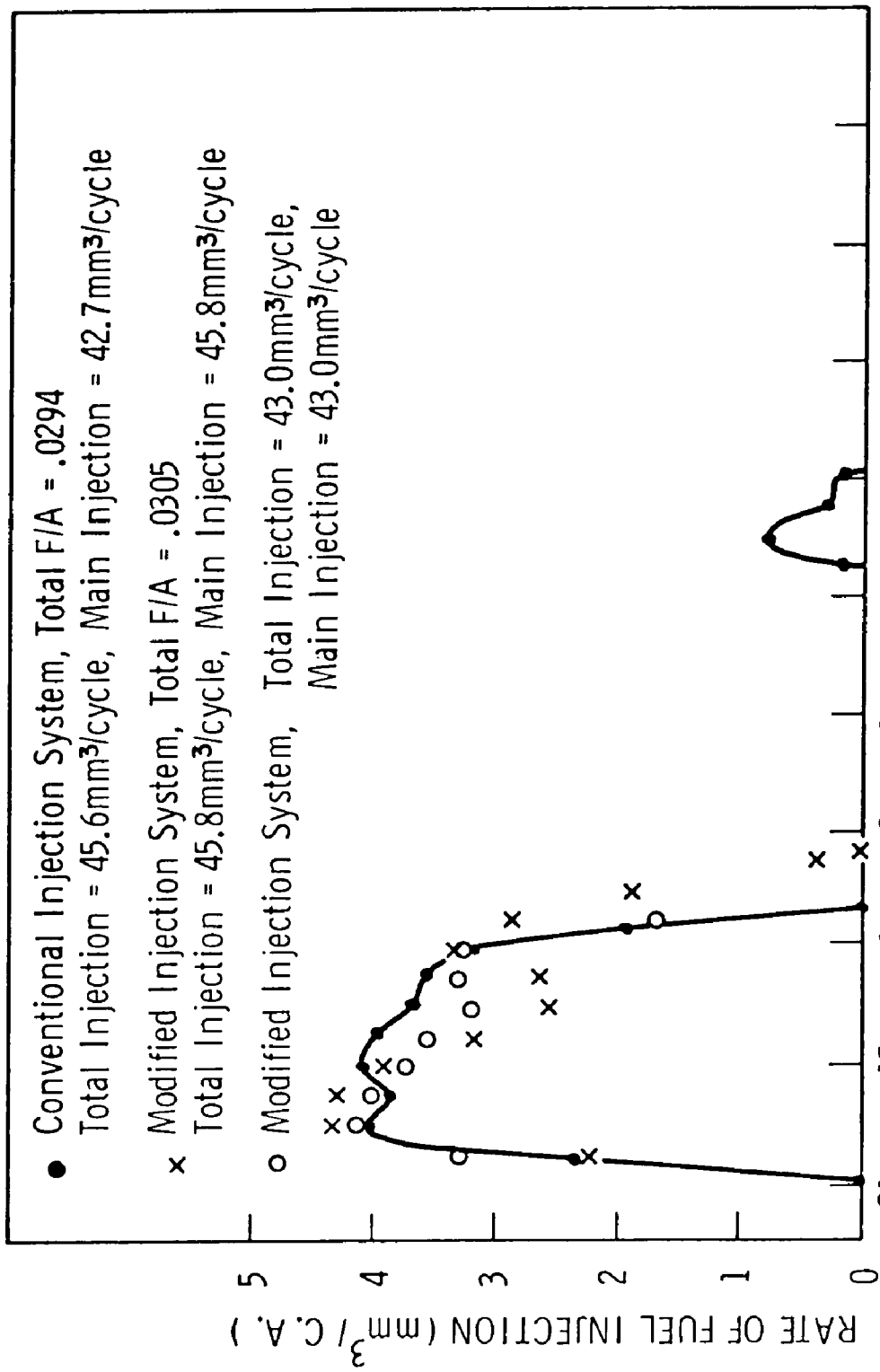


Figure 6.1 Comparison of the Rate of Injection Diagrams Used at an Engine Speed of 1200 rpm

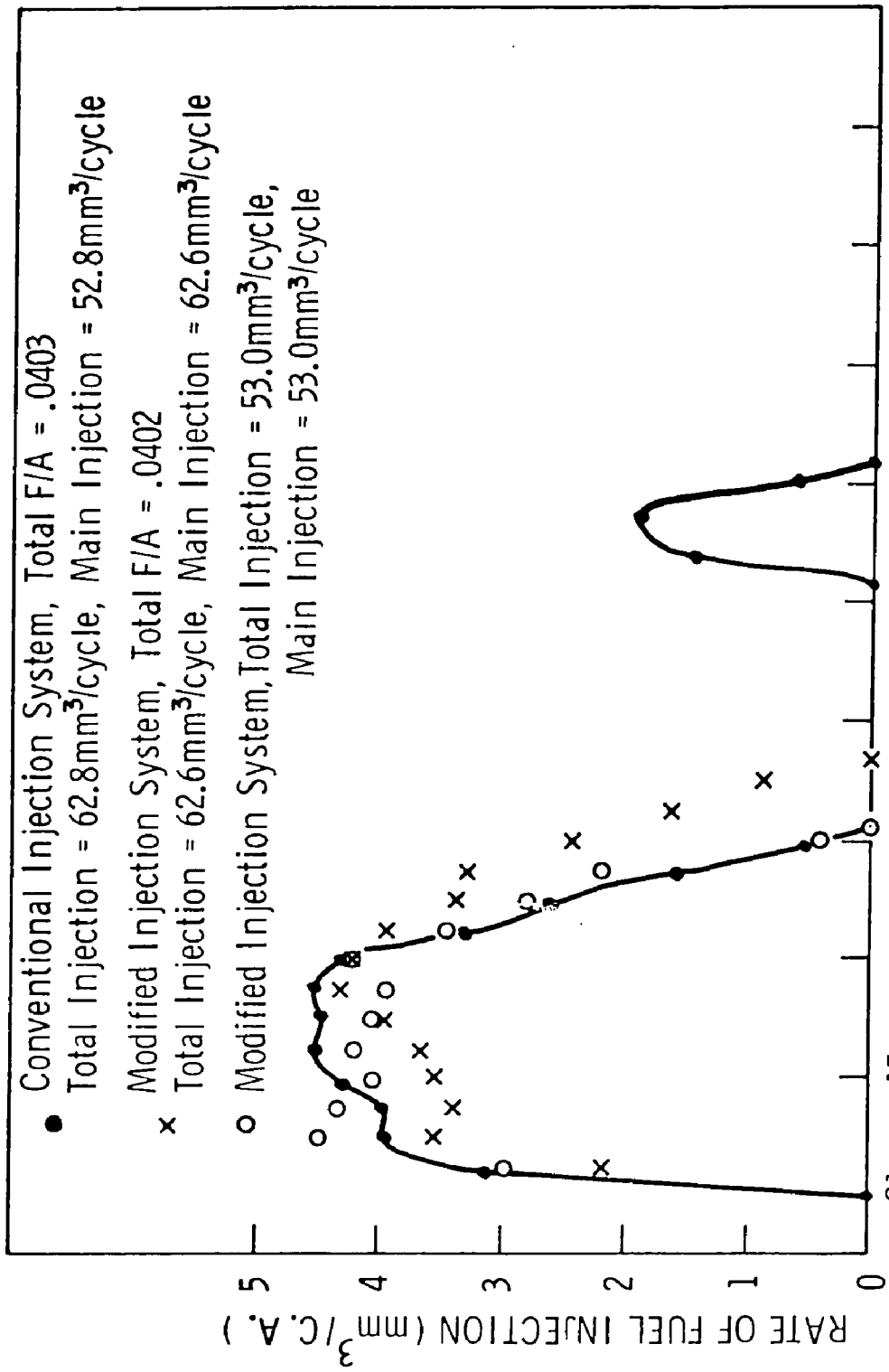


Figure 6.2 Comparison of the Rate of Injection Diagrams Used at an Engine Speed of 1200 rpm

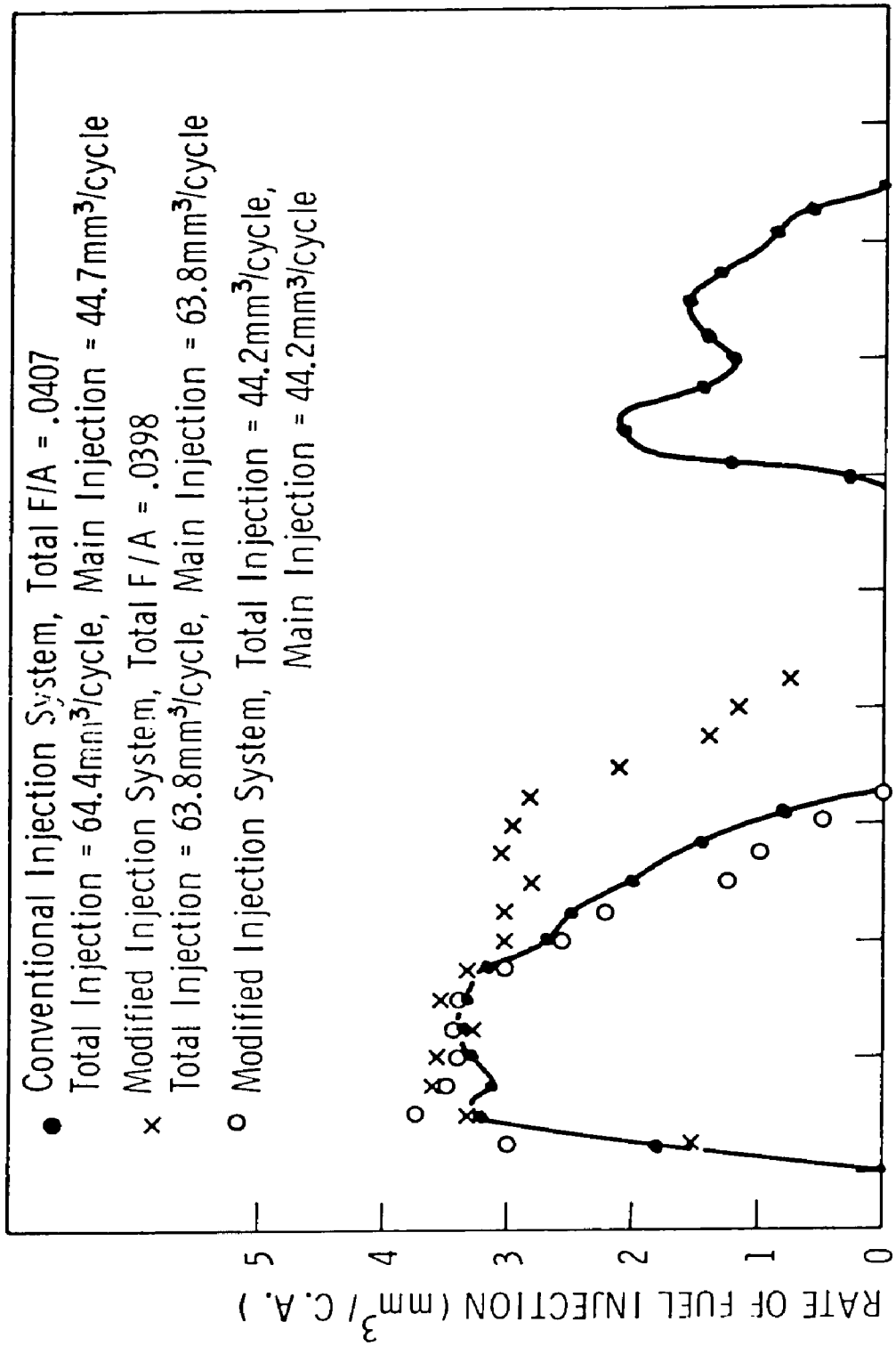


Figure 6.3 Comparison of the Rate of Injection Diagrams Used at an Engine Speed of 1800 rpm

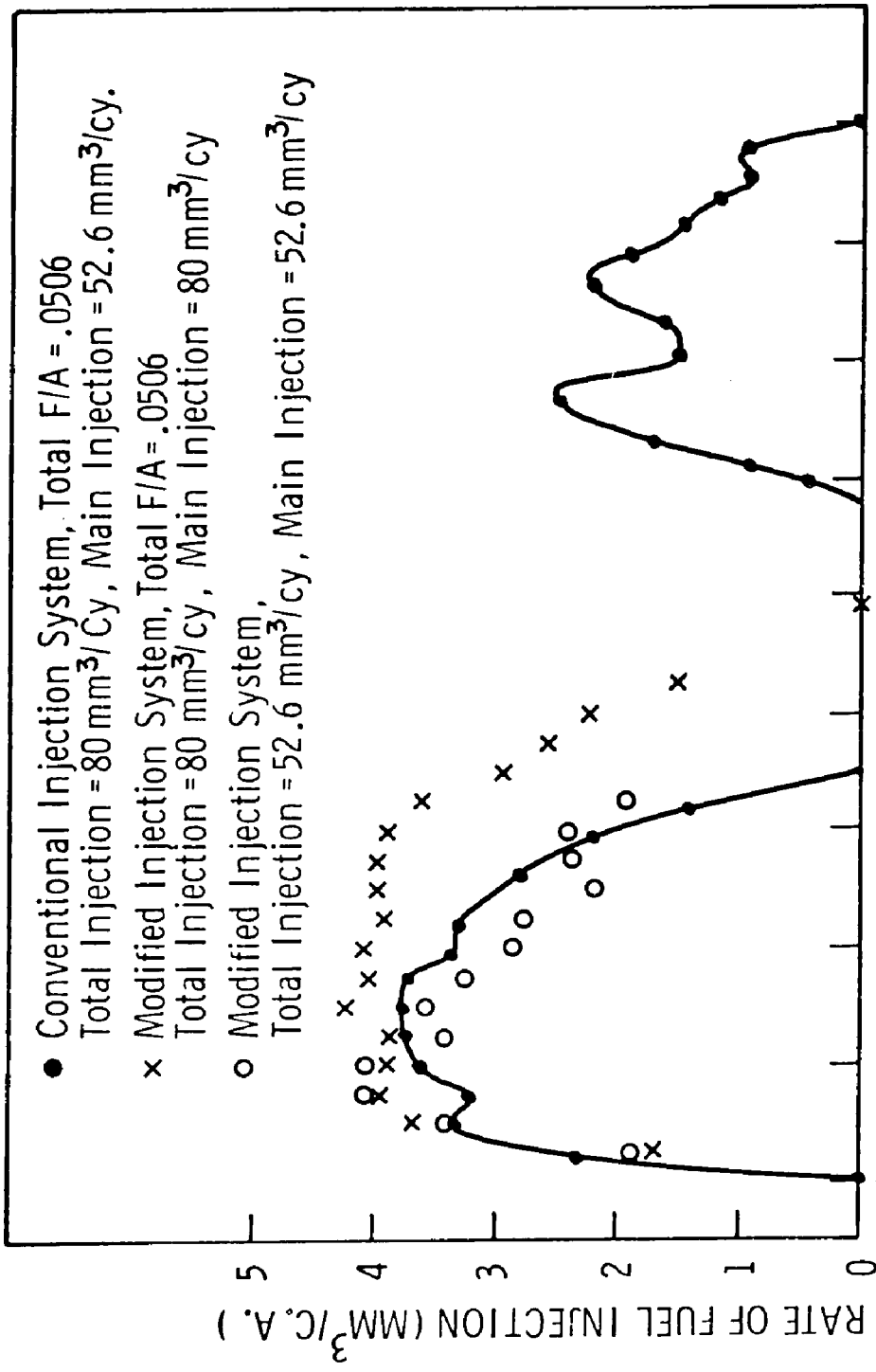


Figure 6.4 Comparison of the Rate of Injection Diagrams Used at an Engine Speed of 1800 rpm

runs common to both cases.

6.1 Results for Case I

The results obtained by comparing test runs Series I and II are presented and discussed in this section. Figure 6.5 shows the effect of secondary injection on percent reduction of BMEP. It shows that for all speeds, increasing the quantity of fuel injected as secondary injection reduces the BMEP. This reduction effect is greatest for engine speeds of 1800 rpm where as seen in Chapter III, the secondary injection percent is greatest. The figure also shows that the percent reduction of BMEP is maximum at a certain quantity of secondary injected fuel per cycle, after which it stays about the same or drops off a little.

Figure 6.6 shows the effect of secondary injection on the percent increase of BSFC. As secondary injection increases for a given speed so does the percent increase of BSFC until a maximum is reached where further increase of secondary injection does not affect the percent increase of BSFC.

Figure 6.7 shows the effect of secondary injection on percent increase of smoke. It shows that increasing secondary injection also causes an increase in smoke for all speeds. The percent increase is greatest at 1200 rpm and least at 2400 rpm. In fact, the percent increase is negative (decrease for most of the 2400 rpm test runs). The reason for this is that at 2400 rpm secondary injection begins very late at about 30°ATDC. At this point, the temperatures and pressures are such that the secondary injected fuel vaporizes, but does not burn. It therefore contributes to very high hydrocarbon in the exhaust, but

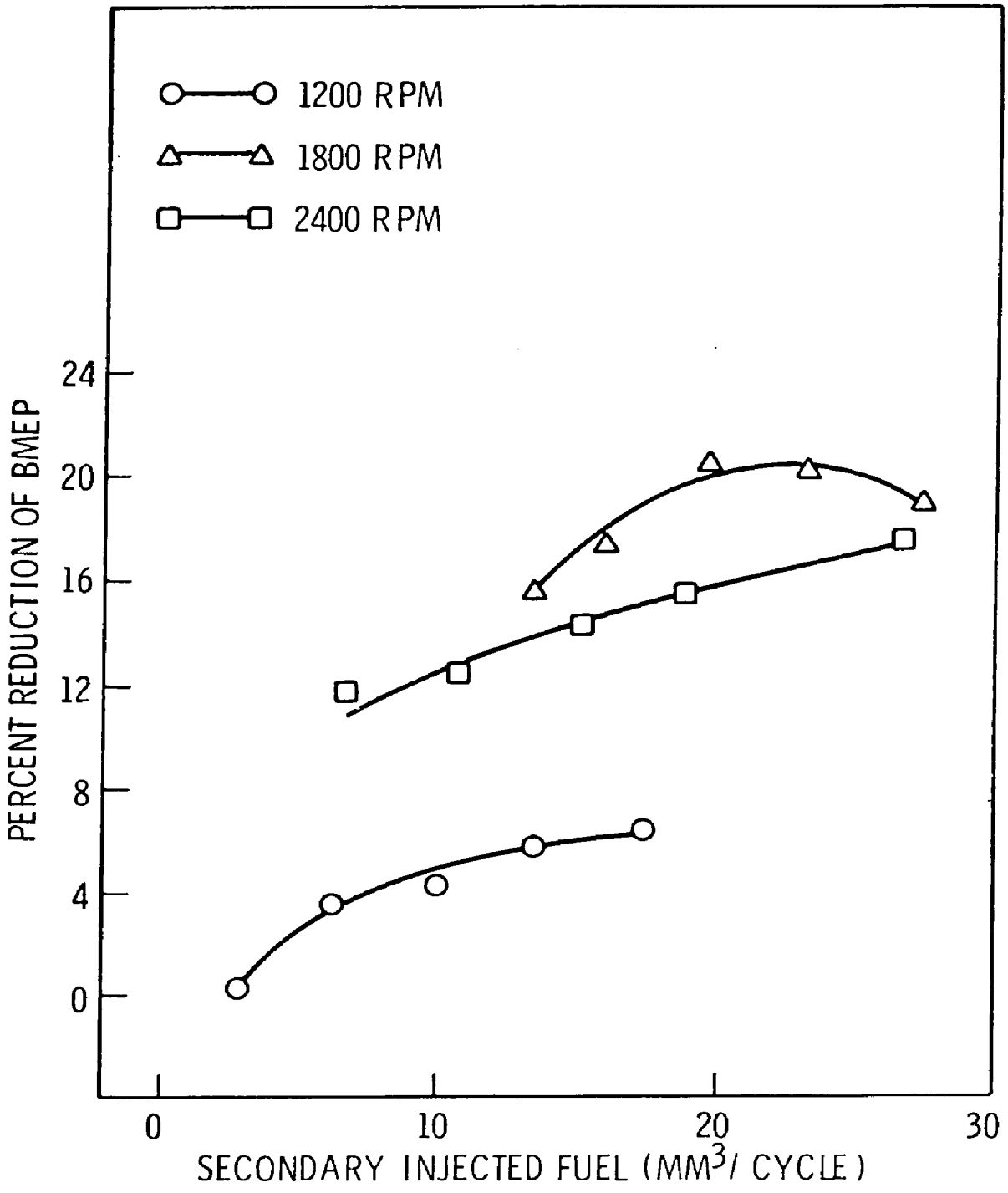


Figure 6.5 Effect of Secondary Injection on Percent Reduction of BMEP for Various Engine Speeds (Case I)

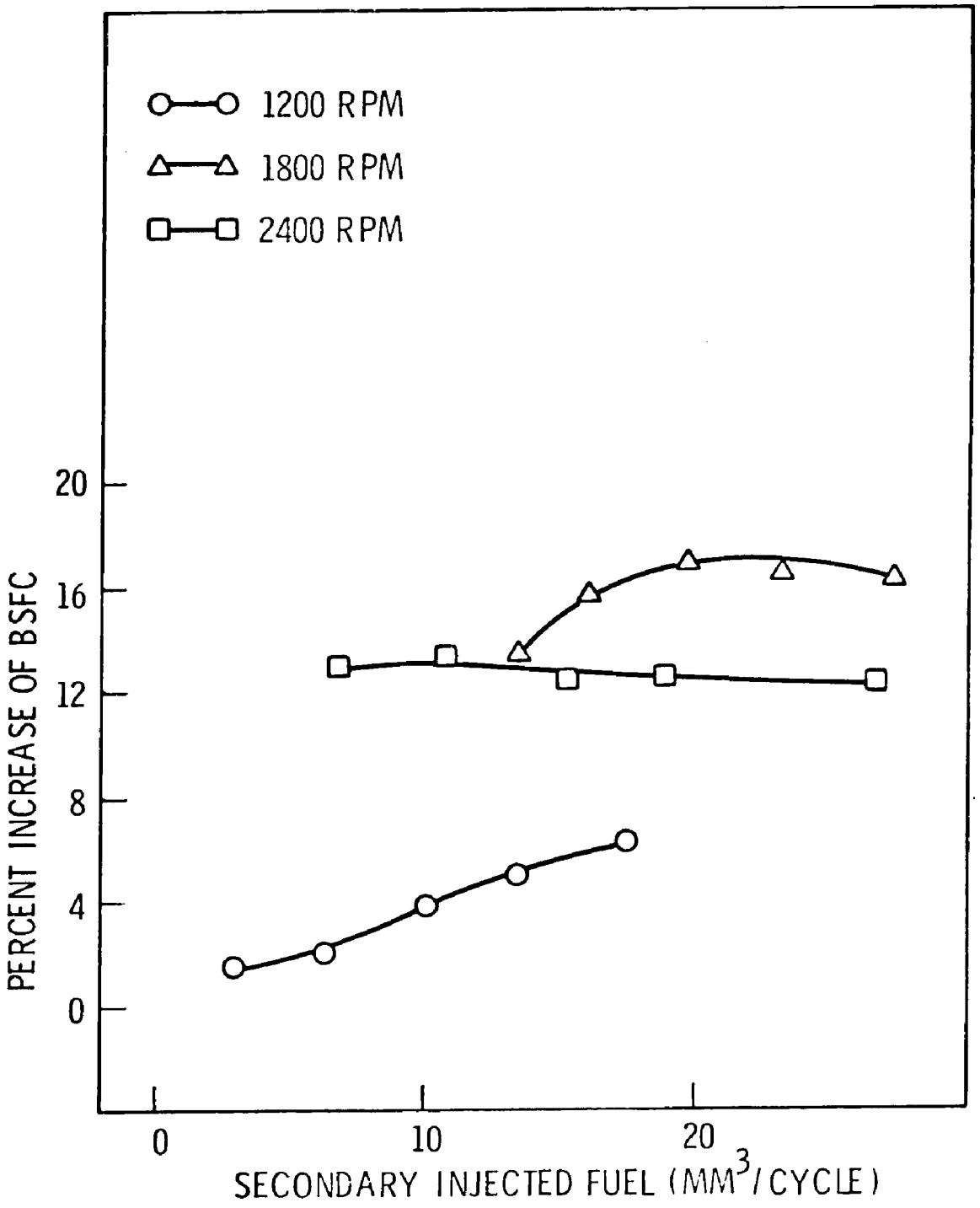


Figure 6.6 Effect of Secondary Injection on Percent Increase of BSFC for Various Engine Speeds (Case I)

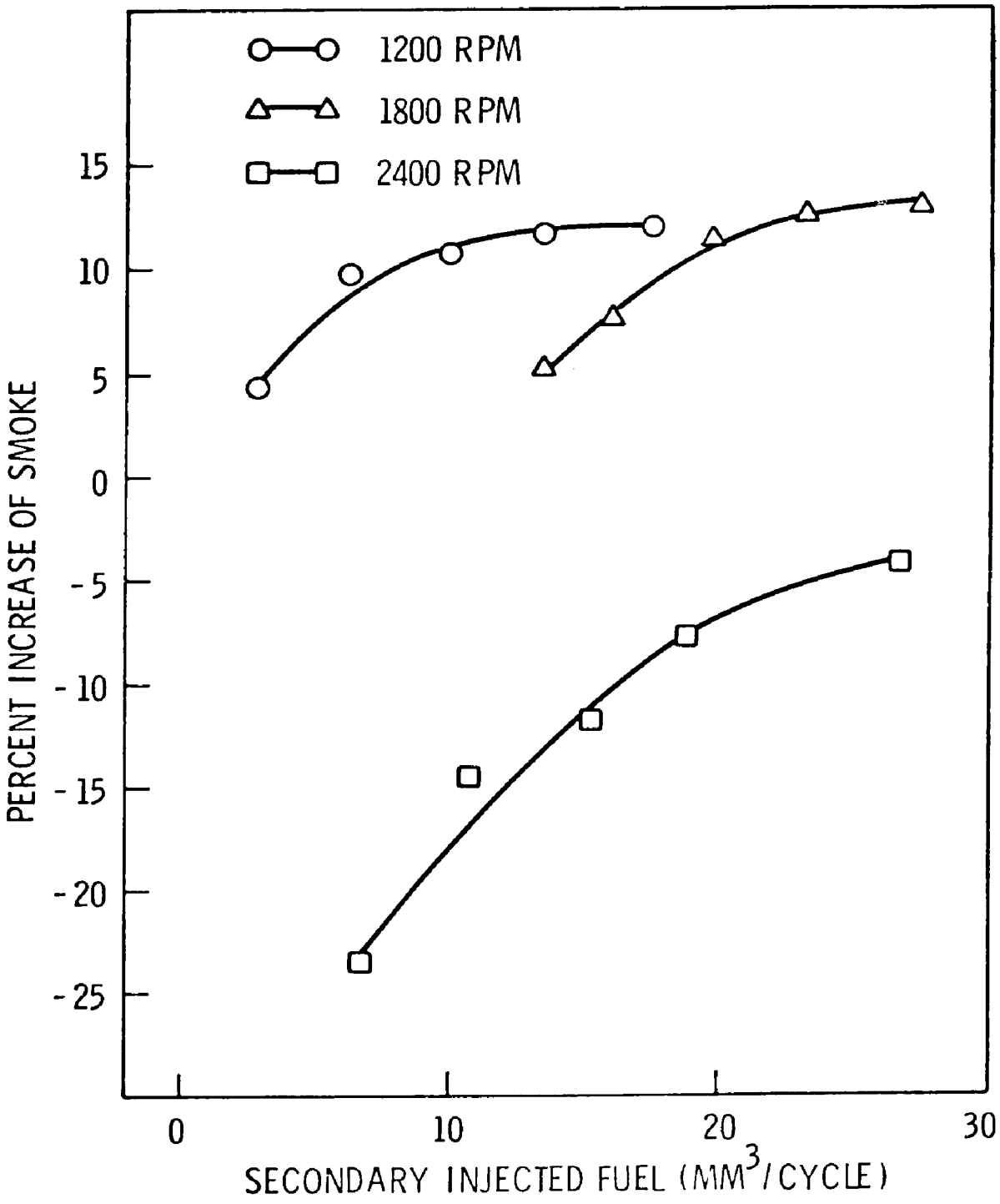


Figure 6.7 Effect of Seconday Injection on Percent Increase of Smoke for Various Engine Speeds (Case I)

does not contribute any smoke. The smoke contribution in this case is only from the main injection whose fuel-air ratio is less than the total fuel-air ratio.

Figure 6.8 shows the effect of secondary injection on percent increase of unburned hydrocarbon. It shows an increase of unburned hydrocarbon with an increase of secondary injection. The percent increase of unburned hydrocarbons is greatest for the 2400 rpm test runs as discussed in the previous paragraph.

Figure 6.9 shows the effect of secondary injection on percent increase of specific hydrocarbon emission. The trend is the same as for unburned hydrocarbons, showing that specific hydrocarbons increase with secondary injection for all speeds.

Similar figures for exhaust temperature and oxides of nitrogen are not presented here because for this case; the effect of secondary injection on exhaust temperature and oxides of nitrogen was negligible.

6.2 Results for Case II

The results obtained by comparing test runs Series I and III are presented and discussed in this section. Figure 6.10 shows the effect of secondary injection on percent increase of BMEP. It shows that the accompanying secondary injection for Series I test runs, because of the resulting increase in fuel-air ratio, causes an increase of BMEP over test runs for Series III. This increase reaches a maximum for a given speed and then begins to drop.

Figure 6.11 shows the effect of secondary injection on percent reduction of BSFC. It shows that as secondary injection is increased, the percent reduction of BSFC also increases mainly because of the

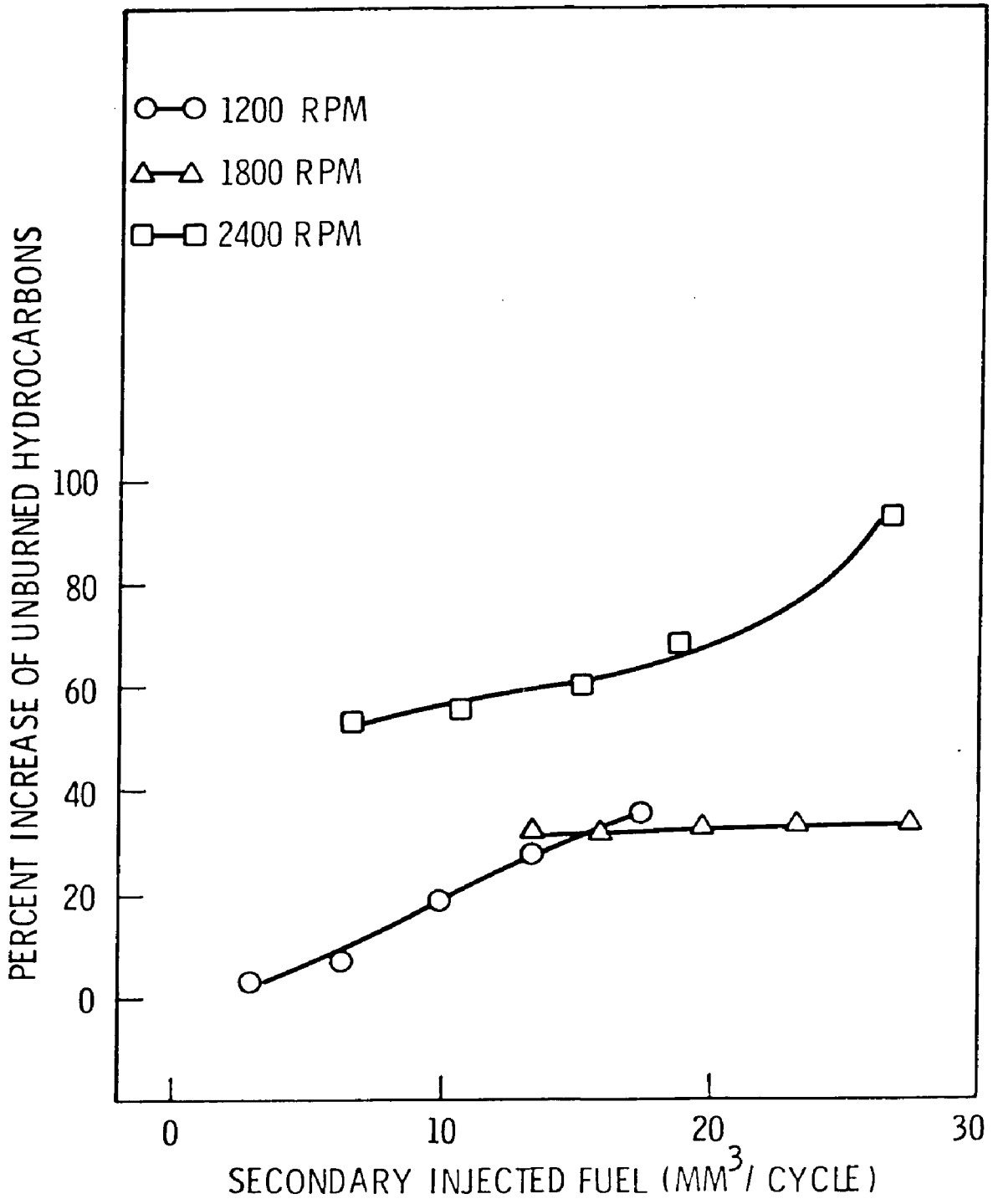


Figure 6.8 Effect of Secondary Injection on Percent Increase of Unburned Hydrocarbons For Various Engine Speeds (Case I)

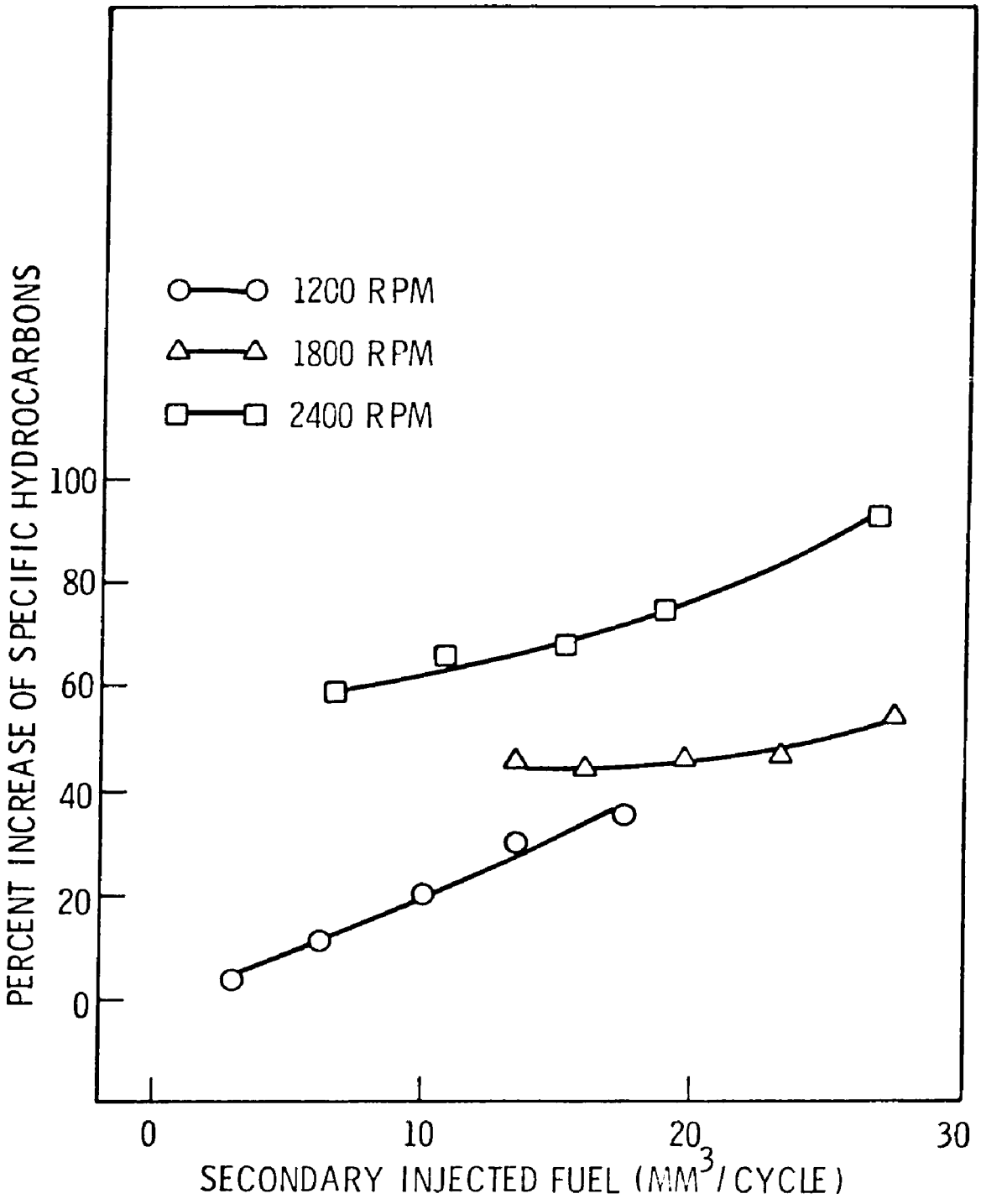


Figure 6.9 Effect of Secondary Injection on Percent Increase of Specific Hydrocarbon Emissions (Case I)

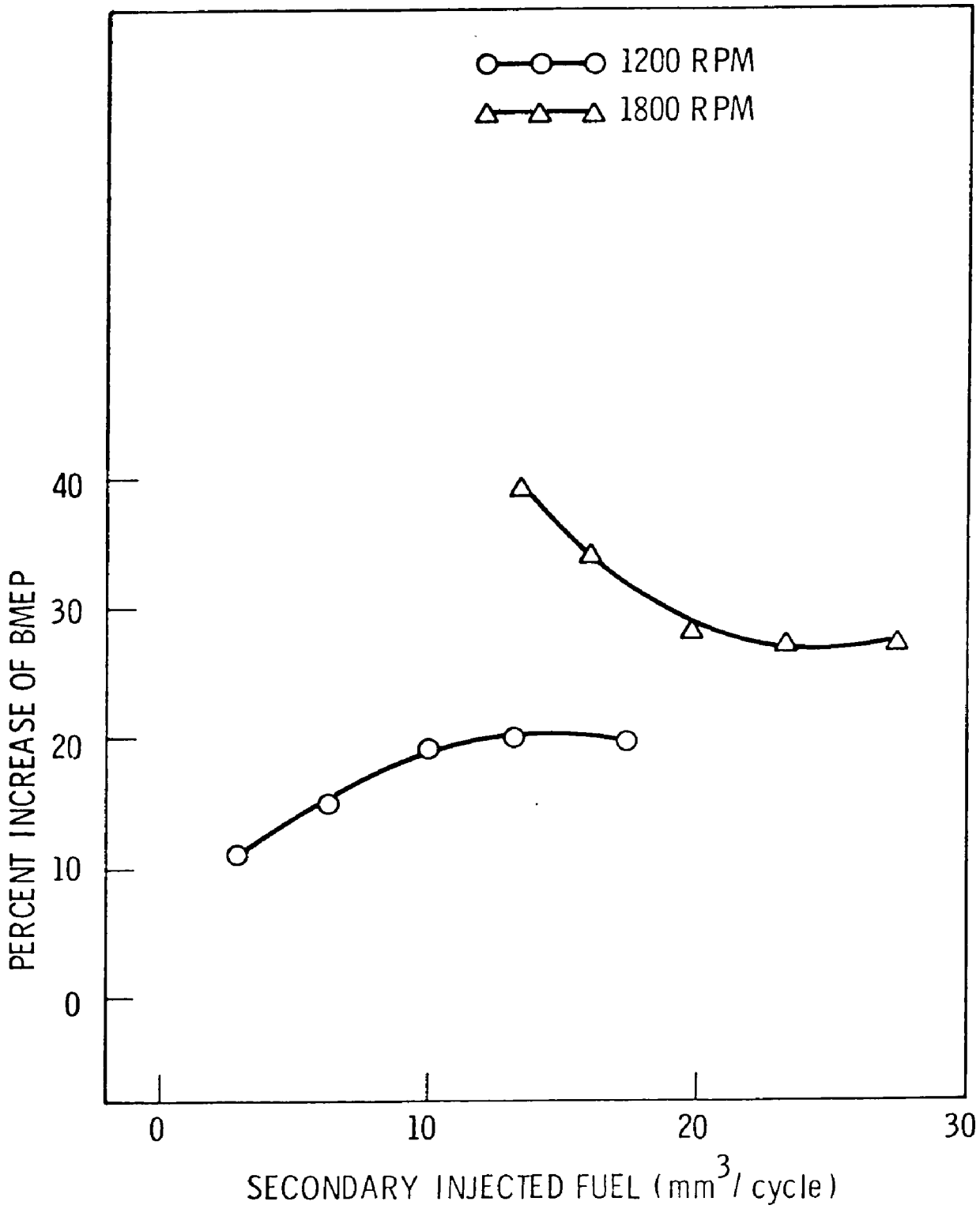


Figure 6.10 Effect of Secondary Injection on Percent Increase of BMEP (Case II)

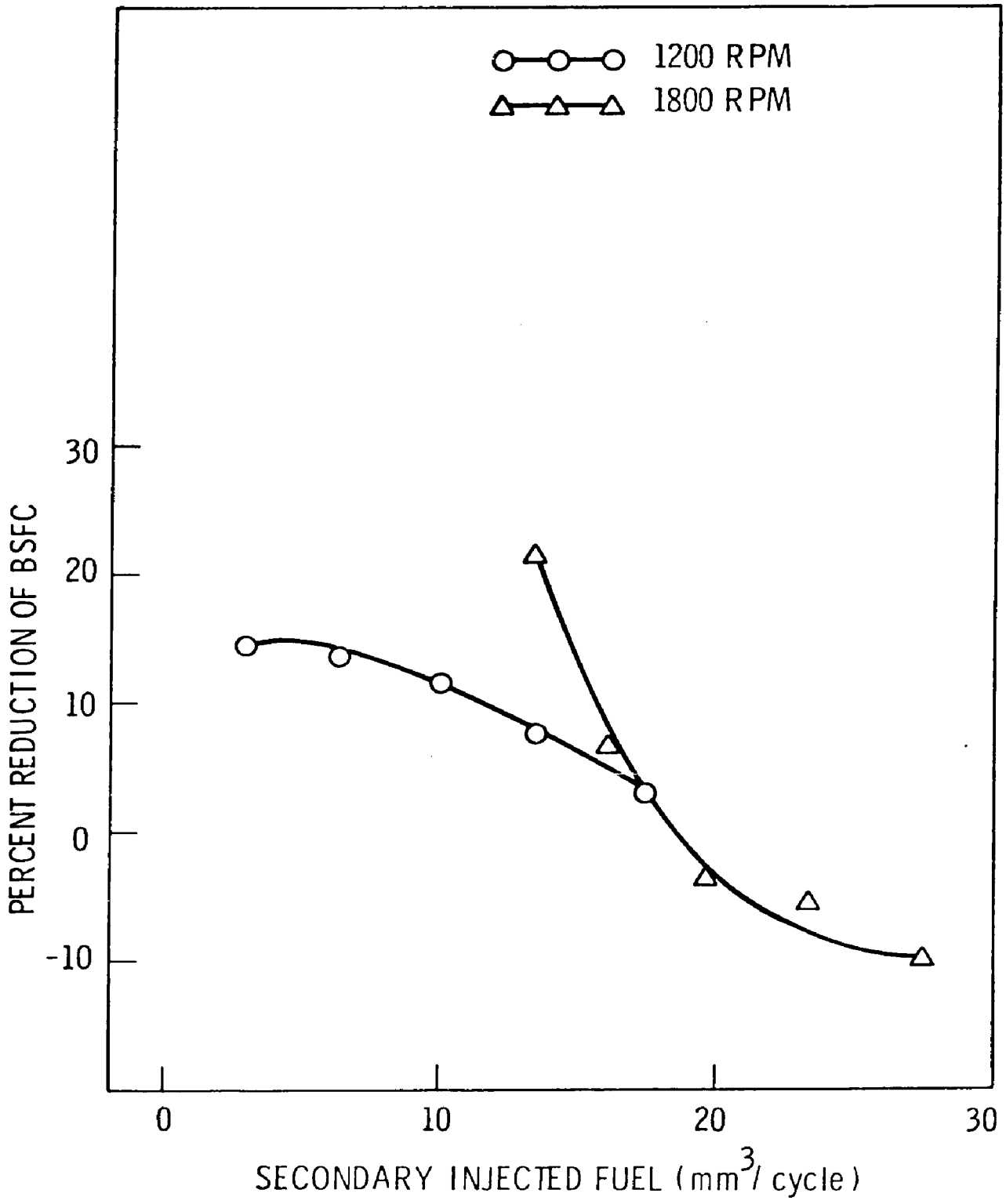


Figure 6.11 Effect of Secondary Injection on Percent Reduction of BSFC (Case II)

effection of increasing fuel-air ratio. This increase reaches its maximum value for a given speed and then begins to drop. It is seen that for the 1800 rpm condition, the effect is to cause a percent increase of BSFC after a secondary injected fuel of about 18 mm^3/cycle.

Figure 6.12 shows the effect of secondary injection on smoke. It shows that increasing secondary injection results in an increase of smoke. Like the other results, it also shows that for a given speed there is a quantity of secondary injection per cycle that produces maximum smoke.

Figures 6.13 and 6.14 show the effect of secondary injection on percent increase of unburned hydrocarbon and specific hydrocarbon emission respectively. They show an initial increase of hydrocarbons with increasing secondary injection, however, as the secondary injection increases further, the trend is reversed. The negative percent increase (decrease) of hydrocarbons at high secondary injection can be attributed to the effect of increasing fuel-air ratio on hydrocarbons and also the resulting higher temperatures with higher fuel-air ratios. These high temperatures can cause hydrocarbon combustion in the exhaust line and mixing tank resulting in the apparent decrease of hydrocarbons shown in the figures.

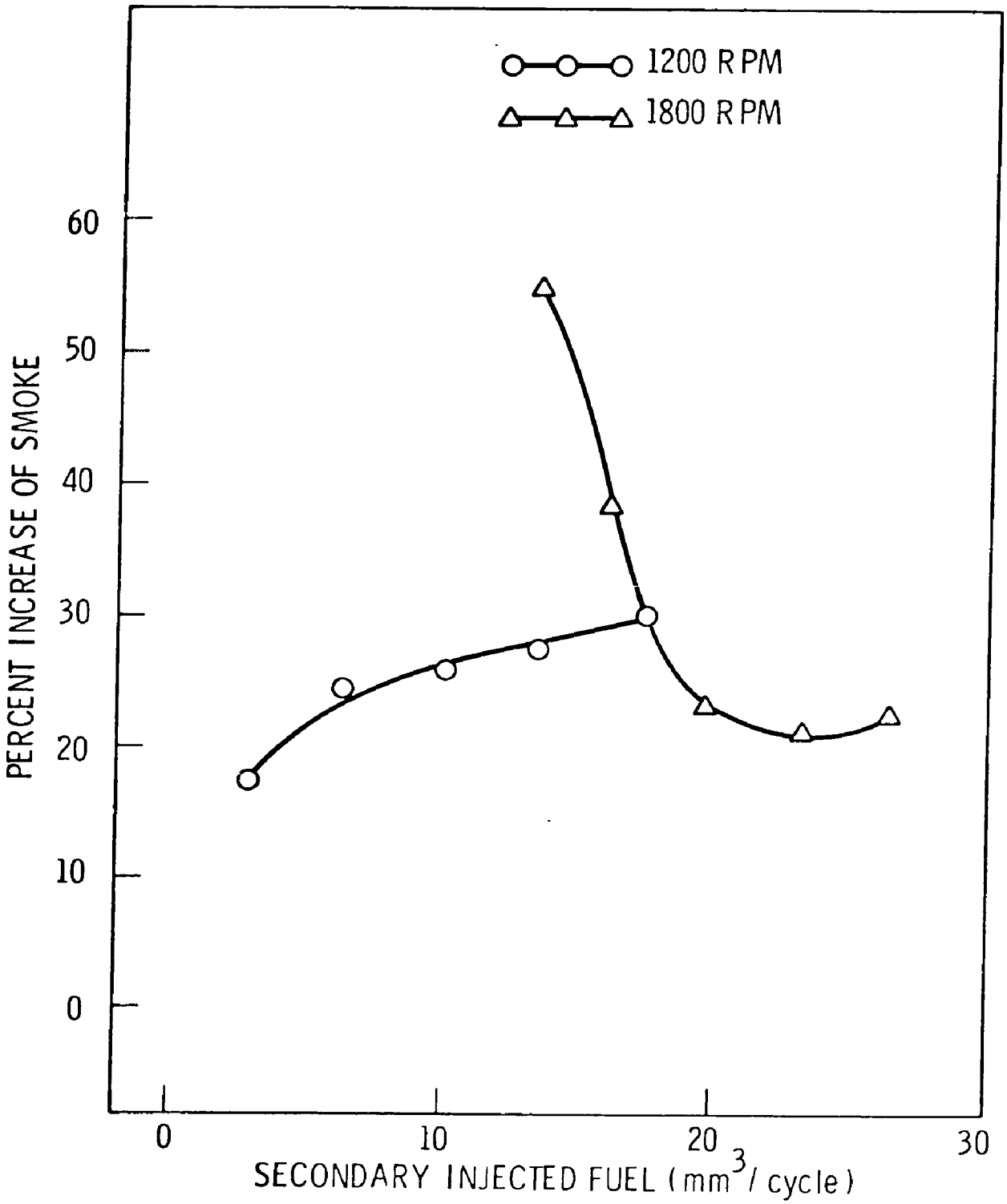


Figure 6.12 Effect of Secondary Injection on Percent Increase of Smoke (Case II)

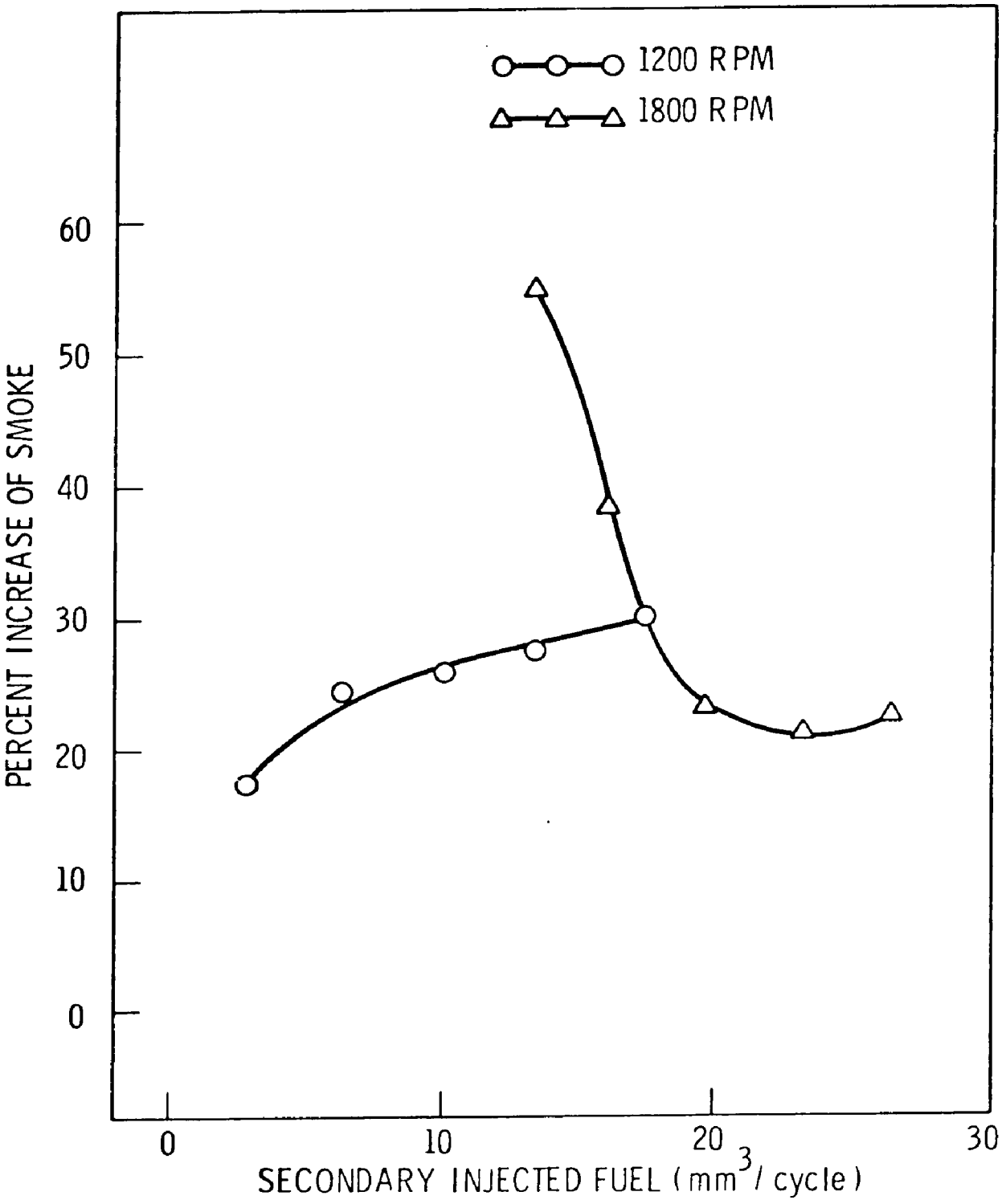


Figure 6.12 Effect of Secondary Injection on Percent Increase of Smoke (Case II)

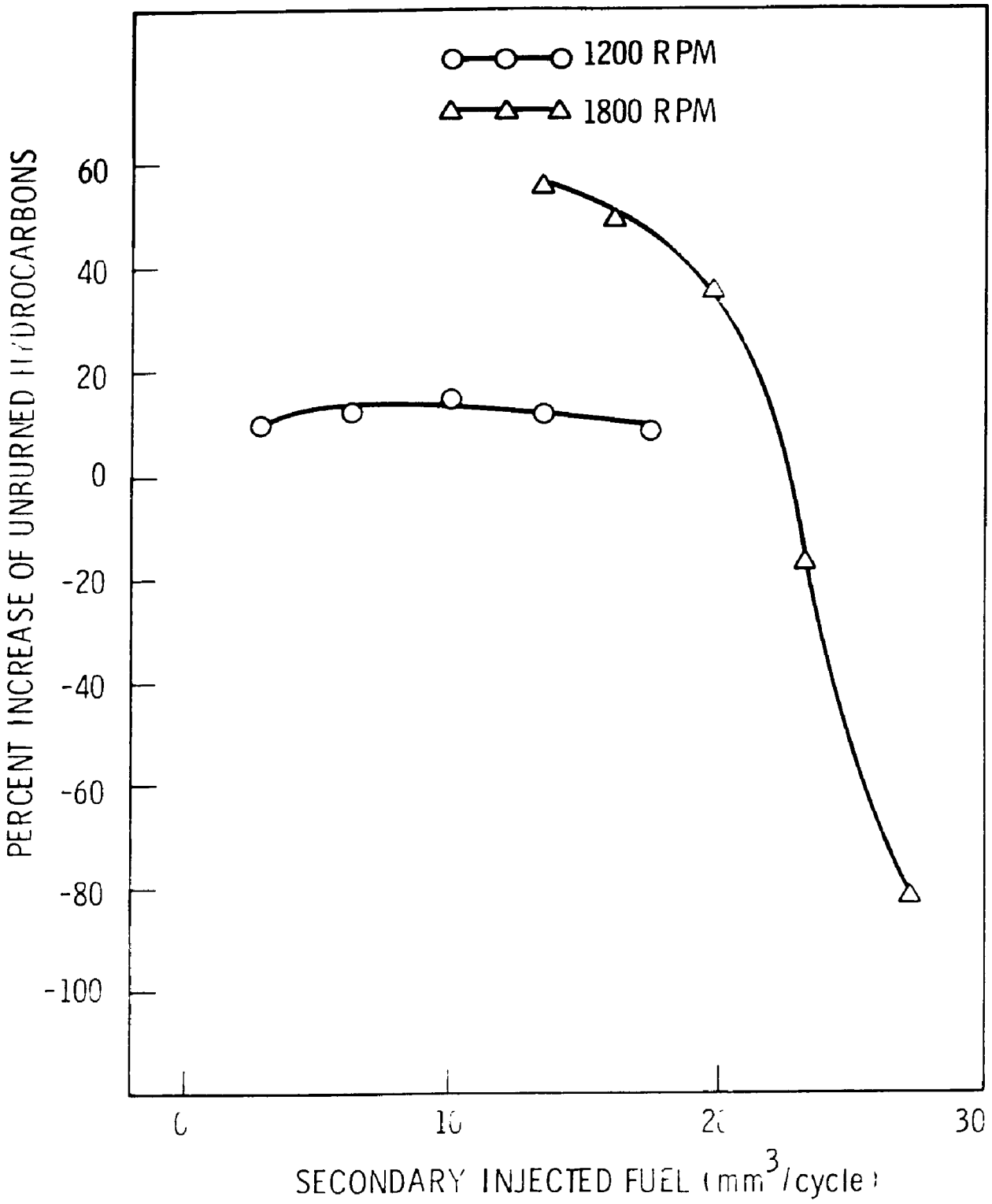


Figure 6.13 Effect of Secondary Injection on Percent Increase of Unburned Hydrocarbons (Case II)

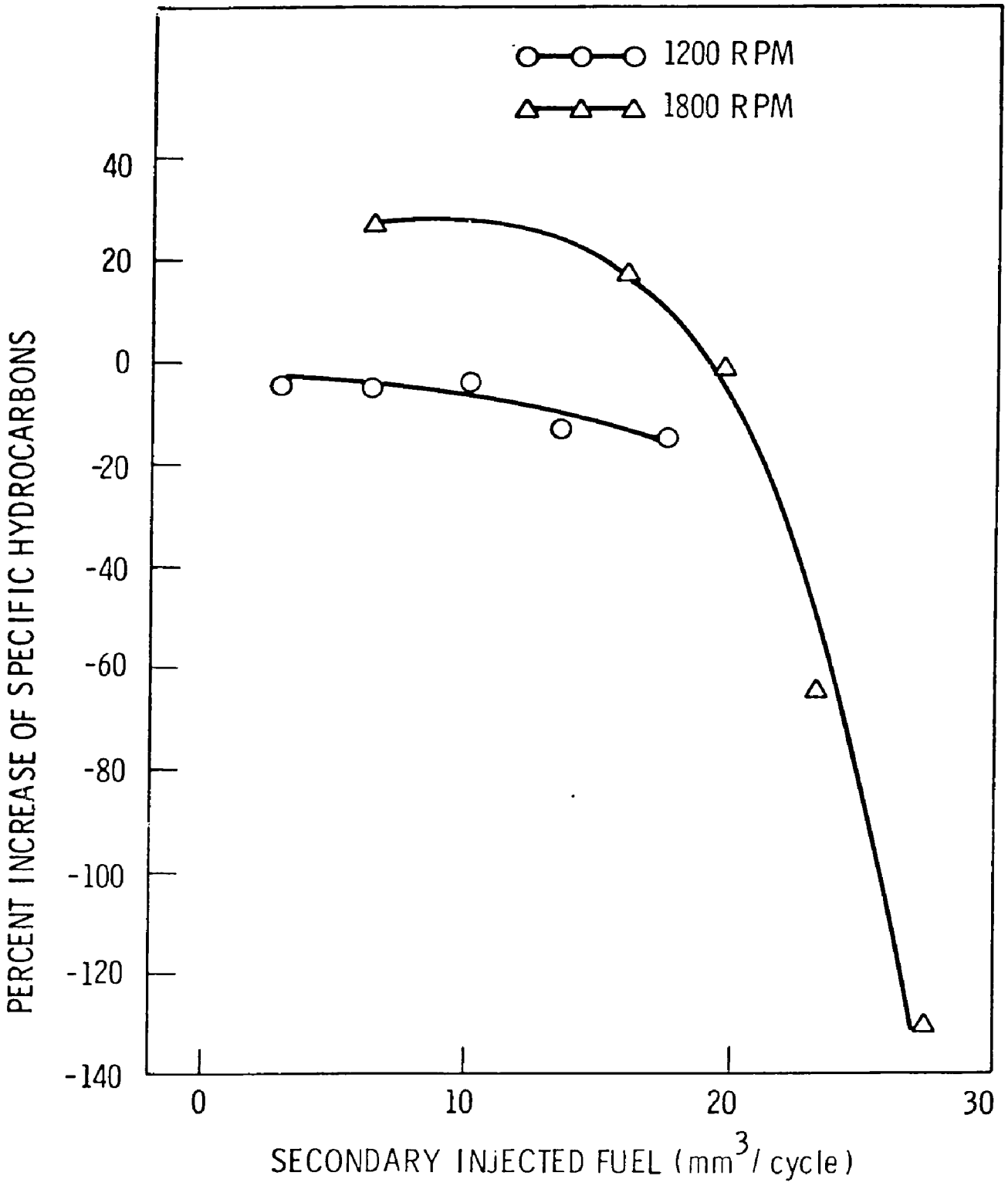


Figure 6.14 Effect of Secondary Injection on Percent Increase of Specific Hydrocarbon Emission (Case II)

CHAPTER VII

GENERAL DISCUSSION

The significant factors, that can determine the nature of combustion of a secondary injected fuel are:

a) Pentration, atomization, and distribution of fuel spray

b) Availability of oxygen

c) Mixing of fuel and air

d) Time available for combustion

In this chapter, an attempt is made to quantitatively discuss these factors as they relate to secondary injection in order to shed some more light on the experimental results presented in the previous two chapters.

Spray penetration has been extensively studied over a long period of time (11), (28), (37). (46), and it has been observed that fuel spray penetration increases with increasing injection pressure and decreases with increasing combustion chamber pressure. All the correlations given for either small or medium-size droplets as do exist in diesel fuel sprays, indicate that spray penetration is roughly proportional to the square root of the pressure drop across the nozzle. From the fuel line and combustion chamber pressure traces, a computation of the square root of the average pressure drop across the nozzle is made as a rough estimate of the relative average spray penetration for each test run. These are tabulated in Appendix A. It clearly shows that for all speeds, the spray tip penetration is more for the main injection than for secondary injection.

For high-speed diesel engines where only a short time is avail-

able for combustion, a high degree of atomization is required to ensure a droplet lifetime much shorter than the time available for combustion. A mean drop size has been defined for a spray by Sauter as a measure of the atomization of the spray. This is called Sauter mean diameter and is defined as the diameter of a drop having the same surface area to volume ratio as the spray. Many studies of droplet sizes in nozzles have been carried out by various investigators. Knight (28) has presented the following correlation for the SMD of a spray and fuel nozzle characteristics.

$$SMD\ (\mu) = 220\ (\Delta P)^{-.458}(Q)^{.209}(\nu_f)^{.215}$$

where:

SMD = Sauter mean diameter (microns)

ΔP = Pressure across nozzle (psi)

Q = Flow rate (lbm/hr)

ν_f = Kinematic viscosity of fuel (centistokes)

Shipinski (40) modified this expression in the fashion of Austen and Lyn (2) to account for the two orifices in series in the injection nozzle, the needle seat orifice, and the nozzle holes orifice. The modified expression is:

$$SMD(\mu) = 220\ (\Delta P)^{-.458}(Q)^{.209}(\nu_f)^{.215}\left(\frac{A_{orf}}{A(t)_{eff}}\right)^{.916}$$

where:

A_{orf} = the exit orifice area (in^2)

$A(t)_{eff}$ = the effective orifice area across which ΔP is measured, (in^2)

This equation has been used to compute the average spray droplet size for both main and secondary injections, and the results are tabulated in Appendix A. It is seen that in general the secondary injected fuel has average droplets larger than the corresponding main injected fuel. The percentage difference ranges from a low of about 4 percent for test run No. 1 to a high of about 50 percent for test run No. 9.

To completely understand the effect of availability of oxygen, one must have data on the spatial temporal fuel-air ratio in the combustion chamber. No quantitative theoretical or experimental data is readily available on the variation of local fuel-air ratio with time. It is self-evident, however, that when secondary injection occurs, the fuel is injected into a mixture of swirling air and combustion products of the main injection. It is therefore expected that the local fuel-air ratios will be a direct function of the overall fuel-air ratio, and the turbulent mixing due to swirl and to a lesser extent on squish. The higher the swirl the better the mixing of the secondary injected fuel and air, and the higher the degree of completeness of combustion.

The factor that has the strongest influence on the burning of the secondary injected fuel is the time available for combustion. If the secondary injection occurs early in the cycle, fairly close to the top dead center, it can still burn completely and contribute to engine power and reduce emissions. If, however, the secondary injection occurs late in the cycle, a few degrees before the exhaust valve opens, it contributes nothing to engine power and this injected fuel has to show in high hydrocarbon readings. If temperatures are high enough for carbon formation, high smoke readings also result. The timing and period of secondary injection therefore determine the time available

for the combustion of the secondary injected fuel. The timing and period of secondary injection of the test runs are tabulated in Appendix A. The timing is about a constant for any fixed speed while the duration increases as load and secondary injected fuel are increased.

CHAPTER VIII

CONCLUSIONS

The results presented in this thesis show the following:

1. Secondary injection generally occurs at conditions of simultaneously high load and speed in conventional jerk pump type fuel injection systems. The secondary injection percent of the total injection is almost a linear function of load (fuel-air ratio) for a constant engine speed. An increase in load (fuel-air ratio) caused a corresponding increase of secondary injection. For a fixed load, however, there is an optimum speed for which secondary injection is a maximum.

2. It is possible to control the high pressure transients in a diesel fuel injection system by a redesign of the spill port holes and delivery valve. In so doing, secondary injections are completely eliminated over a wide range of engine operating conditions while the main injection is not significantly altered.

3. Secondary injection has a significant effect on diesel engine performance. For a given quantity of fuel injected per cycle, a secondary injecting case will result in a decrease of engine power output (BMEP) and increase fuel consumption (BSFC) over a case without secondary injection. The decrease in power output and increase in fuel consumption depend on the timing of secondary injection, duration of secondary injection, pressure differential across nozzle during secondary injection and a number of other engine variables. For the experimental conditions and engine used in this test, a maximum power reduction of 20.5% and maximum fuel consumption increase of 17% were

observed at the same point of 1800 rpm engine speed and about 21 mm^3/ cycle secondary injected fuel.

4. Secondary injection has a profound effect on some diesel engine exhaust emissions. Again for a given quantity of fuel injected per cycle, a secondary injection case will in general increase smoke, unburned hydrocarbons, and specific hydrocarbons over a case without secondary injection. Exhaust temperatures and oxides of nitrogen showed no noticable differences. Maximum smoke increase of about 13.5 percent was observed for engine speeds of 1200 rpm and 1800 rpm. For 2400 rpm tests, a surprising smoke reduction was observed, while increase of unburned hydrocarbons and specific hydrocarbons of up to 92 percent occurred.

APPENDIX A

FUEL INJECTION TEST RESULTS - SERIES I THROUGH III

TABLE V

FUEL INJECTION TEST RESULTS - SERIES I

(Runs with Conventional Injection System)

Run No.	1	2	3	4	5
Engine Speed, rpm	1200	1200	1200	1200	1200
Fuel-Air Ratio	.0294	.0351	.0449	.0449	.0484
Total Inj., mm^3/cycle	45.6	54.7	62.8	69.0	75.5
Main Inj., mm^3/cycle	42.7	48.4	52.8	55.6	58.1
Sec. Inj., mm^3/cycle	2.9	6.3	10.0	13.4	17.4
Sec. Inj., percent	6.34	11.50	15.90	19.40	23.10
Main Inj., S.M.D., microns	17.5	17.7	16.7	16.6	16.7
Sec. Inj., S.M.D., microns	18.3	19.8	20.9	21.6	20.7
Discharge Coefficient	.443	.431	.453	.442	.458
Main Inj. Period, °C.A.	16.8	18.2	18.9	19.6	20.0
Sec. Inj. Timing, °ATDC	10.5	10.5	9.5	10.5	8.0
Sec. Inj. Period, °C.A.	4.6	6.9	6.9	7.5	10.5
Main Inj. Ave. $\Delta P^{1/2}$, $(lbf)^{1/2}$/in.	50	51.6	53.4	55.2	55.7
Sec. Inj. Ave. $\Delta P^{1/2}$, $(lbf)^{1/2}$/in.	34.65	34.8	36.2	36.7	37.1

TABLE VI

FUEL INJECTION TESTS RESULTS - SERIES I

(Runs with Conventional Injection Systems)

Run No.	6	7	8	9	10
Engine Speed, rpm	1800	1800	1800	1800	1800
Fuel-Air Ratio	.0303	.0345	.0407	.0456	.0506
Total Inj., mm^3/cycle	48.0	54.5	64.4	71.9	80.0
Main Inj., mm^3/cycle	34.6	38.5	44.7	48.7	52.6
Sec. Inj., mm^3/cycle	13.4	16.0	19.7	23.2	27.4
Sec. Inj., percent	27.96	29.4	30.6	32.24	34.28
Main Inj., S.M.D., microns	16.6	16.9	16.3	16.0	15.8
Sec. Inj., S.M.D., microns	22.3	24.9	24.6	24.8	23.5
Discharge Coefficient	.428	.437	.460	.466	.476
Main Inj. Period, °C.A.	19.5	20.0	21.0	22.5	23.0
Sec. Inj. Timing, °ATDC	15.0	13.5	13.5	13.5	12
Sec. Inj. Period, °C.A.	13.5	13.5	16.0	18.0	20.5
Main Inj. Ave. $\Delta P^{1/2}$, $(lbf)^{1/2}$/in.	53.7	53.8	56.8	58.5	60.3
Sec. Inj. Ave. $\Delta P^{1/2}$, $(lbf)^{1/2}$/in.	34.1	31.2	31.8	32.2	34.3

TABLE VII

FUEL INJECTION TEST RESULTS - SERIES I

(Runs with Conventional Injection System)

Run No.	11	12	13	14	15
Engine Speed, rpm	2400	2400	2400	2400	2400
Fuel-Air Ratio	.0293	.0347	.0400	.0445	.0508
Total Inj., mm^3/cycle	45.7	54.7	62.8	69.8	80.6
Main Inj., mm^3/cycle	39.0	44.0	48.3	51.0	53.9
Sec. Inj., mm^3/cycle	6.7	10.7	15.2	18.8	26.7
Sec. Inj., percent	14.7	19.5	23.0	27.0	33.1
Main Inj., S.M.D., microns	17.2	17.4	17.6	16.5	16.5
Sec. Inj., S.M.D., microns	20.5	20.8	21.3	18.8	22.3
Discharge Coefficient	.569	.602	.632	.639	.643
Main Inj. Period, °C.A.	23	24	25	25.5	26
Sec. Inj. Timing, °ATDC	30	30	30	30	27
Sec. Inj. Period, °C.A.	9	10	11	12	22
Main Inj. Ave. $\Delta P^{1/2}$,$(lbf)^{1/2}$/in.	54.5	54.4	56.0	59.5	57.3
Sec. Inj. Ave. $\Delta P^{1/2}$,$(lbf)^{1/2}$/in.	37.0	39.8	41.0	45.3	37.7

TABLE VIII

FUEL INJECTION TEST RESULTS - SERIES II

(Runs with Modified Injection System-No Secondary Injection)

Run No.	16	17	18	19	20
Engine Speed, rpm	1200	1200	1200	1200	1200
Fuel-Air Ratio	.0305	.0349	.0402	.0443	.0492
Total Inj., mm^3/cycle	45.8	54.3	62.6	69.0	77.3
Main Inj., mm^3/cycle	45.8	54.3	62.6	69.0	77.3
Sec. Inj., mm^3/cycle	--	--	--	--	--
Sec. Inj., percent	--	--	--	--	--
Main Inj., S.M.D., microns	20.6	18.4	17.7	17.9	18.0
Sec. Inj., S.M.D., microns	--	--	--	--	--
Discharge Coefficient	.589		.440		.491
Main Inj. Period, °C.A.	17	20	22	23	25
Sec. Inj. Timing, °ATDC	--	--	--	--	--
Sec. Inj. Period, °C.A.	--	--	--	--	--
Main Inj. Ave. $\Delta P^{1/2}$, $(lbf)^{1/2}$/in.	42.4	47.6	51.1	51.5	51.5
Sec. Inj. Ave. $\Delta P^{1/2}$, $(lbf)^{1/2}$/in.	-	--	--	--	--

TABLE IX

FUEL INJECTION TEST RESULTS - SERIES II

(Runs with Modified Injection System-No Secondary Injection)

Run No.	21	22	23	24	25
Engine Speed, rpm	1800	1800	1800	1800	1800
Fuel-Air Ratio	.0300	.0353	.0398	.0450	.0509
Total Inj., mm^3/cycle	47.3	56.0	63.8	71.0	80.2
Main Inj., mm^3/cycle	47.3	56.0	63.8	71.0	80.2
Sec. Inj., mm^3/cycle	--	--	--	--	--
Sec. Inj., percent	--	--	--	--	--
Main Inj., S.M.D., microns	20.3	20.1	20.1	20.2	19.1
Sec. Inj., S.M.D., microns	--	--	--	--	--
Discharge Coefficient	.699		.621		.653
Main Inj. Period, °C.A.	19.5	25.0	29.0	30.0	31.5
Sec. Inj. Timing, °ATDC	--	--	--	--	--
Sec. Inj. Period, °C.A.	--	--	--	--	--
Main Inj. Ave. $\Delta P^{1/2}$, $(lbf)^{1/2}$/in.	46.1	46.0	45.1	46.2	50.0
Sec. Inj. Ave. $\Delta P^{1/2}$, $(lbf)^{1/2}$/in.	--	--	--	--	--

TABLE X

FUEL INJECTION TEST RESULTS-SERIES II

(Runs with Modified Injection System-No Secondary Injection)

Run No.	26	27	28	29	30
Engine Speed, rpm	2400	2400	2400	2400	2400
Fuel-Air Ratio	.0296	.0343	.0402	.0456	.0478
Total Inj., mm^3/cycle	46.5	53.7	62.5	71.7	75.5
Main Inj., mm^3/cycle	46.5	53.7	62.5	71.7	75.5
Sec. Inj., mm^3/cycle	--	--	--	--	--
Sec. Inj., percent	--	--	--	--	--
Main Inj., S.M.D., microns	20.5	19.3	19.2	18.8	18.6
Sec. Inj., S.M.D., microns	--	--	--	--	--
Discharge Coefficient	.614		.649		.622
Main Inj. Period, °C.A.	30.0	33.0	35.0	36.5	37.5
Sec. Inj. Timing, °ATDC	--	--	--	--	--
Sec. Inj. Period, °C.A.	--	--	--	--	--
Main Inj. Ave. $\Delta P^{1/2}$, $(lbf)^{1/2}$/in.	44.1	48.1	49.1	51.7	52.3
Sec. Inj. Ave. $\Delta P^{1/2}$, $(lbf)^{1/2}$/in.	--	--	--	--	--

TABLE XI

FUEL INJECTION TEST RESULTS - SERIES III

(Runs with Modified Injection System-No Secondary Injection)

Run No.	31	32	33	34	35
Engine Speed, rpm	1200	1200	1200	1200	1200
Fuel-Air Ratio	.0272	.0306	.0343	.0343	.0380
Total Inj., mm^3/cycle	43.0	48.2	53.0	56.0	59.0
Main Inj., mm^3/cycle	43.0	48.2	53.0	56.0	59.0
Sec. Inj., mm^3/cycle	--	--	--	--	--
Sec. Inj., percent	--	--	--	--	--
Main Inj., S.M.D., microns	19.8	19.6	20.6	20.5	20.4
Sec. Inj., S.M.D., microns	--	--	--	--	--
Discharge Coefficient	.595		.629		.567
Main Inj. Period, °C.A.	16	18.0	18.5	19.5	20
Sec. Inj. Timing, °ATDC	--	--	--	--	--
Sec. Inj. Period, °C.A.	--	--	--	--	--
Main Inj. Ave. $\Delta P^{1/2}$, $(lbf)^{1/2}$/in.	45.1	45.6	43.1	43.3	43.7
Sec. Inj. Ave. $\Delta P^{1/2}$, $(lbf)^{1/2}$/in.	--	--	--	--	--

TABLE XII

FUEL INJECTION TEST RESULTS - SERIES III

(Runs with Modified Injection System-No Secondary Injection)

Run No.	36	37	38	39	40
Engine Speed, rpm	1800	1800	1800	1800	1800
Fuel-Air Ratio	.0217	.0245	.0276	.0303	.0327
Total Inj., mm^3/cycle	34.3	38.8	44.2	48.3	52.3
Main Inj., mm^3/cycle	34.3	38.8	44.2	48.3	52.3
Sec. Inj., mm^3/cycle	--	--	--	--	--
Sec. Inj., percent	--	--	--	--	--
Main Inj., S.M.D., microns			23.1		20.8
Sec. Inj., S.M.D., microns	--	--	--	--	--
Discharge Coefficient			.883		.749
Main Inj. Period, °C.A.	17	18	19	19.5	22
Sec. Inj. Timing, °ATDC	--	--	--	--	--
Sec. Inj. Period, °C.A.	--	--	--	--	--
Main Inj. Ave. $\Delta P^{1/2}$, $(lbf)^{1/2}$/in.			39.7		46.9
Sec. Inj. Ave. $\Delta P^{1/2}$, $(lbf)^{1/2}$/in.	--	--	--	--	--

APPENDIX B

ENGINE PERFORMANCE AND EMISSION RESULTS-

SERIES I THROUGH III

TABLE XIII

ENGINE PERFORMANCE AND EMISSION RESULTS - SERIES I

(Runs with Conventional Injection System)

Run No.	1	2	3	4	5
Engine Speed, rpm	1200	1200	1200	1200	1200
Fuel-Air Ratio	.0294	.0351	.0403	.0449	.0484
BHP	4.80	6.16	7.65	8.56	9.37
BMEP, psi	44.5	57.3	71.0	79.5	86.9
BSFC, lbm/bhp-hr.	.662	.606	.573	.563	.563
Exh. Temperature, °F.	700	805	890	965	1040
Oxides of Nitrogen, ppm	1230	1300	1440	1520	1580
Smoke, Bosch Number	4.6	6.1	7.0	7.6	8.3
Unburned Hydrocarbons, ppm	1500	1700	1850	1800	1700
Specific Hydrocarbon Emission, gm/bhp-hr.	7.62	6.8	6.05	5.07	4.53

TABLE XIV

ENGINE PERFORMANCE AND EMISSION RESULTS - SERIES I

(Runs with Conventional Injection System)

Run No.	6	7	8	9	10
Engine Speed, rpm	1800	1800	1800	1800	1800
Fuel-Air Ratio	.0303	.0345	.0407	.0456	.0506
BHP	6.16	7.54	9.25	10.41	11.47
BMEP, psi	38.2	46.6	57.2	64.7	71.0
BSFC, lbm/bhp-hr.	.817	.757	.730	.722	.731
Exh. Temperature, °F.	830	930	1040	1125	1185
Oxides of Nitrogen, ppm	1010	1060	1170	1250	1280
Smoke, Bosch Number	5.7	6.5	7.4	7.9	8.5
Unburned Hydrocarbons, ppm	1600	1600	1400	900	600
Specific Hydrocarbon Emission, gm/bhp-hr.	9.68	7.98	5.71	3.25	2.15

TABLE XV

ENGINE PERFORMANCE AND EMISSION RESULT -SERIES I

(Runs with Conventional Injection System)

Run No.	11	12	13	14	15
Engine Speed, rpm	2400	2400	2400	2400	2400
Fuel-Air Ratio	.0293	.0347	.0400	.0445	.0508
BHP	6.4	8.9	10.72	11.87	13.01
BMEP, psi	29.7	41.3	49.8	55.1	60.4
BSFC, lbm/bhp-hr.	.998	.858	.817	.824	.865
Exh. Temperature, °F	830	945	1060	1150	1250
Oxides of Nitrogen, ppm	900	1040	1060	1200	1210
Smoke, Bosch Number	4.7	5.5	5.9	6.5	7.0
Unburned Hydrocarbons, ppm	1500	1450	1250	1000	700
Specific Hydrocarbon Emission, gm/bhp-hr.	11.5	8.14	5.88	4.23	2.74

TABLE XVI

ENGINE PERFORMANCE AND EMISSION RESULTS - SERIES II

(Runs with Modified Injection System - No Secondary Injection)

Run No.	16	17	18	19	20
Engine Speed, rpm	1200	1200	1200	1200	1200
Fuel-Air Ratio	.0305	.0349	.0402	.0443	.0492
BHP	5.03	6.51	7.89	9.02	10.16
BMEP, psi	46.6	60.4	73.1	83.7	94.4
BSFC, lbm/bhp-hr.	.636	.583	.555	.534	.531
Exh. Temperature, °F.	690	805	855	975	1050
Oxides of Nitrogen, ppm	1230	1400	1480	1500	1560
Smoke, Bosch Number	4.4	5.3	6.2	6.8	7.4
Unburned Hydrocarbons, ppm	1500	1600	1500	1300	1100
Specific Hydrocarbon Emission, gm/bhp-hr.	7.25	6.03	4.63	3.57	2.73

TABLE XVII

ENGINE PERFORMANCE AND EMISSION RESULTS - SERIES II

(Runs with Modified Injection System - No Secondary Injection)

Run No.	21	22	23	24	25
Engine Speed, rpm	1800	1800	1800	1800	1800
Fuel-Air Ratio	.0300	.0353	.0398	.0450	.0509
BHP	7.02	9.24	10.95	12.32	13.7
BMEP, psi	43.5	57.2	67.8	76.3	84.8
BSFC, lbm/bhp-hr.	.705	.636	.601	.604	.613
Exh. Temperature, °F	815	920	985	1080	1165
Oxides of Nitrogen, ppm	1000	1100	1260	1280	1280
Smoke, Bosch Number	5.5	6.0	6.4	6.9	7.5
Unburned Hydrocarbons, ppm	1050	1100	900	700	300
Specific Hydrocarbon Emission, gm/bhp-hr.	5.6	4.48	3.1	2.15	.832

TABLE XVIII

ENGINE PERFORMANCE AND EMISSION RESULTS - SERIES II

(Runs with Modified Injection System - No Secondary Injection)

Run No.	26	27	28	29	30
Engine Speed, rpm	2400	2400	2400	2400	2400
Fuel-Air Ratio	.0296	.0343	.0402	.0456	.0478
BHP	7.46	10.04	12.1	13.91	14.6
BMEP, psi	35.0	46.6	56.2	64.6	67.8
BSFC, lbm/bhp-hr.	.871	.746	.722	.720	.723
Exh. Temperature, °F.	850	950	1070	1150	1200
Oxides of Nitrogen, ppm	870	940	1010	1180	1210
Smoke, Bosch Number	5.9	6.3	6.8	7.0	7.2
Unburned Hydrocarbons, ppm	700	650	500	300	200
Specific Hydrocarbon Emission, gm/bhp-hr.	4.65	3.20	2.05	1.08	.693

TABLE XIX

ENGINE PERFORMANCE AND EMISSION RESULTS - SERIES II

(Runs with Modified Injection System - No Secondary Injection)

Run No.	31	32	33	34	35
Engine Speed, rpm	1200	1200	1200	1200	1200
Fuel-Air Ratio	.0272	.0306	.0342	.0360	.0380
BHP	4.25	5.21	6.30	6.94	7.68
BMEP, psi	39.98	48.2	58.56	64.72	71.14
BSFC, lbm/bhp-hr.	.753	.697	.632	.602	.575
Exh. Temperature, °F.	675	730	805	850	890
Oxides of Nitrogen, ppm	1040	1230	1390	1440	1460
Smoke, Bosch Number	3.8	4.6	5.2	5.5	5.8
Unburned Hydrocarbons, ppm	1350	1500	1580	1580	1560
Specific Hydrocarbon Emission, gm/bhp-hr.	7.96	7.10	6.25	5.70	5.18

TABLE XX

ENGINE PERFORMANCE AND EMISSION RESULTS - SERIES III

(Runs with Modified Injection System - No Secondary Injection)

Run No.	36	37	38	39	40
Engine Speed, rpm	1800	1800	1800	1800	1800
Fuel-Air Ratio	.0217	.0245	.0276	.0303	.0327
BHP	3.7	5.0	6.6	7.4	8.3
BMEP, psi	23.0	31.1	40.9	46.7	51.3
BSFC, lbm/bhp-hr.	.996	.798	.708	.690	.661
Exh. Temperature, °F	630	690	755	805	850
Oxides of Nitrogen, ppm	830	900	960	1000	1050
Smoke, Bosch Number	2.5	3.7	4.9	5.5	5.8
Unburned Hydrocarbons, ppm	700	860	1000	1050	1090
Specific Hydrocarbon Emission, gm/bhp-hr.	6.99	6.52	5.72	5.4	4.95

REFERENCES

1. Anders, U.W.P., "The Dynamic Delivery Rate and the Hydraulic Similarity of Injection Pumps for High-Speed Engines," ASME Paper No. 71-DGP-3, April 18-22, 1971.

2. Austen, A.E.W. and Lyn, W-T, "Relation Between Fuel Injection and Heat Release in a Direct-Injection Engine and the Nature of the Combustion Process," Proc. Instr. Mech. Engr., Automobile Div., 1960-61.

3. Bascom, R. C., Broersing, L.C., and Wubfhorst, D.E., "Design Factors that Affect Diesel Emissions," SAE Paper 710484, June 1971.

4. Becchi, G.A., "Analytical Simulation of Fuel Injection in Diesel Engines," SAE Paper 710568, June 7-11, 1971.

5. Becchi, G.A. and Guglielmotti, A., "Influence of Some Particular Fuel Injection Phenomena on Diesel Engine Performances," Proc. Instn. Mech. Engrs., London, Vol. 184, Pt. 3J, 1969-70.

6. Bolt, J.A. and Henein, N.A., "The Effect of Some Engine Variables on Ignition Delay and Other Combustion Phenomena in a Diesel Engine," Proc. Instn. Mech. Engrs., London, Vol. 187, Pt. 3J, 1969-70.

7. Bolt, J.A., El-Erian, M.F., Duerr, J. and Miklos, A., "Diesel Engine Combustion and Emissions," Technical Paper No. 11796 submitted to the U.S. Army-Tank Automotive Command, Warren, Mi., Sept. 1972.

8. Bradbury, C.H., "Stationary Compression Engines," London, E & F. N. Spon. Ltd., 1950.

9. Breitenbach, L.P., and Shelef, M., "Development of a Method for the Analysis of NO_2 and NH_3 by NO-measuring Instruments," J. Air Poll. Control Assoc., Vol. 23, no. 2, 1973.

10. Burman, P.G., DeLuca, F., "Fuel Injection and Controls for Internal Combustion Engines," N.Y., Simmons-Boardman Publ. Corp., 1962.

11. Burt, R. and Troth, K.A., "Penetration and Vaporization of Diesel Fuel Sprays," Proc. Instn. Mech. Engrs., London, Vol. 187, Pt. 3J, 1969-70.

12. Cook, Harvey A., "Diesel Engine Cycle Analysis of Relationships of Fuel Injection to Fuel Compression Ignition Characteristics and Best Fuel Utilization," SAE Paper 650449, 1965.

13. Daniel, W.A. and Wentworth, J.T., "Exhaust Gas Hydrocarbons-Genesis and Exodus," SAE Paper 486B, March 12-16, 1962.

14. Dolenc, A. and Lees, R., "Some Aspects of the Development of the OVA24 Traction Engine," Proc. Inst. Mech. Engrs., Vol. 183, Pt. 3b, 1968-69.

15. El-Erian, M.F., "Simulation and Control of Transient Flow in the Diesel Injection System," Ph.D. thesis, University of Michigan, April 1972.

16. El-Erian, M.F., Wylie, E.B., and Bolt, J.A., "Analysis and Control of Transient Flow in the Diesel Injection System, Part I - The Analytical Control Method," SAE Paper 730661, June 18-22, 1973.

17. El-Erian, M.F., Wylie, E.B., and Bolt, J.A., "Analysis and Control of Transient Flow in the Diesel Inection System, Part II - Design Results of Controlled After Injection," SAE Paper 730663, June 18-22, 1973.

18. Flynn, P.F. and Johnson, J.H., "High Output Single Cylinder Research Engine," Final Tech. Report, Int'l Harvester Co., Ceed Engine Engr., Jan. 1957.

19. Ford, H.S., Merrion, D.F., and Hames, R.J., "Reducing Hydrocarbons and Odor in Diesel Exhaust by Fuel Injection Design," SAE Paper 700734, Sept. 14-17, 1970.

20. Gross-Gronomski, L., "Diesel Smoke - Flame Cooling as the Main Cause," Automobile Engineer, Vol. 541, Dec. 1964.

21. Henein, N.A., "Combustion and Emission Formation in Fuel Sprays Injected in Swirling Air," SAE Paper 710220, Jan. 11-15, 1971.

22. Henein, N.A. and Bolt, J.A., "The Effect of Some Fuel and Engine Factors on Diesel Smoke," SAE Paper 690557, Aug. 1969.

23. Hodgeson, J.A., et. al., "Application of a Chemiluminescence Detector for the Measurement of Total Oxides of Nitrogen and Ammonia in the Atmosphere," AIAA Paper 71-1067, Nov. 1971.

24. Johnson, J.H., Sienicki, E.J. and Zeck, O.F., "A Flame Ionization Technique for Measuring Total Hydrocarbons in Diesel Exhaust," SAE Paper 680419, May 1968.

25. Judge, Arthur W., "High-Speed Diesel Engine," London, Chapman & Hall, Sixth Ed., 1967.

26. Khan, I.M., "Formation and Combustion of Carbon in a Diesel Engine," Proc. Instn. Mech. Engrs., London, Vol. 184, Pt. 3J, 1969-70.

27. Khan, I.M. and Green, A.C., "Scheduling Injection Timing For Reduction of Diesel Emissions," SAE Paper 750337, Feb. 1975.

28. Knight, B.E., "Communication on the Performance of a Type of Swirl Atomizer," Proc. Inst. of Mech. Eng., 1955.

29. Lustgarten, G. and Dolenc, A., "Development of Injection System for Medium-Speed Diesel Engine with Quiescent-Type Combustion Chamber," Proc. Instn. Mech. Engrs., London, Vol. 184, Pt. 3J, 1969-70.

30. Lyn, W-T, "The Spectrum of Diesel Combustion Research," Keynote Address, Proc. Instn. Mech. Engrs., London, Vol. 184, Pt. 3J, 1969-70.

31. MacFarlane, J.J., and Holderness, F.H., "Laboratory Studies of Carbon Formation in Fuel-Rich Flames at High Pressures," Proc. Instn. Mech. Engrs., London, Vol. 184, Pt. 3J, 1969-70.

32. Mansfield, W.P., "A New Servo-Operated Fuel Injection System for Diesel Engines," SAE Paper 650432, May 1965.

33. McConnell, G., "Oxides of Nitrogen in Diesel Engine Exhaust Gas: Their Formation and Control," Inst. Mech. Engrs., London, 1963-64.

34. Newhall, H.K. and Starkman, E.S., "Direct Spectroscopic Determination of Nitric Oxide in Reciprocating Engine Cylinders," SAE Paper 670122, Jan. 1967.

35. Parks, M.V., Polonski, C., Tove, R., "Penetration of Diesel Fuel Sprays in Gases," SAE Paper 660747, Oct. 1966.

36. Pearsall, H.W., "Measuring the Total Hydrocarbons in Diesel Exhaust," SAE Paper 670089, Jan. 1967.

37. Schweitzer, P.H., "Penetration of Oil Sprays," Penn. State Col. Bull. No. 46, Eng. Exp. Sta., July 1937.

38. Shahed, S.M., Chiu, W.S., and Yumlu, V.S., "A Preliminary Model for the Formation of Nitric Oxide in Direct Injection Diesel Engines and its Application in Parametric Studies," SAE Paper 730083, Jan. 1973.

39. Shipinski, J.H., "Relationships Between Rates-of-Injection and Rates-of-Heat Release in Diesel Engines," Ph.D. thesis, Dept. of Mech. Eng., University of Wisconsin, June 1967.

40. Shipinski, J., Myers, P.S., and Uyehara, O.A., "A Spray-Droplet Model for Diesel Combustion," Proc. Instn. Mech. Engrs., London, Vol. 187, Pt. 3J, 1969-70.

41. Sigsby, John E., et al., "Chemiluminescent Method for Analysis of Nitrogen Compounds in Mobile Source Emissions (NO, NO_2 and NH_3)," Environmental Science and Technology, Vol. 7, No. 1, Jan. 1973.

42. Springer, K.J., and Dietzmann, H.E., "Diesel Exhaust Hydrocarbon Measurement - A Flame Ionization Method," SAE Paper 700106, Jan. 1970.

43. Tateishi, M., Kushiyama, T., and Nagae, Y., "Elimination of Secondary Injection in Diesel Fuel Injection," Bulletin of the JSME, Vol. 16, No. 93, March 1973.

44. Taylor, C.F., and Taylor, E.S., "The Internal Combustion Engine," Int'l Textbook Co., Scranton, Pa., 1966.

45. Taylor, D.H.C. and Walsham, B.E., "Combustion Process in a Medium Speed Diesel Engine," Proc. Instn. Mech. Engrs., London, Vol. 184, Pt. 3J, 1969-70.

46. Wakuri, Y., Fufii, M., Amitani, T., and Tsuneya, R., "Studies on the Penetration of Fuel Spray in a Diesel Engine," Bulletin of JSME, Vol. 3, No. 9, 1960.

47. Walder, C.J., "Reduction of Emissions from Diesel Engines," SAE Paper 730214, Jan. 1973.

48. Wilson, R.P., Muir, E.B., and Pellicciotti, F.A., "Emissions Study of a Single-Cylinder Diesel Engine," SAE Paper 740123, Feb. 1974.

49. Wylie, E.B., Bolt, J.A., and El-Erian, M.F., "Diesel Fuel Injection System Simulation and Experimental Correlation," SAE Paper 710569, June 1971.

50. Yumlu, V.S. and Carey, A.W., "Exhaust Emission Characteristics of Four-Stroke, Direct Injection, Compression Ignition Engines," SAE Paper 680420, May 1968.